

Oncology and Translational Medicine

Volume 7 • Number 5 • October 2021

Identification of microRNA-21 as a valuable diagnostic marker of oral squamous cell carcinoma and potential target

Hua Yang, Yuxue Wei, Gangli Liu 195

Cone beam computed tomography-guided differences among registration methods for lung cancer and the effects of tumor position, treatment model, and tumor size on positioning errors

Jiayu Du, Jie Tang, Qian Zhang, Xiaojie Ma 203

Ultrasound-guided No Touch liver pedicle microwave ablation in hepatocellular carcinoma treatment

Dan Wang, Shu Zhu, Peng Zhu, Yi Cheng, Hongchang Luo, Jianhua Wang 209

SMARCC1 copy number variation is related to metastatic colon cancer: an investigation based on TCGA data

Libo Feng, Yu Liu, Dong Xia, Xiaolong Chen 216

Oncology and Translational Medicine

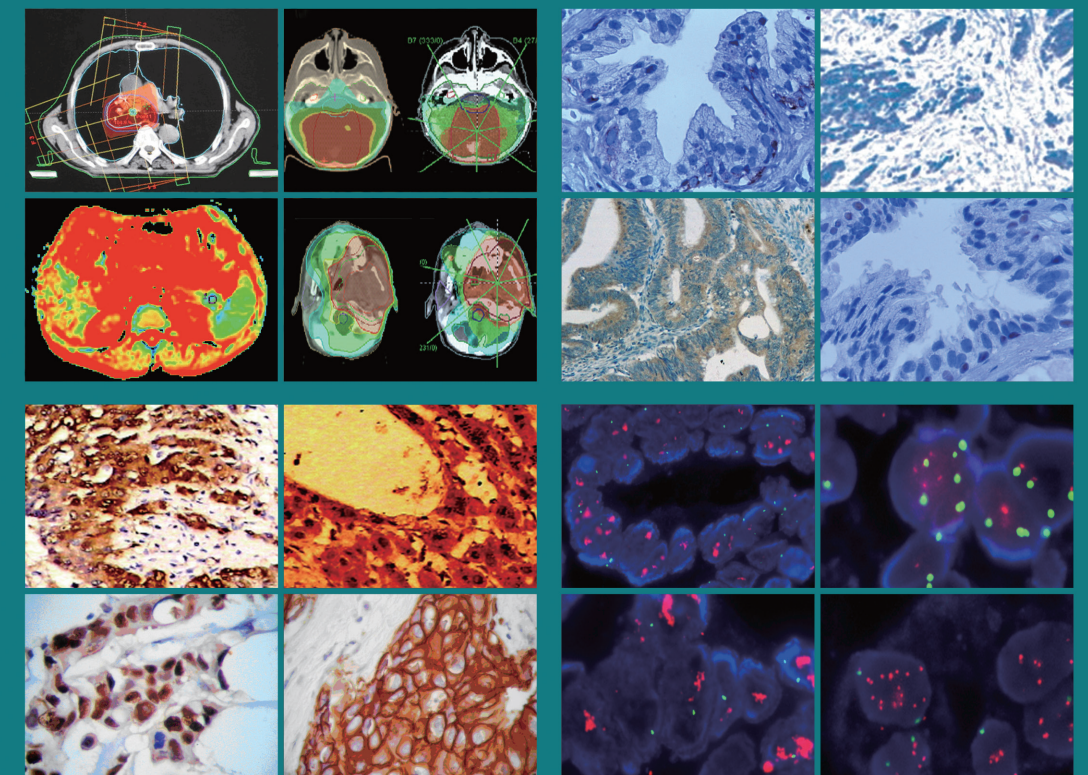
Volume 7 • Number 5 • October 2021

pp 195-243

Oncology and Translational Medicine

肿瘤学与转化医学（英文）

ISSN 2095-9621
CN 42-1865/R



Online First
Immediately Online

otm.tjh.com.cn

Faster
publication!

邮发代号: 38-121

ISSN 2095-9621



GENERAL INFORMATION
» otm.tjh.com.cn

Volume 7
Number 5
October 2021





Honorary Editors-in-Chief

W.-W. Höpker (Germany)
Yan Sun (China)

Editors-in-Chief

Anmin Chen (China)
Shiying Yu (China)

Associate Editors

Yilong Wu (China)
Shukui Qin (China)
Xiaoping Chen (China)
Ding Ma (China)
Hanxiang An (China)
Yuan Chen (China)

Editorial Board

A. R. Hanauske (Germany)
Adolf Grünert (Germany)
Andrei Iagaru (USA)
Arnulf H. Hölscher (Germany)
Baoming Yu (China)
Bing Wang (USA)
Binghe Xu (China)
Bruce A. Chabner (USA)
Caicun Zhou (China)
Ch. Herfarth (Germany)
Changshu Ke (China)
Charles S. Cleeland (USA)
Chi-Kong Li (China)
Chris Albanese (USA)
Christof von Kalle (Germany)
D Kerr (United Kingdom)
Daoyu Hu (China)
Dean Tian (China)
Di Chen (USA)
Dian Wang (USA)
Dieter Hoelzer (Germany)
Dolores J. Schendel (Germany)
Dongfeng Tan (USA)
Dongmin Wang (China)
Ednin Hamzah (Malaysia)
Ewerbeck Volker (Germany)
Feng Li (China)
Frank Elsner (Germany)
Gang Wu (China)
Gary A. Levy (Canada)
Gen Sheng Wu (USA)
Gerhard Ehninger (Germany)
Guang Peng (USA)
Guangying Zhu (China)
Gunther Bastert (Germany)
Guoan Chen (USA)
Guojun Li (USA)

Guoliang Jiang (China)
Guoping Wang (China)
H. J. Biersack (Germany)
Helmut K. Seitz (Germany)
Hongbing Ma (China)
Hongtao Yu (USA)
Hongyang Wang (China)
Hua Lu (USA)
Huaqing Wang (China)
Hubert E. Blum (Germany)
J. R. Siewert (Germany)
Ji Wang (USA)
Jiafu Ji (China)
Jianfeng Zhou (China)
Jianjie Ma (USA)
Jianping Gong (China)
Jihong Wang (USA)
Jilin Yi (China)
Jin Li (China)
Jingyi Zhang (Canada)
Jingzhi Ma (China)
Jinyi Lang (China)
Joachim W. Dudenhausen (Germany)
Joe Y. Chang (USA)
Jörg-Walter Bartsch (Germany)
Jörg F. Debatin (Germany)
JP Armand (France)
Jun Ma (China)
Karl-Walter Jauch (Germany)
Katherine A. Siminovitch (Canada)
Kongming Wu (China)
Lei Li (USA)
Lei Zheng (USA)
Li Zhang (China)
Lichun Lu (USA)
Lili Tang (China)
Lin Shen (China)
Lin Zhang (China)
Lingying Wu (China)
Luhua Wang (China)
Marco Antonio Velasco-Velázquez (Mexico)
Markus W. Büchler (Germany)
Martin J. Murphy, Jr (USA)
Mathew Casimiro (USA)
Matthias W. Beckmann (Germany)
Meilin Liao (China)
Michael Buchfelder (Germany)
Norbert Arnold (Germany)
Peter Neumeister (Austria)
Qing Zhong (USA)
Qinghua Zhou (China)
Qingyi Wei (USA)

Qun Hu (China)
Reg Gorczynski (Canada)
Renyi Qin (China)
Richard Fielding (China)
Rongcheng Luo (China)
Shenjiang Li (China)
Shenqiu Li (China)
Shimosaka (Japan)
Shixuan Wang (China)
Shun Lu (China)
Sridhar Mani (USA)
Ting Lei (China)
Ulrich Sure (Germany)
Ulrich T. Hopt (Germany)
Ursula E. Seidler (Germany)
Uwe Kraeuter (Germany)
W. Hohenberger (Germany)
Wei Hu (USA)
Wei Liu (China)
Wei Wang (China)
Weijian Feng (China)
Weiping Zou (USA)
Wenzhen Zhu (China)
Xianglin Yuan (China)
Xiaodong Xie (China)
Xiaohua Zhu (China)
Xiaohui Niu (China)
Xiaolong Fu (China)
Xiaoyuan Zhang (USA)
Xiaoyuan (Shawn) Chen (USA)
Xichun Hu (China)
Ximing Xu (China)
Xin Shelley Wang (USA)
Xishan Hao (China)
Xiuyi Zhi (China)
Ying Cheng (China)
Ying Yuan (China)
Yixin Zeng (China)
Yongjian Xu (China)
You Lu (China)
Youbin Deng (China)
Yuankai Shi (China)
Yuguang He (USA)
Yuke Tian (China)
Yunfeng Zhou (China)
Yunyi Liu (China)
Yuquan Wei (China)
Zaide Wu (China)
Zefei Jiang (China)
Zhangqun Ye (China)
Zhishui Chen (China)
Zhongxing Liao (USA)

Oncology and Translational Medicine

October 2021 Volume 7 Number 5

Contents

Identification of microRNA-21 as a valuable diagnostic marker of oral squamous cell carcinoma and potential target

Hua Yang, Yuxue Wei, Gangli Liu 195

Cone beam computed tomography-guided differences among registration methods for lung cancer and the effects of tumor position, treatment model, and tumor size on positioning errors

Jiayu Du, Jie Tang, Qian Zhang, Xiaojie Ma 203

Ultrasound-guided No Touch liver pedicle microwave ablation in hepatocellular carcinoma treatment

Dan Wang, Shu Zhu, Peng Zhu, Yi Cheng, Hongchang Luo, Jianhua Wang 209

SMARCC1 copy number variation is related to metastatic colon cancer: an investigation based on TCGA data

Libo Feng, Yu Liu, Dong Xia, Xiaolong Chen 216

CircBAGE2 (hsa_circ_0061259) regulates CCND1 and PDCD10 expression by functioning as an miR-103a-3p 'sponge' to alter the proliferation and apoptosis of prostate cancer cells

Chunlei Zhang, Dan Liu (Co-first author), Qinjin Tian, Qi Yang, Xiaoyuan Zi, Yinghao Sun 221

Evaluation of endocrine therapy combined with intensity modulated radiation therapy in patients with advanced prostate cancer

Xiulong Ma, Hongbing Ma, Dongli Ruan 229

A case of sorafenib-induced severe thrombocytopenia during treatment of unresectable hepatocellular carcinoma

Xiaoying Quan, Xiaoyan Chen, Lei, Chunzhi Wu, Xiaoli Jia, Bin Ye 235

Special IgD- λ type multiple myeloma based on bone marrow cell morphology: A case report

Xiaofang Zhang, Yanqing Zhang, Yungang Zhang, Chuanke Wan, Ling Xu, Ruimin Li 239

Aims & Scope

Oncology and Translational Medicine is an international professional academic periodical. The Journal is designed to report progress in research and the latest findings in domestic and international oncology and translational medicine, to facilitate international academic exchanges, and to promote research in oncology and translational medicine as well as levels of service in clinical practice. The entire journal is published in English for a domestic and international readership.

Copyright

Submission of a manuscript implies: that the work described has not been published before (except in form of an abstract or as part of a published lecture, review or thesis); that it is not under consideration for publication elsewhere; that its publication has been approved by all co-authors, if any, as well as – tacitly or explicitly – by the responsible authorities at the institution where the work was carried out.

The author warrants that his/her contribution is original and that he/she has full power to make this grant. The author signs for and accepts responsibility for releasing this material on behalf of any and all co-authors. Transfer of copyright to Huazhong University of Science and Technology becomes effective if and when the article is accepted for publication. After submission of the Copyright Transfer Statement signed by the corresponding author, changes of authorship or in the order of the authors listed will not be accepted by Huazhong University of Science and Technology. The copyright covers

the exclusive right and license (for U.S. government employees: to the extent transferable) to reproduce, publish, distribute and archive the article in all forms and media of expression now known or developed in the future, including reprints, translations, photographic reproductions, microform, electronic form (offline, online) or any other reproductions of similar nature.

Supervised by

Ministry of Education of the People's Republic of China.

Administered by

Tongji Medical College, Huazhong University of Science and Technology.

Submission information

Manuscripts should be submitted to:
<http://otm.tjh.com.cn>
dmedizin@sina.com

Subscription information

ISSN edition: 2095-9621
CN: 42-1865/R

■ Subscription rates

Subscription may begin at any time. Remittances made by check, draft or express money order should be made payable to this journal. The price for 2021 is as follows: US \$ 30 per issue; RMB ¥ 28.00 per issue.

Database

Oncology and Translational Medicine is abstracted and indexed in EMBASE, Index Copernicus, Chinese Science and Technology Paper Citation Database (CSTPCD), Chinese Core Journals Database, Chinese Journal Full-text Database (CJFD), Wanfang

Data; Weipu Data; Chinese Academic Journal Comprehensive Evaluation Database.

Business correspondence

All matters relating to orders, subscriptions, back issues, offprints, advertisement booking and general enquiries should be addressed to the editorial office.

Mailing address

Editorial office of
Oncology and Translational Medicine
Tongji Hospital
Tongji Medical College
Huazhong University of Science and Technology
Jie Fang Da Dao 1095
430030 Wuhan, China
Tel.: +86-27-69378388
Email: dmedizin@sina.com

Printer

Changjiang Spatial Information
Technology Engineering Co., Ltd.
(Wuhan) Hangce Information
Cartography Printing Filial, Wuhan,
China
Printed in People's Republic of China

Editors-in-Chief

Anmin Chen
Shiyong Yu

Managing director

Jun Xia

Executive editors

Yening Wang
Jun Xia
Jing Chen
Qiang Wu

Identification of microRNA-21 as a valuable diagnostic marker of oral squamous cell carcinoma and potential target*

Hua Yang¹, Yuxue Wei¹, Gangli Liu² (✉)

¹ Department of Stomatology, People's Hospital of Lanling County, Linyi 276000, China

² Department of Oral and Maxillofacial Surgery, Hospital of Stomatology, School of Stomatology, Qilu Medical College, Shandong University, Jinan 250012, China

Abstract

Objective The aim of the study was to summarize the diagnostic value of miR-21 as a biomarker in oral squamous cell carcinoma (OSCC) using a review of the literature and data from the cancer genome atlas (TCGA) database.

Methods Data from TCGA database was sorted and analyzed by bioinformatics to determine the expression level of miR-21 in OSCC. Further, we searched for relevant articles in Embase, PubMed/Medline, Scopus, and Web of Science published before March 2021, extracted the data, and conducted quality assessment. The bivariate meta-analysis model with Stata 16.0 was used to analyze the diagnostic value of miR-21 for OSCC.

Results A total of 304 related articles were identified, and seven were selected for meta-analysis. The diagnostic results after analysis were as follows: sensitivity 0.76 [95% confidence interval (CI), 0.57–0.88]; specificity 0.77 (95% CI, 0.58–0.89); positive likelihood ratio 3.34 (95% CI, 1.58–7.08); negative likelihood ratio 0.31 (95% CI, 0.15–0.63); diagnostic odds ratio 10.75 (95% CI, 2.85–40.51); and area under the curve 0.83 (95% CI, 0.80–0.86). The Deeks' funnel chart showed that there was no potential bias ($P = 0.54$). Prediction analysis of the potential target genes of miR-21 was performed via the biological website, and DAVID was used to cross target genes for gene ontology (GO) annotation function analysis.

Conclusion The results showed that miR-21-3p and miR-21-5p were significantly more highly expressed in OSCC tissues than in normal tissues ($P < 0.05$), and the results of the meta-analysis indicated that they could be used as potential biomarkers in the diagnosis of OSCC. In addition, 58 potential target genes of miR-21 were significantly enriched in 28 GO annotation functional pathways, which provided a biological basis for further clinical diagnostic value research.

Key words: miR-21; oral squamous cell carcinoma (OSCC); diagnostic meta-analysis; target gene prediction

Received: 11 May 2021

Revised: 20 September 2021

Accepted: 8 October 2021

Oral squamous cell carcinoma (OSCC) accounts for 90% of oral and maxillofacial tumors and is the sixth most common type of malignant tumor worldwide^[1]. Its incidence and mortality have not been affected by the improvement of surgical techniques, which is recognized as a serious problem. Traditional detection methods have several limitations, including expensive inspection fees and low specificity. Thus far, early detection and treatment are the best therapeutic strategies. Therefore, identification of new diagnostic markers for the early

detection of OSCC is a potential treatment option. MicroRNAs (miRNAs), endogenous non-coding small RNAs with a length of 18–25 nucleotides, are considered as potential cancer biomarkers for early detection and diagnosis. Increasing evidence have shown that miRNA can be used as a new and non-invasive biomarker for the early diagnosis of various types of cancer^[2–3]. miR-21 is located on chromosome 17p23.1, which is an oncogenic miRNA that promotes carcinogenesis through anti-apoptotic effects. miR-21 is highly expressed in

✉ Correspondence to: Gangli Liu. Email: liugangli@sdu.edu.cn

* Supported by a grant from the National Natural Science Foundation of China (No. 81402298).

© 2021 Huazhong University of Science and Technology

many cancers, including gastric, esophageal, ovarian, and breast cancer. Inhibition of its expression can lead to tumor shrinkage and has a significant impact on the chemoresistance of tumors^[4-5]. Gombos and other studies have shown that miR-21 is highly expressed in oral cancer tissues, and miR-21 can be used as a non-invasive biomarker for the diagnosis and detection of other cancers^[6]. However, the diagnostic value of miR-21 in OSCC requires further confirmation. Therefore, in this meta-analysis, we screened and summarized the diagnostic value of miR-21 as a biomarker in OSCC and analyzed its potential target genes and related enrichment pathways, which are necessary for effective diagnosis and treatment of OSCC patients.

Materials and methods

Download and organization of the cancer genome atlas (TCGA) database

We downloaded all of the miRNA-related transcriptome data of OSCC from the TCGA database (<https://portal.gdc.cancer.gov/>) and drew pictures using the “beeswarm” package in the R software.

Literature search

We searched the Embase, PubMed/Medline, Scopus, and Web of Science databases, for articles published before March 2021. We searched for synonyms of OSCC and miR-21 as keywords through the keyword MeSH function in PubMed, and relevant documents were collected comprehensively and systematically.

Literature inclusion and exclusion criteria

Inclusion and exclusion of the literature were completed separately and integrated by two individuals. The inclusion criteria were as follows: miR-21 diagnosis data – sensitivity or specificity, the control group information of healthy patients can be obtained from the literature or by contacting the author; the exclusion criteria included: inability to provide valid data such as sensitivity and specificity, non-human studies, non-clinical studies, reviews, conference abstracts, case reports, and repeated published studies.

Literature quality evaluation and data extraction

The quality of the literature was evaluated using QUADAS-2; the items in the QUADAS list were applied to each article, and the answer was determined to be “yes,” “no,” or “unclear.” Two researchers rated the literature according to the scoring criteria, and articles with inconsistent scores were re-scored by group discussion. The data extraction information included the name of the first author, publication, year, country/region, ethnicity,

sample size, specimen and cancer type, detection method, true positive, false positive, true negative, and false negative numbers.

Statistical processing

Statistical analysis was performed using Stata version 16.0; the bivariate meta-analysis model was used to calculate the relevant values, the comprehensive sensitivity and specificity, diagnostic odds ratio (DOR), positive likelihood ratio (PLR), and negative likelihood ratio (NLR). Analysis of the summary receiver operating characteristic curve (SROC) and the calculation of the area under the curve (AUC) were carried out to evaluate the value of the overall diagnosis of miR-21 in cancer detection and diagnosis; the data used the hierarchical summary receiver operating characteristic model (HSROC) model for further confirmation. Spearman's correlation coefficient and ROC plane analysis evaluated the heterogeneity of threshold effects. The heterogeneity of non-threshold effects was detected by Q test and discordance index (I^2), where $P < 0.10$ or $I^2 > 50\%$ indicates that there is obvious heterogeneity between studies. Fagan nomograms verified pre-test probability, likelihood ratio, and post-test probability; Deeks' funnel chart was used to test bias.

miR-21 target gene analysis

Three online target gene prediction tools, namely TargetScan (http://www.targetscan.org/vert_71/), miRDB (<http://mirdb.org/>), and PicTar (<https://pictar.mdc-berlin.de/>), were used to predict the potential target genes of miR-21 (including miR-21-3p and miR-21-5p). Further, we used the VennDiagram package in the R software to draw a Venn diagram of the three databases to take the intersection for subsequent analysis.

Functional enrichment analysis of target genes

The online tool DAVID (<http://david.abcc.ncifcrf.gov/>) was used to perform gene ontology functional enrichment analysis (GO analysis) on the intersecting target genes, and $P < 0.01$ was set as the significance threshold to obtain the top 28 statistically significant GO annotation analyses.

Results

Expression level of miR-21 in different tissues

Through the download and analysis of TCGA database, the expression levels of miR-21-3p and miR-21-5p in OSCC and normal tissues were sorted out, and the results showed that both were significantly highly expressed in OSCC ($P = 0.021$ and $P = 0.04$; Fig. 1), which further illustrated that the study of miR-21 is of great significance for OSCC patients.

Literature review

A total of 304 documents were obtained from the online database. A total of 88 duplicate documents were removed by two authors, leaving 216 documents; 168 articles were initially screened by reading document titles, keywords, and abstracts, and 136 documents were retained; 41 documents were eliminated by reading the full text and following the exclusion rules. Finally, a total of seven articles, including 609 studies (359 OSCC patient groups and 250 control groups) were included in the meta-analysis. A flow chart of the literature selection is shown in Fig. 2. The basic information of the seven included meta-analysis documents and the results of QUADAS-2. The results of the literature quality evaluation are shown in Table 1.

Threshold effect and heterogeneity analysis

This study examined the threshold effect by drawing the ROC curve and calculating the Spearman correlation coefficient between the logarithm of sensitivity and the logarithm of (1-specificity). The results showed that the ROC curve did not reveal a shoulder-arm-like distribution (Fig. 3); Spearman's correlation coefficient was 0.19, and the *P* value was 0.04, both of which indicate no threshold effect; $I^2 = 94\%$ indicated heterogeneity, and the meta-analysis revealed heterogeneity caused by non-threshold effects. Since only seven studies were included in this meta-analysis, meta-regression analysis could not be performed to investigate the source of heterogeneity.

Analysis of meta consolidated statistics

The pooled sensitivity and specificity of miR-21 for the diagnosis of OSCC were 0.77 (95% CI, 0.58–0.89) and

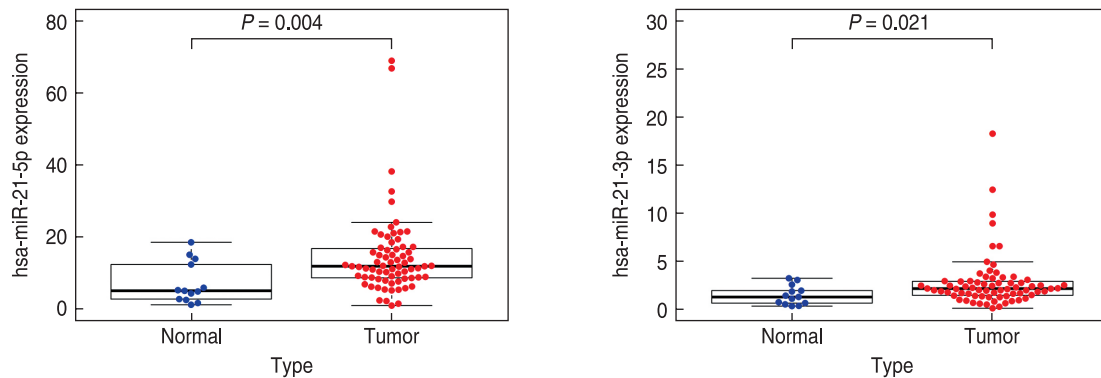


Fig. 1 The expression levels of miR-21-3p and miR-21-5p. The gene expression profiling data of OSCC tissues and normal samples in TCGA database were chosen to analyze the mRNA levels of miRNA-21-5p (*P* = 0.04) and miRNA-21-3p (*P* = 0.021)

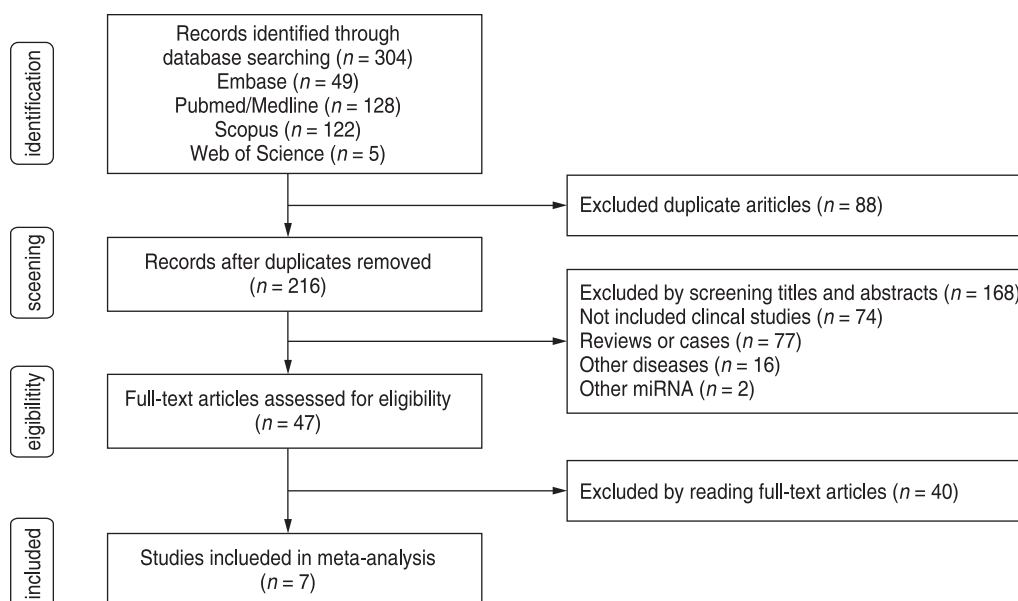


Fig. 2 Flow chart of articles selection

Table 1 Characteristics of publications included in the meta-analysis

First author	Year	Country	Ethnicity	Cancer type	Sample type	Test method	Cutoff	Cases/controls	QUADAS-2
Karimi [7]	2020	Iran	Caucasian	OSCC	Serum	RT-qPCR	\	20/20	5
Lu [8]	2019	China	Asian	Oral cancer	Serum	RT-qPCR	\	82/53	6
Mahmood [9]	2019	Pakistan	Caucasian	Oral cancer	Plasma	RT-qPCR	35 Ct	100/100	7
Ren [10]	2014	China	Asian	OSCC	Blood	RT-qPCR	9646	58/32	5
He [11]	2016	China	Asian	OTSCC	Tissue	RT-qPCR	\	19/20	6
Zahran [12]	2015	Egypt	Caucasian	OSCC	Salivary	RT-qPCR	\	20/20	5
Supic [13]	2017	Serbia	Caucasian	Tongue carcinoma	Tissue	RT-qPCR	938	60/5	5

Note: OSCC, oral squamous cell carcinoma; OTSCC, oral tongue squamous cell carcinoma; RT-qPCR, reverse transcription–polymerase chain reaction; QUADAS, quality assessment of diagnostic accuracy studies

0.76 (95% CI, 0.57–0.88; Fig. 4), and the PLR was 3.34 (95% CI, 1.58–7.08), NLR was 0.31 (95% CI, 0.15–0.63; Fig. 5), and DOR was 10.75 (95% CI, 2.85–40.51; Fig. 6). The AUC of miR-21 was 0.83 (95% CI, 0.80–0.86; Fig. 7). These results indicated that miR-21 was highly accurate at differentiating OSCC patients from controls. To assess the clinical utility of the index test, Fagan nomograms were used to predict the increasing inerrability of a positive diagnosis using the value of the test. As shown in Fig. 8, the pre-test probability was 50%, and a positive result of post-test probability was raised to 77%, whereas a negative result of post-test probability decreased to 24%. All pooled estimates indicated that miR-21 had a relatively moderate to high accuracy in distinguishing OSCC patients from healthy individuals in this analysis.

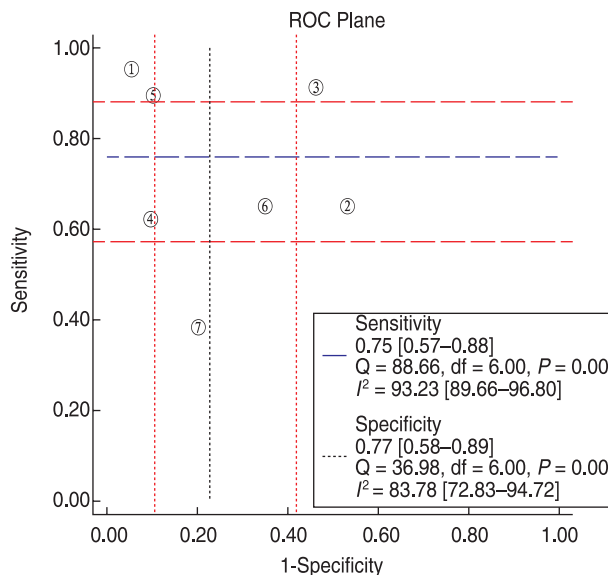


Fig. 3 ROC curve of miR-21

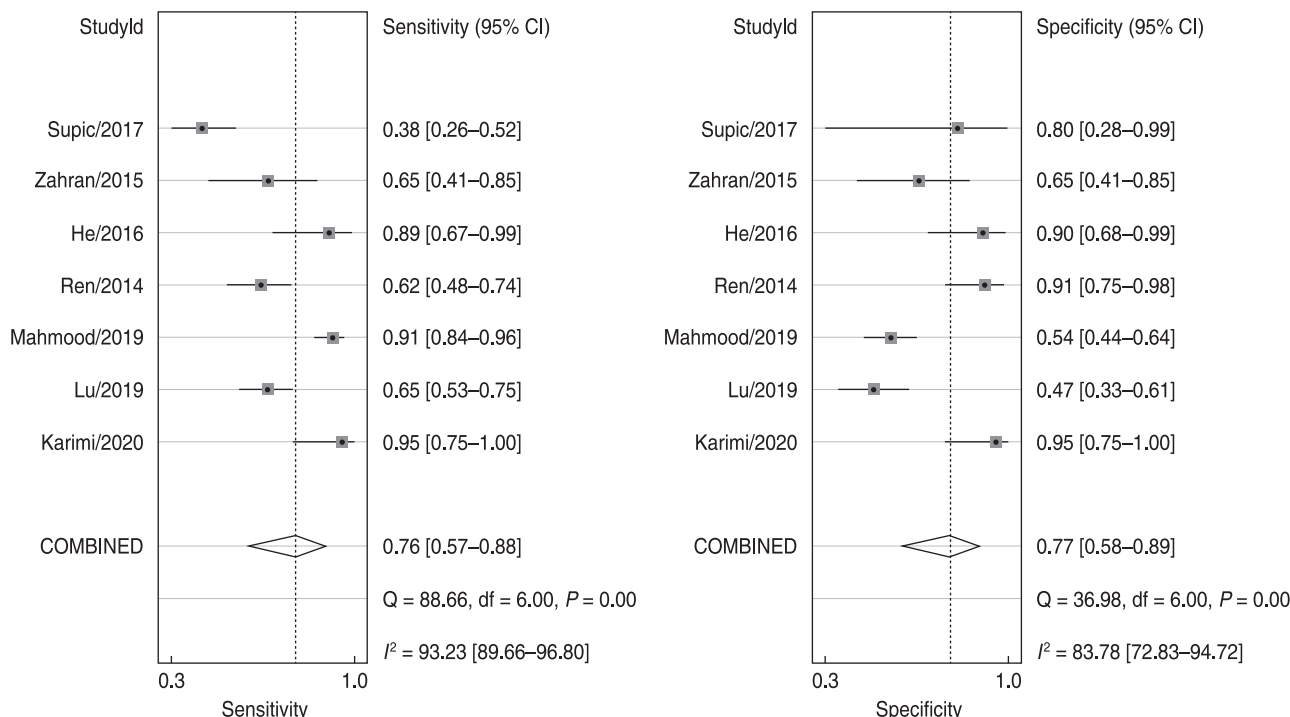


Fig. 4 The sensitivity and specificity of miR-21

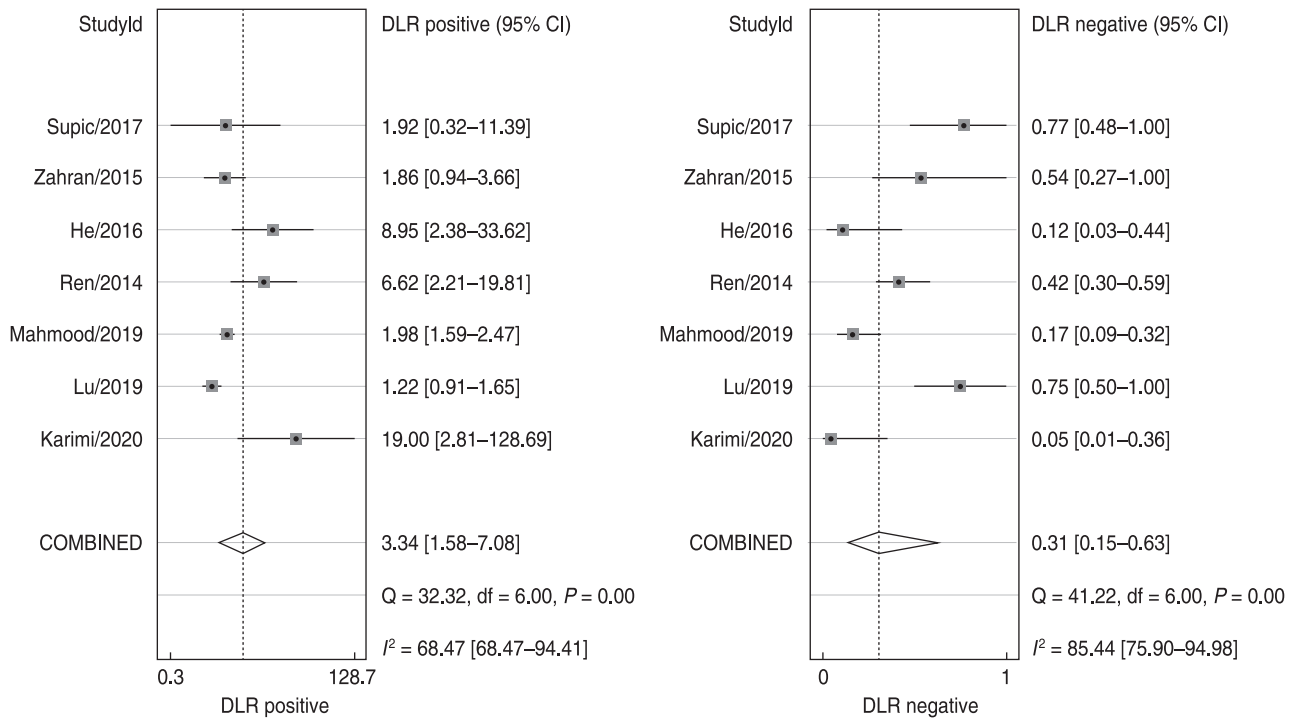


Fig. 5 The PLR and NLR values of miR-21

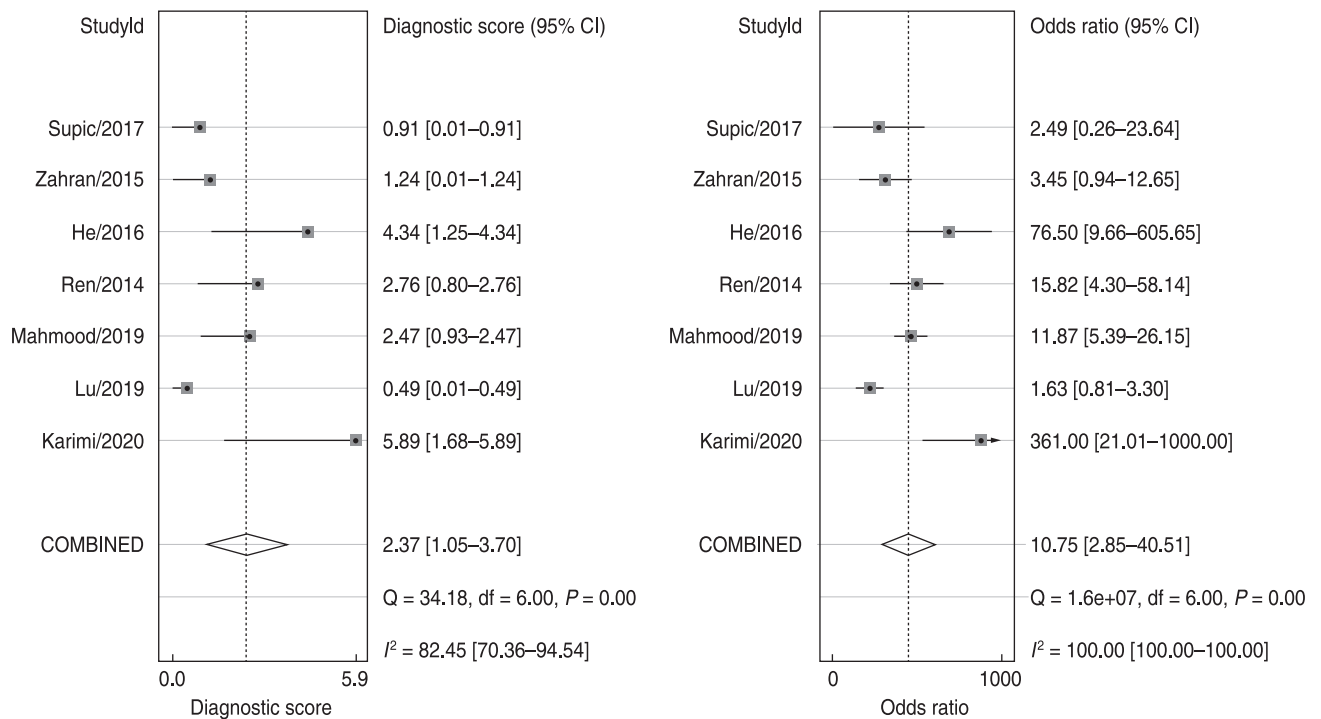


Fig. 6 The DOR value of miR-21

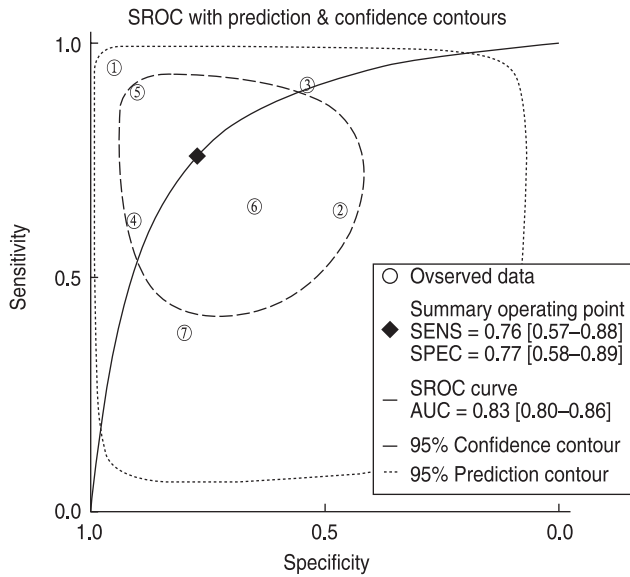


Fig. 7 SROC curve of miR-21

Assessment of publication bias

The results of Deeks’ funnel chart analysis using Stata are shown in Fig. 9. The results showed that the slope coefficient was $P = 0.54$, suggesting no significant publication bias among the documents included in the meta-analysis.

MiR-21 target gene prediction analysis

The number of potential miR-21 target genes predicted by the three online databases, TargetScan, miRDB, and PicTar, were 4048, 1064, and 137, respectively, and a Venn diagram was drawn to take the intersection of the above results, and 58 predicted target genes were obtained (Fig. 10).

Prediction of the GO function annotation for the potential target gene

GO analysis was performed on 58 target genes, and biological pathway enrichment analysis was performed using functional annotation in the DAVID database. Based on analysis of the whole human genome, we identified that the target genes of miR-21 were significantly enriched in 28 functional pathways ($P < 0.01$), of which 47 intersection target genes were enriched in protein binding functional pathways, and 30 were enriched in the nucleus functional pathway (Fig. 11).

Discussion

OSCC has a high morbidity and fatality rate; therefore, early diagnosis of the disease and effective prognosis of patients are particularly important [14]. Traditional diagnostic examinations are expensive and have poor

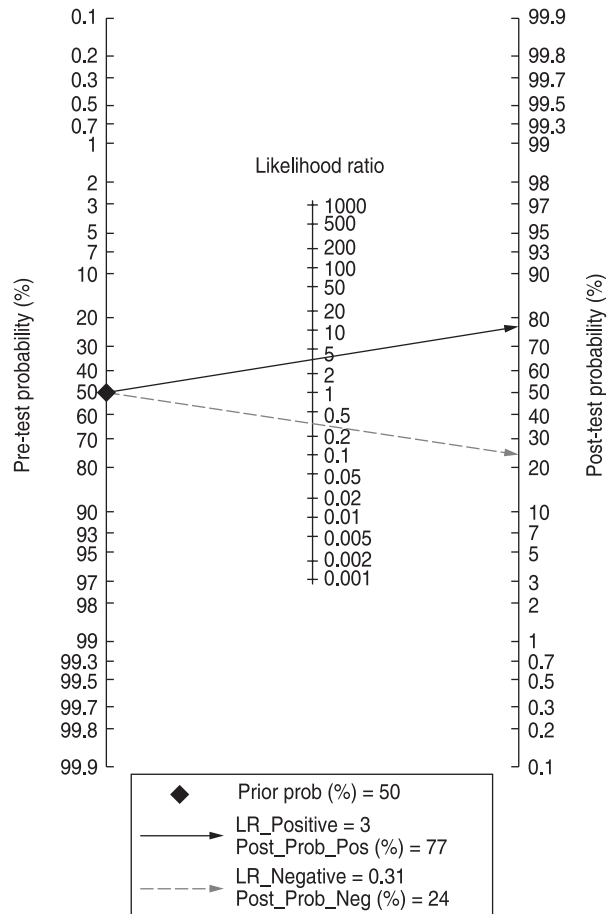


Fig. 8 Fagen nomogram of miR-21

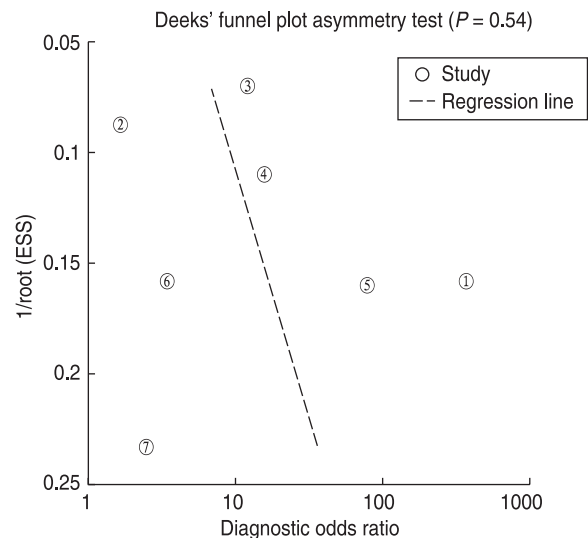


Fig. 9 miR-21 diagnosis of OSCC publication bias funnel chart

sensitivity and specificity; therefore, a new approach is required. As a new OSCC biomarker, miRNAs are involved in cell growth, development, differentiation,

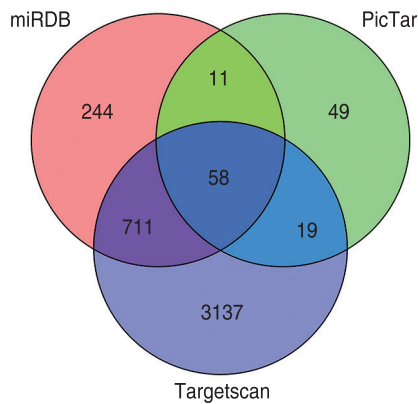


Fig. 10 Venn diagram of predicted target genes

and apoptosis, and their expression is closely related to the diagnosis, staging, progression, prognosis, and response to treatment^[15]. This is expected to become a therapeutic target for most diseases and is an important step towards gene therapy for human diseases^[16]. Among them, miR-21 is a dysregulated miRNA that has been studied in OSCC, and its overexpression in serum or tissue is related to tumor size and distant metastasis. Studies have shown that miR-21 can regulate a variety of cancer-related target genes, and the serum miR-21 of OSCC patients is upregulated significantly, which could be used as a biomarker of OSCC prognosis^[9, 17]. In this study, the expression of miR-21-3p and miR-21-5p was first analyzed in OSCC and normal tissues, which illustrated the importance of miR-21 in OSCC patients.

The meta-analysis in this study was used to evaluate the diagnostic value of miR-21 in OSCC testing. The

combined PLR was 3.34 (95% CI, 1.58–7.08), NLR was 0.31 (95% CI, 0.15–0.63), and the positive rate of miR-21 in the OSCC case group was 3.3 times compared to that of the control group; the negative rate of miR-21 was 31% of that in the control group; and the DOR was 10.75 (95% CI, 2.85–40.51). The above results indicated that miR-21 as a biomarker for the diagnosis of OSCC is highly reliable and accurate, and its clinical value is considerable. Fagan’s nomogram revealed that if the pre-test probability was 50%, the positive probability after the test increased to 77% when the PLR was 3.3, and the negative probability after the test decreased to 24% when the NLR was 0.31, indicating miR-21 is relatively reliable for cancer detection and treatment.

The discussion of heterogeneity in this study may be restricted by several limitations, as follows: (1) The number of available studies and the number of participants were small; (2) The data are mainly from Asian and Caucasian participants, which may lead to incomplete ethnic coverage; (3) Sample collection was performed via various methods, including blood, saliva, and tissues, which may cause differences in the results; (4) The cut-off value of miR-21 could not be determined as a whole, because each study used different cut-off values; (5) The analysis of this study was retrospective, and selective bias can reduce the credibility of the results; (6) Published research only contained English, which may lead to the neglect of research published in other languages.

Furthermore, prediction analysis revealed that miR-21 has 58 potential target genes, which are mostly enriched in protein binding and nuclear function pathways, according to the results of the GO function annotation. In addition, six potential target genes (*STAT3*, *PDCD4*,

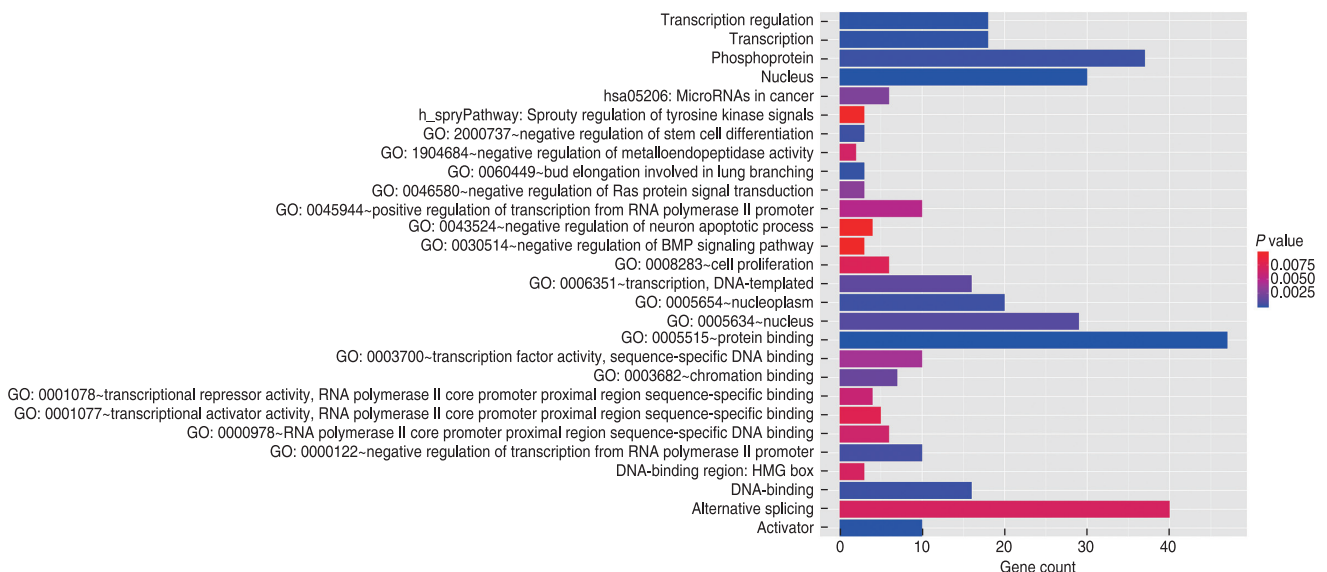


Fig. 11 GO function annotation diagram of potential target genes

TIMP3, *SPRY2*, *RECK*, and *CDC25A*) were enriched in pathway – hsa05206: microRNAs in cancer, and OSCC is a type of malignant tumor, indicating that there is a strong correlation between miR-21 and OSCC.

In summary, the results of this meta-analysis revealed that miR-21 can effectively distinguish OSCC patients from healthy controls and could potentially be used as a supplement to improve the accuracy of existing diagnostic methods. Future research should focus on the combined use of miR-21 and other biomarkers to further improve the accuracy of OSCC diagnosis.

Conflicts of interest

The authors indicated no potential conflicts of interest.

References

- Warnakulasuriya S. Global epidemiology of oral and oropharyngeal cancer. *Oral Oncol*, 2009, 45: 309–316.
- Jansson MD, Lund AH. MicroRNA and cancer. *Mol Oncol*, 2012, 6: 590–610.
- Binmadi NO, Basile JR, Perez P, *et al.* miRNA expression profile of mucoepidermoid carcinoma. *Oral Dis*, 2018, 24: 537–543.
- Wang B, Zhang QY. The expression and clinical significance of circulating microRNA-21 in serum of five solid tumors. *J Cancer Res Clin Oncol*, 2012, 138: 1659–1666.
- Chen Y. Progress in lung cancer treatment. *Oncol Transl Med*, 2015, 1: 3–4.
- Gombos K, Horváth R, Szele E, *et al.* miRNA expression profiles of oral squamous cell carcinomas. *Anticancer Res*, 2013, 33: 1511–1517.
- Karimi A, Bahrami N, Sayedyahosseini A, *et al.* Evaluation of circulating serum 3 types of microRNA as biomarkers of oral squamous cell carcinoma; A pilot study. *J Oral Pathol Med*, 2020, 49: 43–48.
- Lu ZY, He QT, Liang JF, *et al.* miR-31-5p is a potential circulating biomarker and therapeutic target for oral cancer. *Mol Ther Nucleic Acids*, 2019, 16: 471–480.
- Mahmood N, Hanif M, Ahmed A, *et al.* Circulating miR-21 as a prognostic and predictive biomarker in oral squamous cell carcinoma. *Pak J Med Sci*, 2019, 35: 1408–1412.
- Ren WH, Qiang C, Gao L, *et al.* Circulating microRNA-21 (MIR-21) and phosphatase and tensin homolog (PTEN) are promising novel biomarkers for detection of oral squamous cell carcinoma. *Biomarkers*, 2014, 19: 590–596.
- He QT, Chen ZJ, Cabay RJ, *et al.* microRNA-21 and microRNA-375 from oral cytology as biomarkers for oral tongue cancer detection. *Oral Oncol*, 2016, 57: 15–20.
- Zahran F, Ghalwash D, Shaker O, *et al.* Salivary microRNAs in oral cancer. *Oral Dis*, 2015, 21: 739–747.
- Supic G, Zeljic K, Rankov AD, *et al.* miR-183 and miR-21 expression as biomarkers of progression and survival in tongue carcinoma patients. *Clin Oral Investig*, 2018, 22: 401–409.
- Rivera C, Venegas B. Histological and molecular aspects of oral squamous cell carcinoma (Review). *Oncol Lett*, 2014, 8: 7–11.
- Volinia S, Calin GA, Liu CG, *et al.* A microRNA expression signature of human solid tumors defines cancer gene targets. *Proc Natl Acad Sci USA*, 2006, 103: 2257–2261.
- Wu W, Sun M, Zou GM, *et al.* MicroRNA and cancer: Current status and prospective. *Inter J Cancer*, 2007, 120: 953–960.
- Sayed D, Rane S, Lypowy J, *et al.* MicroRNA-21 targets Sprouty2 and promotes cellular outgrowths. *Mol Biol Cell*, 2008, 19: 3272–3282.

DOI 10.1007/s10330-021-0494-4

Cite this article as: Yang H, Wei YX, Liu GL. Identification of microRNA-21 as a valuable diagnostic marker of oral squamous cell carcinoma and potential target. *Oncol Transl Med*, 2021, 7: 195–202.

Cone beam computed tomography-guided differences among registration methods for lung cancer and the effects of tumor position, treatment model, and tumor size on positioning errors*

Jiayu Du^{1,3}, Jie Tang^{1,3}, Qian Zhang^{1,3}, Xiaojie Ma^{1,2} (✉)

¹ Department of Oncology, Affiliated Hospital of North Sichuan Medical College, Nanchong 637000, China

² Department of Radiation Oncology, North Sichuan Medical College, Nanchong 637000, China

³ Department of Clinical Medicine, North Sichuan Medical College, Nanchong 637000, China

Abstract

Objective To explore the differences in three different registration methods of cone beam computed tomography (CBCT)-guided down-regulated intense radiation therapy for lung cancer as well as the effects of tumor location, treatment mode, and tumor size on registration.

Methods This retrospective analysis included 80 lung cancer patients undergoing radiotherapy in our hospital from November 2017 to October 2019 and compared automatic bone registration, automatic grayscale (t + r) registration, and automatic grayscale (t) positioning error on the X-, Y-, and Z-axes under three types of registration methods. The patients were also grouped according to tumor position, treatment mode, and tumor size to compare positioning errors.

Results On the X-, Y-, and Z-axes, automatic grayscale (t + r) and automatic grayscale (t) registration showed a better trend. Analysis of the different treatment modes showed differences in the three registration methods; however, these were not statistically significant. Analysis according to tumor sizes showed significant differences between the three registration methods ($P < 0.05$). Analysis according to tumor positions showed differences in the X- and Y-axes that were not significant ($P > 0.05$), while the autopsy registration in the Z-axis showed the largest difference in the mediastinal and hilar lymph nodes ($P < 0.05$).

Conclusion The treatment mode was not the main factor affecting registration error in lung cancer. Three registration methods are available for tumors in the upper and lower lungs measuring < 3 cm; among these, automatic gray registration is recommended, while any gray registration method is recommended for tumors located in the mediastinal hilar site measuring < 3 cm and in the upper and lower lungs ≥ 3 cm.

Key words: lung cancer; IMRT; positioning error; registration method; CBCT; different tumor locations; different treatment modes; tumor size

Received: 29 June 2021

Revised: 21 August 2021

Accepted: 15 September 2021

Lung cancer is one of the most common malignant tumors worldwide, ranking first in incidence and mortality [1], with men significantly more affected than women. Radiotherapy is the primary treatment for patients with lung cancer [2–4]. However, in chest tumor radiotherapy, the target area is easily affected by organ movement, resulting in reduced radiotherapy accuracy,

which has become the main reason for radiotherapy failure in lung cancer in recent years [5]. Therefore, accurate positioning is an important part of the radiotherapy process, as this directly affects the therapeutic efficacy of tumor radiotherapy [6]. The implementation of precise radiotherapy includes increased requirements for accuracy and positioning repeatability. At present,

✉ Correspondence to: Xiaojie Ma. Email: 992437730@qq.com

* Supported by grants from the Nanchong City School Cooperation Project (No. 18SXHZ0542), Hubei Chen Xiaoping Science and Technology Development Foundation Project (No. CXPJH11900002-037), and Sichuan Medical Research Youth Innovation Project (No. Q18031).

© 2021 Huazhong University of Science and Technology

it is mainly solved and verified using a medical image registration strategy before performing radiotherapy [7-8]. In clinical practice, cone beam computed tomography (CBCT)-guided automatic registration is mainly used, in which the fusion registration of CBCT is generally performed by doctors and technicians in the radiotherapy room, who randomly choose among bone, gray-scale, or manual registration according to their clinical experience. Finally, the error in patient body position is adjusted based on the results of fusion registration; the disadvantage lies in the randomization of the registration mode during the precise radiotherapy process and the lack of unified and fixed standards or norms, which inevitably lead to inconsistent registration results in the same patient and ultimately affect the overall treatment effects. The present study retrospectively analyzed differences between the three registration methods used for intensity-modulated radiotherapy in 80 lung cancer patients as well as the effects of tumor positions, treatment modes, and tumor lengths on registration, to provide a scientific basis for the clinical selection of appropriate and reasonable registration modes.

Materials and methods

Clinical data

This study included a total of 80 lung cancer patients who received radiotherapy in the Department of Radiotherapy of the Affiliated Hospital of North Sichuan Medical College between November 2017 and October 2019. Among them, 70 and 10 patients received radical radiotherapy and postoperative adjuvant radiotherapy, respectively, including 68 male and 12 female patients, 48 upper lungs, 13 middle lungs, and 19 lower lungs. The median age of the patients was 61 years. All patients were confirmed to have lung cancer by histopathological examination, including squamous cell carcinoma ($n = 26$), adenocarcinoma ($n = 27$), small cell ($n = 26$), and atypical carcinoid ($n = 1$).

Patient fixation and CT positioning

Our hospital currently uses the SIEMENS SOMATOM Emotion CT scanning thermoplastic positioning system. When positioned under the CT scan simulation machine, all patients were placed in the supine position, with both hands clasping their elbows to cross to the forehead. This position is comfortable and easily repeated. A thermoplastic positioning film was used to fix it on the carbon fiber board. The "+" mark on the upper front centerline and the left and right body sides of the patient's thermoplastic film was positioned to coincide with the laser lead bead mold and a lead bead with a diameter of approximately 2 mm was placed as the body surface mark for the reference coordinate system. A CT scan was

performed after all the molds were cooled and shaped. The scanning layer thickness was 5 mm. Conventional reconstruction images were used to obtain image data from the positioning CT. After the scan, the image was transmitted to the Monaco radiotherapy planning system to delineate and plan the target area.

Patient positioning and CBCT registration

Two experienced technicians positioned the patient on a linear accelerator treatment bed (Elekta Synergy) in a fixed. The patient position was adjusted so that the body membrane marker line coincided with the indoor laser at the axial, coronal, and sagittal intersection, which was used as the basis for positioning. CBCT images were collected by the Elekta XVI registration system and registered with the target images transmitted by the planning system. The registration and verification were performed by two deputy chief physicians and doctors with professional titles. The two physicians unanimously identified them as effective registrations and used the average value of each registration error as the registration error data. The left and right directions were defined as the X-axis, the head and foot directions were defined as the Y-axis, and the front and back directions were defined as the Z-axis to determine the translation and rotation errors in each of these axes, respectively. All patients underwent all three registration methods (bone, gray-scale [translation + rotation] (t + r), and gray-scale [translation] (t)) to compare the differences among the three registration methods in all three axes.

Grouping of patients

The patients were grouped according to tumor location (upper, middle, and lower lung), treatment mode (radical or postoperative radiotherapy), and tumor length (≥ 3 cm and < 3 cm) and the errors in each group under different registration methods were compared.

Data processing

Analysis was performed using IBM SPSS for Windows, version 22.0. The errors in measurement data between the three registration methods were assessed by analysis of variance (ANOVA), with post hoc tests used for pairwise comparison between groups. T-tests were used to compare the data between groups. The positioning errors of patients according to tumor location, treatment mode, and tumor size under the three registration modes were compared using two-factor ANOVA and multiple comparisons, with linear regression used to determine the quantitative relationship of interdependence between two variables. A P value < 0.05 indicated that the sample difference was statistically significant.

Results

Basic patient information

This study included a total of 80 patients (68 males and 12 females) with a median age of 61 years. Ten and 70 patients received postoperative radiotherapy and radical radiotherapy, respectively. There were 48 cases of upper lung cancer, 13 cases of middle lung cancer, and 19 cases of lower lung cancer. Thirty-three patients had tumors measuring ≥ 3 cm and 47 patients had tumors measuring < 3 cm (Table 1).

Comparisons of the differences among automatic bone, automatic gray-scale (t + r) and automatic gray-scale (t) registration on the X-, Y-, and Z-axes

Automatic bone, automatic gray-scale (t + r), and automatic gray-scale (t) registration were used for each patient. The results showed no significant differences between the three registration methods on the X-, Y-, and Z-axes; however, automatic gray-scale (t + r) and automatic gray-scale (t) registration showed a better

trend (Fig. 1).

Comparisons of positioning errors on the X-, Y-, and Z-axes among lung cancer patients with different tumor locations under the three registration modes

There were no significant differences among the registration errors of the three registration methods on the X- and Y-axes according to tumor location ($P > 0.05$). On the Z-axis, there were no significant differences in registration error between lung cancer tumor sites using automatic gray-scale and automatic gray-scale (t) matching, but there was a significant difference using automatic bone matching ($P < 0.05$). The difference in the values of the middle lung was the highest, while those of the upper and lower lungs were low (Fig. 2).

Comparisons of positioning errors on the X-, Y-, and Z-axes among patients receiving different treatment modes for lung cancer under the three registration methods

There were no significant differences in registration errors among automatic bone, automatic gray-scale (t + r), and automatic gray-scale (t) registration on the X-, Y-, and Z-axes. Moreover, different treatment methods for lung cancer showed no significant effect on the choice of registration methods for patients with lung cancer.

Comparisons of the positioning errors on the X-, Y-, and Z-axes among patients with different lung cancer tumor sizes under the three registration methods

For tumors < 3 cm, there were no significant differences in the registration errors among automatic bone, automatic gray-scale (t + r), and automatic gray-scale (t) registration methods on the X-, Y-, and Z-axes ($P > 0.05$). For tumors ≥ 3 cm, there was no significant difference in errors between automatic bone, automatic gray-scale (t + r), and automatic gray-scale (t) registration on the X- and Z-axes ($P > 0.05$). However, on the Y-axis, the positioning error of automatic bone registration was

Table 1 Basic conditions of patients and general characteristics of tumors

Feature	No. of patients
Age (years)	61
Gender	
Male	68
Female	12
Treatment	
Radical radiotherapy	70
Postoperative radiotherapy	10
Tumor site	
Upper lung	48
Middle lung	13
Lower lung	19
Tumor length (cm)	
≥ 3	33
< 3	47

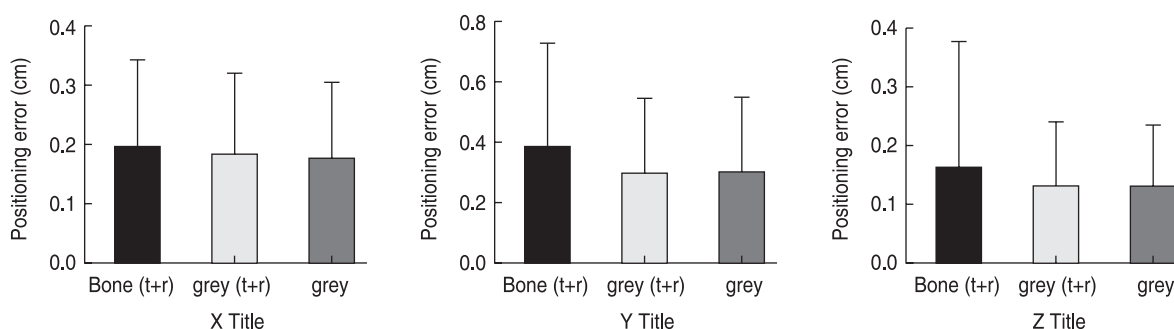


Fig. 1 Analysis of the difference of the positioning errors in the X, Y, and Z axis directions under the three registration methods

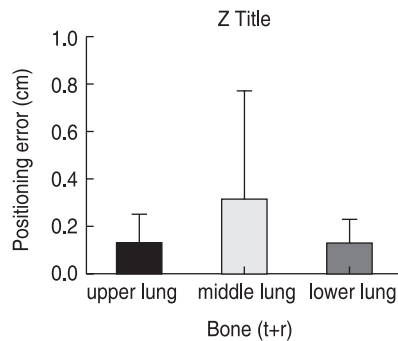


Fig. 2 The difference analysis of the positioning error in the Z-axis direction under the automatic bone registration method between different tumor sites

significantly larger than that of automatic gray-scale (t + r), and automatic gray-scale (t) registration ($P < 0.05$) (Fig. 3).

Discussion

Lung cancer is a common malignant tumor in the clinic and also ranks first for deaths among malignant tumors^[9]. Radiotherapy is one of the main treatment methods for patients with lung cancer and can effectively prevent local recurrence in patients. This treatment also plays a very important role in many aspects, such as improving the local control rate and improving the overall survival rate of patients^[10-11]. With the continuous development of radiotherapy equipment and technology, radiotherapy has entered the era of intensity-modulated radiotherapy for “accurate positioning, accurate planning, and accurate positioning”^[12]. Accurate measurement and correction of the target location and intra-fractional errors in tumor radiotherapy have gradually become the focus of domestic oncology and radiotherapy physicians, physicists, and technicians^[13]. Several studies^[14-16] have shown that movement of the centers of GTV95 and CTV95 by 5 mm can result in a dose change to the tumor as high as 21%. Thus, pre-radiotherapy positioning verification is critical. In the current postural standard of tumor radiotherapy: the allowable range of translation error is < 5 mm, the allowable range of rotation error is < 3 mm, and CBCT is an important means of positioning verification before radiotherapy. In the clinic, automatic registration is routinely used under CBCT guidance, with manual registration performed in individual special cases. Automatic registration is fast and simple, which not only saves time but also has high precision and has been unanimously adopted in the clinic. The two types of automatic registration methods—automatic bone registration and automatic grayscale registration—can be subdivided into automatic grayscale (t) registration and automatic grayscale registration.

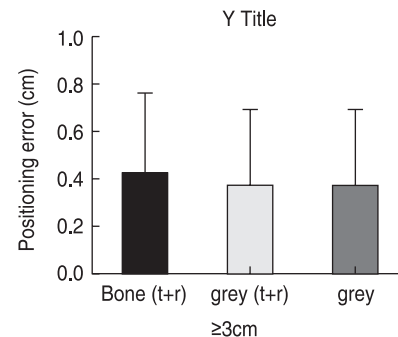


Fig. 3 Analysis of the difference in positioning errors in the Y-axis direction in the tumor ≥ 3 cm group under different registration methods

At present, there is no guideline for choosing the appropriate registration method in the clinic. This selection mainly depends on the experience and habits of radiotherapy doctors and physicists, and the registration method is randomized. To address this problem and provide a basis for a standardized registration model of lung cancer, we retrospectively analyzed the registration data of 80 patients with lung cancer undergoing radiotherapy. Our results showed that there was no statistical difference among the three registration methods in the X-, Y-, and Z-axes, but that automatic grayscale registration and automatic grayscale registration (t) showed a better trend than automatic bone registration. This result is consistent with the results reported by Li *et al.*^[17-18]. The reason for this finding may be related to the anatomical structure of chest tumors as lung cancer tissue is rich in soft tissue, the tissue is closely connected, and the relative position is relatively fixed, while the bony markers around the lung cancer tissue are less available for reference and have a large degree of displacement, are easily affected by posture and breathing, and are not fixed. In this study, considering the mediastinal anatomy, the use of grayscale registration appears to be more reasonable, and manual registration can be combined with manual registration if necessary^[19].

Domestic and foreign studies have identified tumor location as an important factor affecting the positioning error in patients undergoing radiotherapy for lung cancer^[20-22]. Our analysis of the influence of different tumor positions on positioning showed that a tumor location on the X-stroke Y-axis was not the key factor affecting positioning error. On the Z-axis, we observed no significant differences in registration errors between groups with different tumor sites using automatic gray level (t + r) and automatic gray (t) registration; however, for automatic bony registration, the difference in the value of the middle lung was the highest, while that of the upper and lower lung was low. This is consistent with the findings reported by Tan^[21]. The explanation for

this observation may be that tumors in the middle lung are affected by respiratory mobility to a certain extent; moreover, those adjacent to the heart are also affected by the heartbeat^[20–22]. Thus, the difference in the registration phase based on bony markers was greater than that of grayscale registration. Therefore, all three registration methods can be used for tumors of the upper and lower lung, while automatic bony registration should not be used if it can be avoided for tumors in the middle lung.

Furthermore, regarding the effects of tumor size on positioning, in the group with tumor size <3 cm, all three registration methods were available on the X-, Y-, and Z-axes; in contrast, in the group with tumor size > 3 cm group, both automatic gray (t + r) and automatic gray (t) registration on the Y-axis showed better results. Sarudis^[22] reported a correlation between tumor size and respiratory movement. The reason for this finding may be that the larger the tumor, the more likely it is to be affected by posture, respiratory degree, heartbeat, and diaphragm contraction. Moreover, the chest bone marks are less and easily affected; thus, the automatic bone matching error is larger. Therefore, the use of automatic grayscale registration is appropriate^[24–25].

The results of the present study showed that in lung cancer, automatic bony, automatic grayscale, and automatic grayscale (t) registration are recommended for tumors in the upper and lower lung measuring <3 cm, especially the latter two methods. For tumors located in the middle lung measuring <3 cm and tumors in the upper and lower lung measuring ≥3 cm, either automatic grayscale or automatic grayscale (t) registration can be used. This study included only two patients with middle lung tumors measuring ≥ 3 cm; thus, additional studies with larger sample sizes are needed.

Conflicts of interest

The authors indicated no potential conflicts of interest.

References

- Ren XC, Liu YE, Li J, *et al.* Progress in image-guided radiotherapy for the treatment of non-small cell lung cancer. *World J Radiol*, 2019, 11: 46–54.
- Prezzano KM, Ma SJ, Hermann GM, *et al.* Stereotactic body radiation therapy for non-small cell lung cancer: A review. *World J Clin Oncol*, 2019, 10: 14–27.
- Kulbida R, Mathes A, Loeser J. Beneficial effects of hirudotherapy in a chronic case of complex regional pain syndrome. *J Integr Med*, 2019, 17: 383–386.
- Coroller TP, Grossmann P, Hou Y, *et al.* CT-based radiomic signature predicts distant metastasis in lung adenocarcinoma. *Radiother Oncol*, 2015, 114: 345–350.
- Ren XC, Liu YE, Li J, *et al.* Progress in image-guided radiotherapy for the treatment of non-small cell lung cancer. *World J Radiol*, 2019, 11: 46–54.
- Zhang WT, Tong YH, Li Z, *et al.* Research on the setup error of 4D-CBCT applied to lung cancer SBRT. *J Med Theory Pract*, 2019, 32: 1346–1348.
- Peng J, Zhang Z, Wang J, *et al.* Is internal target volume accurate for dose evaluation in lung cancer stereotactic body radiotherapy? *Oncotarget*, 2016, 7: 22523–22530.
- Nabavizadeh N, Elliott DA, Chen Y, *et al.* Image guided radiation therapy (IGRT) practice patterns and IGRT's impact on workflow and treatment planning: results from a National Survey of American Society for Radiation Oncology Members. *Int J Radiat Oncol Biol Phys*, 2016, 94: 850–857.
- Ricco A, Hanlon A, Lanciano R. Propensity score matched comparison of intensity modulated radiation therapy vs stereotactic body radiation therapy for localized prostate cancer: a survival analysis from the National Cancer Database. *Front Oncol*, 2017, 7: 185.
- Cuomo JR, Sharma GK, Conger PD, *et al.* Novel concepts in radiation-induced cardiovascular disease. *World J Cardiol*, 2016, 8: 504–519.
- Li YC, Cheng PJ, Chen WJ, *et al.* Comparative study of positioning errors of two fixation techniques in stereotactic radiotherapy for lung cancer. *Chin J Oncol (Chinese)*, 2017, 44: 600–604.
- Li LP, Deng Y, Luo TG, *et al.* The role of precise posture fixation in image-guided radiotherapy of lung cancer. *Cancer Res Prev Treat*, 2018, 45: 758–761.
- Zhou AM, Deng XB, Xiong QQ. Efficacy of intensity-modulated conformal radiotherapy for lung cancer and its influence on left ventricular diastolic function. *Chin Med Innovat (Chinese)*, 2019, 16: 21–25.
- Thureau S, Dubray B, Modzelewski R, *et al.* FDG and FMISO PET-guided dose escalation with intensity-modulated radiotherapy in lung cancer. *Radiat Oncol*, 2018, 13: 208.
- Delishaj D, Ursino S, Pasqualetti F, *et al.* Set-up errors in head and neck cancer treated with IMRT technique assessed by cone-beam computed tomography: a feasible protocol. *Radiat Oncol J*, 2018, 36: 54–62.
- Rozema R, Doff MH, van Ooijen PM, *et al.* Diagnostic reliability of low dose multidetector CT and cone beam CT in maxillofacial trauma-an experimental blinded and randomized study. *Dentomaxillofac Radiol*, 2018, 47: 20170423.
- Li Y, Ma JL, Chen X, *et al.* 4DCT and CBCT based marginin Stereotactic Body Radiotherapy (SBRT) of nonsmallcell lung tumor adhered to chest wall or diaphragm. *Radiat Oncol*, 2016, 11: 152.
- Shang K, Chi ZF, Wang J, *et al.* Analysis of setup error in IGRT of thoracic esophageal carcinoma. *Chin J Radiat Oncol (Chinese)*, 2015, 24: 70–73.
- Li QR, Chen JX, Ding DQ, *et al.* Analysis of registration error of CBCT images of lung cancer by different personnel. *Pract J Cancer*, 2018, 33: 1245–1248.
- Wang S, Shang D, Meng X, *et al.* Effects of respiratory motion on volumetric and positional difference of GTV in lung cancer based on 3DCT and 4DCT scanning. *Oncol Lett*, 2019, 17: 2388–2392.
- Sarudis S, Karlsson Hauer A, Nyman J, *et al.* Systematic evaluation of lung tumor motion using four-dimensional computed tomography. *Acta Oncol*, 2017, 56: 525–530.
- Tan KV, Thomas R, Hardcastle N, *et al.* Predictors of respiratory-induced lung tumour motion measured on four-dimensional computed tomography. *Clin Oncol (R Coll Radiol)*, 2015, 27: 197–204.
- Xing XF, Meng HM, Cui T, *et al.* Research on the displacement and volume changes of lung tumors during breathing exercise based on four-dimensional CT. *Shanxi Med J (Chinese)*, 2016, 45: 1763–1765.
- Sun XH, Tan LN, Wang ZF, *et al.* Feasibility study of cone-beam

- CT online registration based on target volume in stereotactic body radiotherapy for lung cancer. *Chin J Med Phy (Chinese)*, 2019, 36: 282.
25. Ren XC, Liu YE, Li J, *et al.* Progress in image-guided radiotherapy for the treatment of non-small cell lung cancer. *World J Radiol*, 2019, 11: 46–54.

DOI 10.1007/s10330-021-0499-9

Cite this article as: Du JY, Tang J, Zhang Q, *et al.* Cone beam computed tomography-guided differences among registration methods for lung cancer and the effects of tumor position, treatment model, and tumor size on positioning errors. *Oncol Transl Med*, 2021, 7: 203–208.

Ultrasound-guided No Touch liver pedicle microwave ablation in hepatocellular carcinoma treatment

Dan Wang¹, Shu Zhu¹, Peng Zhu², Yi Cheng³, Hongchang Luo¹, Jianhua Wang³ (✉)

¹ Department of Medical Ultrasound, Tongji Hospital, Tongji Medical College, Huazhong University of Science and Technology, Wuhan 430030, China

² Hepatic Surgery Center, Tongji Hospital, Tongji Medical College, Huazhong University of Science and Technology, Wuhan 430030, China

³ Department of Oncology, Tongji Hospital, Tongji Medical College, Huazhong University of Science and Technology, Wuhan 430030, China

Abstract

Objective This study aimed to investigate the feasibility, safety, and clinical effect of No Touch liver pedicle microwave ablation (NTLP-MWA).

Methods The outcomes of 118 patients diagnosed with hepatocellular carcinoma (HCC) between 2014 and 2015 were retrospectively analyzed. Patients were divided into three groups. In group A, 35 patients underwent ultrasound-guided NTLP-MWA, 27 in Group B were treated with routine microwave ablation (RMWA), and 56 in group C underwent anatomic hepatectomy (AH). The preoperative basic data, intraoperative data, and postoperative data were analyzed among the three groups.

Results The treatment time, intraoperative blood loss, and postoperative liver function (alanine transaminase) in the NTLP-MWA and RMWA groups were significantly different from those in the AH group (all $P < 0.005$). There was no difference in the complete elimination rate and local recurrence within 1 year among the three groups. Treatment was not an independent risk factor for early postoperative recurrence. There was no significant difference in the 5-year overall survival rates among the three groups.

Conclusion NTLP-MWA is safe and reliable, in accordance with the principles of oncology treatment, and worth further promotion in clinical practice.

Key words: ultrasonic guidance; hepatocellular carcinoma; microwave ablation; liver pedicle

Received: 15 July 2021

Revised: 21 August 2021

Accepted: 16 September 2021

Hepatocellular carcinoma (HCC) is one of the five most common malignancies in the world, ranking first in cancer incidence and mortality in China (Chen *et al.* 2014). In some parts of Asia, HCC is the most common cause of cancer-related deaths. The incidence of HCC is increasing significantly in European and American countries (Tan *et al.* 2018). Currently, more than 500,000 new cases are diagnosed each year. China has a high incidence of HCC. According to the World Cancer Report released by the World Health Organization in 2014, China accounts for half of the new cases of HCC and more than half of the total deaths globally (McGuire, 2015).

Therefore, the treatment of HCC has attracted increasing attention worldwide. Surgical treatment has

always been considered the primary treatment for HCC. However, most patients cannot be treated surgically because of tumor anatomical location, tumor size, tumor number, insufficient liver residue, and extrahepatic metastasis. Meanwhile, non-surgical treatment is currently available for most patients with HCC. With the development of medical technology and equipment, it is necessary to regenerate therapeutic strategies for HCC.

In recent years, topical ablation has rapidly developed. Owing to the advantages of minimally invasive, repeatable, real-time monitoring, and high clinical compliance, ultrasound-guided ablation of HCC has become the third major treatment method for HCC after anatomic hepatectomy (AH) and interventional

✉ Correspondence to: Jianhua Wang. Email: superman.4812@163.com

© 2021 Huazhong University of Science and Technology

treatment (Feng *et al.* 2014; Abdelsalam *et al.* 2016; Xu *et al.* 2018). However, for lesions with a diameter between 2 and 5 cm, the conventional multi-antenna and multi-point acupuncture treatment in a polyhedral geometric model is likely to cause residual lesions, leading to incomplete ablation (Berber. 2016; Zaidi *et al.* 2016; Lee *et al.* 2017; Long *et al.* 2016). No touch liver pedicle microwave ablation (NTLP-MWA) is a new method of topical ablation. Before the ablation of the lesion, the hepatic pedicle of the liver segment or subsegment, where the lesion was located, was first destroyed to prevent the metastasis of tumor cells along the portal system. This study aimed to investigate the feasibility, safety, and clinical applications of NTLP-MWA by comparing the outcomes of NTLP-MWA, routine microwave ablation (RMWA) and AH.

Materials and methods

Study population

This study was approved by the institutional review board of Tongji Hospital. Written informed consent was obtained from all the patients. Consecutive, unrelated adult patients ($n=118$, 97 for men; mean age, 56.77 ± 11.08 years) who were treated in the Tongji hepatic surgery center between January 2014 and December 2015 were retrospectively studied if they fulfilled the standard diagnostic criteria for HCC.

Microwave ablation would be administered if the patients did not meet the surgical guidelines, or did not wish to undergo surgical treatment. NTLP-MWA was administered to patients with lesions located in one segment, and the liver pedicle was evident on preoperative ultrasound examination or CT scan. Patients were divided into three groups. In group A, 35 patients underwent ultrasound-guided NTLP-MWA, 27 in group B were treated with RMWA, and 56 in group C underwent AH.

All enrolled patients were required to meet the following conditions: (1) Preoperative diagnoses based on the guidelines of the American Association for the Study of Liver Diseases, and all lesions presented typical manifestations on contrast-enhanced ultrasound, contrast-enhanced CT scan, or magnetic resonance imaging: hyperenhancement in arterial phase, rapid wash-out in portal/late phase; (2) Patients had no vascular infiltration, liver function Child-Pugh class A, American Society of Anesthesiologists score of 2 or less, ICG-R15 less than 15%; (3) Preoperative imaging examination confirmed a single lesion with a diameter of 2–5 cm; (4) The lesion located in a certain liver segment or a sub-hepatic segment; and (5) All patients signed informed consent before treatment. The study was performed in accordance with the Declaration of Helsinki and the ethical guidelines for clinical studies of the local ethics

committee. Patients were excluded if they had obvious portal vein tumor thrombus, distant metastasis, multiple lesions, or a lesion diameter less than 2 cm or greater than 5 cm.

In our study, the basic preoperative data (age, sex, lesion size, alpha-fetoprotein [AFP] level, etc.), operative materials (treatment time, intraoperative blood loss), and postoperative data (postoperative liver function indicators, complications, local recurrence rate, and overall survival rate) of the three groups of patients were observed.

Microwave ablation

Imaging was performed with an Esaote MyLab™ ClassC ultrasound machine (Esaote, Genova, Italy), using an IOT342 appleprobe in open hepatectomy and an LP323 probe in laparoscopic hepatectomy. The probe frequency was 4–10 MHz, and the LP323 probe angle could be up/down 90° and right/left 90° through the two adjustment rods at the tail. Ablation was performed with a model ECO-100A1 microwave tumor ablation system (ECO, Nanjing, China) with a frequency of 2450 MHz, an output power of 0–150 W, and an ECO-100AI8 disposable microwave ablation antenna.

NTLP-MWA

The patients in group A underwent ultrasound-guided NTLP-MWA. Preoperative imaging data of the patients were fully analyzed to assess the route of the hepatic segment or subsegmental pedicle where the lesion was located. During the ablation, conventional ultrasound or laparoscopic ultrasound was first used to insert the microwave antenna into the hepatic pedicle of the liver segment or subsegment where the lesion was located without touching the tumor through the skin, and then the hepatic pedicle was damaged. The power of the microwave tumor ablation system was 60 W, and the duration of single ablation was 4 min. The microwave antenna was then inserted into the lesion and placed in an appropriate position for ablation. The ablation range of the tumor was ensured to be covered by a single antenna multiple times or multiple-antenna single time. The microwave tumor ablation system had a power of 60 W and a single ablation time of 6 min. The actual total ablation time was based on the lesion size. After treatment, the microwave antenna was slowly removed. When approaching the liver capsule, the power was turned on again, and the antenna passage was cauterized to prevent tumor metastasis and bleeding in the antenna passage.

RMWA

RMWA was performed directly in group B. Before ablation, the position and size of the lesion were fully

understood, and the position adjacent to the surrounding important blood vessels and pipelines was designed. Two or three ablation antennas were placed at a spacing of 1–1.5 cm simultaneously, or one ablation antenna was inserted in different positions of the lesion multiple times at intervals of 1–1.5 cm each until the lesion was completely damaged. The ablation range was superimposed on each other in geometric shapes to ensure that the overall ablation range covered the lesion and the surrounding normal liver tissues by approximately 1 cm, and the ablation time and power of each ablation were consistent with those of group A.

Anatomic hepatectomy

AH refers to the complete removal of the hepatic segments supplied by the portal vein and major branches of the hepatic artery surrounding the lesion. Surgery was classified according to Couinaud’s conventional terminology from eight segments of the liver (Couinaud, 1986). Dissection of one or more segments: five segments, extended hepatectomy; Four segments, lobectomy (right hepatectomy); Three segments, left hepatectomy (lobectomy); central hepatectomy, two sections; left lateral segment resection, right anterior or posterior sector resection; and one segment, a wedge resection (Inoue, 2012; Liu *et al.* 2019). Intraoperative ultrasound was used to detect lesion size and location, ruling out any lesions undiscovered in preoperative image evaluation, information about hepatic vascular structures, and location of the lesion in the liver segment that was resected. The Glisson system of the corresponding liver segment or subsegment was selected after dissecting the first hilum or the liver parenchyma, and clipping and dissecting the liver parenchyma along the ischemic line on the liver surface, followed by the dissection of the corresponding liver segment. The Pringle method was used to block the first hilum during the liver parenchyma

dissection procedure (Pringle, 1908).

Statistical analysis

Statistical analyses were performed using Statistical Package for the Social Sciences ver. 25 software (IBM Corp., Armonk, NY, USA). Quantitative data are expressed as mean±standard error of the mean. Statistical analysis was performed using analysis of variance followed by the Tukey-Kramer multiple comparisons test or unpaired two-tailed Student’s *t*-test. Percentages were compared using the chi-squared test or Fisher’s exact test. Multivariate logistic regression analysis was performed on the clinical indicators with statistical differences in univariate analysis to calculate the OR value of each independent risk factor. Statistical significance was set at *P* < 0.05. The Kaplan-Meier method was used to establish the survival curves of the three groups.

A patient was considered lost to follow-up if the last information available was older than 3 months with a total follow-up duration of < 5 years. To estimate the time of OS, the last follow-up assessment or death was measured from the date of treatment.

Results

Patient characteristics and follow-up

Between January 2014 and December 2015, 118 patients were treated in the Tongji Hepatic Surgery Center were divided into 3 groups. The background demographic patient characteristics including sex, age, underlying diseases (history of hypertension, diabetes, or hepatitis), tumor size, cirrhosis, Child-Pugh score, AFP, and liver function, are listed in Table 1.

During the 5-year follow-up, seven patients (5.93%) were lost to follow-up: two in the NTLP-MWA group, five in the AH group, and none in the RMWA group.

Table 1 Baseline characteristics

Variables	Variables			χ ² /F	P
	NTLP-MWA (n=35)	RMWA (n=27)	AH (n=56)		
Gender					
Male	29	22	46	0.020	0.990
Female	6	5	10		
Age	59.80 ± 11.26	56.04 ± 13.11	55.77 ± 11.08	1.940	0.148
Diabetes	4	3	6	0.012	0.994
Hypertension	15	12	27	0.274	0.872
Cirrhosis	27	20	44	0.209	0.901
Tumor size	2.72 ± 0.58	2.78 ± 0.53	2.67 ± 0.44	1.447	0.240
AFP	638.26 ± 1356.76	218.91 ± 393.06	945.06 ± 5121.29	0.371	0.691
pre-ALT	36.91 ± 30.83	29.81 ± 12.17	32.95 ± 18.79	0.818	0.444

NTLP-MWA, No Touch liver pedicle microwave ablation; RMWA, routine microwave ablation; AH, anatomic hepatectomy; AFP, Alpha-fetoprotein; ALT, Alanine aminotransferase

Table 2 Comparison of treatment effect

Group	Patients	Operation time (min)	Intraoperative bleeding (mL)	post-ALT-1d	post-ALT-3d
NTLP-MWA	35	29.91 ± 5.71	15.86 ± 3.53	108.89 ± 92.97	44.49 ± 35.48
RMWA	27	21.00 ± 4.53	14.44 ± 3.49	132.15 ± 68.02	38.19 ± 16.42
AH	56	136.86 ± 9.24	213.13 ± 103.16	141.31 ± 92.70	65.52 ± 45.61
<i>F</i>		3291.869	713.000	4.512	4.383
<i>P</i>		0.000	0.000	0.013	0.015

NTLP-MWA, no Touch liver pedicle microwave ablation; RMWA, routine microwave ablation; AH, anatomic hepatectomy; ALT, Alanine aminotransferase

Comparison of treatment characteristics

Comparing the 3 groups, the median treatment time in the NTLP-MWA group, RMWA group and AH group was 29.91 min (IQR: 24.20–35.62), 21.00 min (IQR: 16.47–25.52), 136.86 min (IQR: 127.62–146.10), respectively. The treatment time in the NTLP-MWA and RMWA groups was significantly shorter than that in the AH group. The intraoperative blood loss in the NTLP-MWA, RMWA, and AH group were 15.86 mL (IQR: 12.33–19.39), 14.44 mL (IQR: 10.95–17.93), 213.13 mL (IQR: 109.97–316.29), respectively. The blood loss in the AH group was significantly higher than that in the NTLP-MWA and RMWA groups. The levels of alanine transaminase in the NTLP-MWA and RMWA groups was lower than that in the AH group on the 1st and 3rd day after treatment (Table 2).

Comparison of postoperative recurrence and survival rate

Reexamination 1 month after the treatment showed no residual lesion in the NTLP-MWA and AH groups, and the complete ablation rate was 100%. In the RMWA

group, one patient had residual lesions, with a complete ablation rate of 96.30%. However, the difference was not statistically significant ($P = 0.183$).

After 1 year of follow-up, a total of 5 patients were lost to follow-up, including two in the NTLP-MWA group and three in the AH group. Five patients relapsed, including 2/33 (6.61%) in the NTLP-MWA group, 2/27 (7.41%) in the RMWA group, and 1/53 (1.89%) in the AH group. No patient died in any of the groups. The local recurrence rate of the AH group was lower than that of the NTLP-MWA and RMWA groups, but the difference was not statistically significant ($P = 0.453$). Univariate analysis showed that treatment was not a risk factor for early recurrence after surgery (Table 3). Logistic multivariate analysis showed that tumor lesions, differentiation degree, and AFP were closely related to early postoperative recurrence, but treatment was not an independent risk factor for early postoperative recurrence (Table 4).

At the end of the 5-year follow-up period, a total of seven patients were lost, including two in the NTLP-MWA group and five in the AH group. The 5-year overall survival rates of the NTLP-MWA, RMWA, and AH groups were 48.48% (16/33), 44.44% (12/27), and 47.06% (24/51), respectively. The overall survival rate of the NTLP-MWA group was slightly higher than that of the other two groups, but the difference was not statistically

Table 3 Comparison of local treatment and recurrence

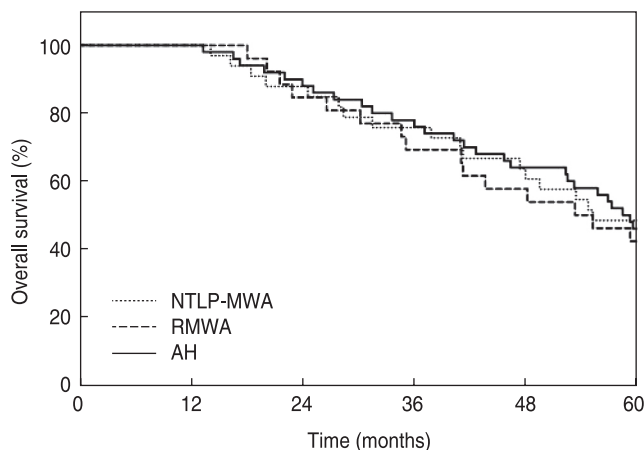
Group	1 month		1 year	
	Local residual	Non-residue	Local residual	Non-residue
NTLP-MWA	0	33	2	31
RMWA	1	26	2	25
AH	0	56	1	52
χ^2	3.399		1.584	
<i>P</i>	0.183		0.453	

NTLP-MWA, no Touch liver pedicle microwave ablation; RMWA, routine microwave ablation; AH, anatomic hepatectomy

Table 4 Multivariate analysis of risk factors for recurrence after 1 year

Group	<i>P</i>	HR (95%CI)
NTLP-MWA (vs. AH)	0.331	29.91 ± 5.71
RMWA (vs. AH)	0.254	21.00 ± 4.53
Tumor size < 3 cm (vs. ≥ 3 cm)	0.046	136.86 ± 9.24
Well tumor differentiation (vs. poor or moderate)	0.046	3291.869
AFP < 400 (vs. ≥ 400)	0.033	0.000

NTLP-MWA, no Touch liver pedicle microwave ablation; RMWA, routine microwave ablation; AH, anatomic hepatectomy; AFP, Alpha-fetoprotein

**Fig. 1** Comparison of 5-year overall survival of three groups

significant ($P = 0.952$) (Fig. 1).

Adverse events

The incidence of complications in the NTLP-MWA and RMWA groups was lower than that in the AH group ($P < 0.05$). No serious complications were found in any of the patients in the two groups during and after treatment, whereas there were different degrees of subxiphoid process pain, right shoulder, and upper arm radial acid distension. In the NTLP-MWA group, two patients had a small amount of peritoneal effusion, and three had pleural effusion. Among them, one patient had pleural effusion and a small amount of peritoneal effusion due to the lesion's proximity to the top of the diaphragm. In the RMWA group, three patients developed pleural effusion, and the complication rate was 11.11% (3/27). In the AH group, all patients reported postoperative incision pain, two cases of liver limitation wound effusion, 12 cases of abdominal cavity effusion, and 15 cases of pleural effusion, including 10 patients simultaneously, appeared as pleural effusion and peritoneal effusion, two cases of hepatic limitations wound effusion, and five with pleural effusion puncture pumping liquid treatment, and the complication rate was 33.93% (19/56).

Discussion

Hepatocellular carcinoma (HCC) is one of the most common digestive tract malignancies in China (Chen *et al.* 2016). With the widespread use of radiological techniques in HCC, an increasing number of HCC patients are now diagnosed at an early stage. Thermal ablation, mainly microwave ablation and radiofrequency ablation, has achieved satisfactory results in the treatment of HCC. Previous studies have shown that 70% of very early-stage HCC patients can achieve a similar 5-year survival rate with thermal ablation and hepatectomy. Several studies have compared the outcomes of radiofrequency ablation (RFA) and hepatectomy and have recommended that RFA be the preferred approach, even if HCC can be removed (Liu *et al.* 2016; Pompili *et al.* 2015; Xu *et al.* 2017). Microwave ablation has a higher ablation frequency, faster heat production, higher internal temperature of the tumor, larger ablation range, shorter ablation time, and easy control of the thermal field. Because it can directly lead to coagulation necrosis of the tumor, microwave ablation has the advantages of being minimally invasive, safe, and repeatable. It is one of the treatment options chosen by the majority of doctors and patients (Lee *et al.* 2014; Cavagnaro *et al.* 2019; Stauffer *et al.* 2003). When the diameter of the HCC was greater than 3 cm, the size of the tumor was irregular, the capsular can be interrupted, and the tumor tissue gasification during the ablation process is serious. Consequently, hyperechoic

with fuzzy boundaries appear in the ablation foci and surrounding areas, which can easily cause ablation leakage and lead to residual lesions (Xu *et al.* 2017; Galanakis *et al.* 2018). Based on these shortcomings, for lesions of larger diameters, microwave ablation can be combined with multiple antennas to significantly expand the ablation volume (Violi *et al.* 2018; Facciorusso *et al.* 2016; Laeseke *et al.* 2009), so that microwave ablation has greater advantages. However, it should be noted that when the lesion volume is large, multi-antenna ablation is performed. The multi-point antenna placement method is susceptible to potential incomplete ablation due to the influence of the lesion location and the doctor's experience in antenna placement, which may lead to tumor recurrence or metastasis.

HCC cells form microinfiltration in the tumor-bearing segment of the liver in several ways: 1) invading the portal system and spreading to the distal end, 2) causing an arteriovenous short circuit to the central countercurrent of the portal vein; and 3) blocking the central countercurrent of the portal vein by tumor thrombus. AH is the first choice for the treatment of HCC by exposing the landmark vascular structure of the liver segment where the lesion is located, ligating the severed hepatic pedicle, and simultaneously removing the lesion and the liver segment to reduce the risk of recurrence of postoperative microfiltration and maximize the volume of the functional liver. The criterion for successful surgery is the treatment of the hepatic pedicle (Zhao *et al.* 2020; Shindoh *et al.* 2016; Li *et al.* 2016).

NTLP-MWA is a combination of routine microwave ablation and management of the hepatic pedicle, which is the key point in AH. First, we should find the hepatic pedicle of the liver segment where the lesion is located. To achieve the effect of ligation and dissociation of the hepatic pedicle in AH, to avoid the metastasis of tumor cells via the portal vein and adhere to the principles of oncology treatment, the first antenna was used to conduct thermal destruction of the hepatic pedicle without contact with the lesion, while the second antenna was used to conduct thermal ablation of the lesion (Fig. 2).

By comparing AH and RMWA, we analyzed the operation time, intraoperative bleeding volume, postoperative complications, postoperative liver function, 1-year local recurrence rate, and overall survival rate of the 118 patients in our study. The NTLP-MWA group and RMWA group compared with the AH group had significantly reduced blood loss, shortened the operation time, and had less influence on the patients, and patients recovered faster after treatment. Compared with the RMWA group, the NTLP-MWA group exhibited less residual tumor tissue and more complete ablation. There were no statistically significant differences in the 1-year and overall survival rates among the three groups.

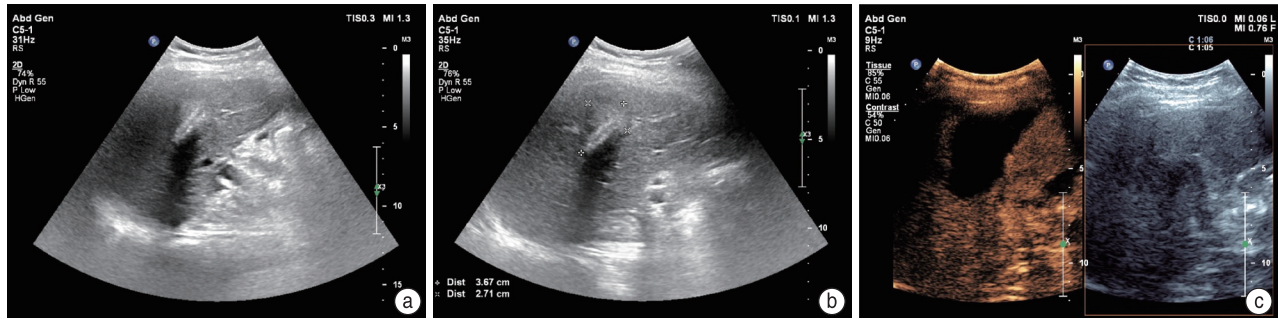


Fig. 2 (a) The lesion was located Segment III of the liver; (b) Two-dimensional sonogram of the lesion after No Touch hepatic pedicle microwave ablation; (c) Postoperative contrast-enhanced ultrasonography showed no contrast agent filling in Segment III of liver

However, it is worth mentioning that the absolute number of patients with local recurrence was higher in both the microwave ablation group and the conventional microwave ablation group than in the hepatectomy group. Our study shows that the NTPL-MWA is an effective and safe treatment. The complete ablation rate for HCC was 100%. There were no significant or serious complications, and a small amount of pleural effusion and peritoneal effusion were acceptable in some patients. In this study, there were two cases of local recurrence within 1 year in the NTPL-MWA group. The authors believe that there are the following reasons: (1) There may be multiple portal vessels supplying blood to the tumor-bearing hepatic segment; (2) In the early stage of the study, the injection accuracy was insufficient or the ablation time was short, and the ablation of the hepatic pedicle was incomplete. To achieve the best ablation effect, it is important to conduct a detailed preoperative imaging evaluation. By comparing the preoperative ultrasound, CT, and magnetic resonance imaging, the vessels in the liver segment where the lesion is located can be identified to avoid loss of the vessels in the hepatic pedicle or the retention of the pedicle during the operation. During the ablation, precise antenna insertion was needed, the optimal route was chosen to avoid the lesion, and the microwave antenna was inserted into the target liver pedicle precisely. In these ways, we could shorten the duration of the microwave ablation and reduce the damage range. When the power was increased to 60 W and microwave ablation was performed for 4 min, the insertion site of the microwave antenna was approximately 2 cm away from the bifurcation of the hepatic pedicle. The ablation achieved satisfactory results and avoided damage to adjacent important structures.

Limitations

A limitation of our study is its retrospective nature. Another limitation is that it was a single-center study without incorporating the results from other centers, and the results may not be comparable to those obtained from other centers. However, a single-center study can avoid

such technical differences.

This study also has the following limitations: because hepatic pedicle microwave ablation is a new minimally invasive technique, the research time is shorter, and no touch technique cannot be used for ablation of some lesions in special sites, which are supplied by multiple branches of the hepatic pedicle. Moreover, the number of cases near the hepatic hilum, diaphragmatic roof, or adjacent large vessels was small. More cases will be included in future studies to extend the follow-up period to achieve more accurate comparative results.

Conclusions

To our knowledge, NTPL-MWA is a new local ablation technique. This new method has great potential in clinical applications, which can reduce the amount of surgical bleeding, shorten the operation time, have less influence on the liver function, and aid faster recovery after surgery. Further research is expected to contribute to its extensive clinical application.

Conflicts of interest

The authors indicated no potential conflicts of interest.

References

1. Chen WQ, Sun KX, Zheng RS, *et al.* Cancer incidence and mortality in China, 2014. *Chin J Cancer Res*, 2018, 30: 1–12.
2. Tan YH, Jiang JY, Wang Q, *et al.* Radiofrequency ablation using a multiple-electrode switching system for hepatocellular carcinoma within the Milan criteria: long-term results. *Int J Hyperthermia*, 2018, 34: 298–305.
3. McGuire S. World cancer report 2014. Geneva, Switzerland: World Health Organization, International Agency for Research on Cancer, WHO Press, 2015. *Adv Nutr*, 2016, 7: 418–419.
4. Feng K, Ma KS. Value of radiofrequency ablation in the treatment of hepatocellular carcinoma. *World J Gastroenterol*, 2014, 20: 5987–5998.
5. Abdelsalam ME, Murthy R, Avritscher R, *et al.* Minimally invasive image-guided therapies for hepatocellular carcinoma. *J Hepatocell Carcinoma*, 2016, 3: 55–61.
6. Xu XL, Liu XD, Liang M, *et al.* Radiofrequency ablation versus hepatic

- resection for small hepatocellular carcinoma: systematic review of randomized controlled trials with meta-analysis and trial sequential analysis. *Radiology*, 2018, 287: 461–472.
7. Berber E. Laparoscopic microwave thermosphere ablation of malignant liver tumors: an initial clinical evaluation. *Surg Endosc*, 2016, 30: 692–698.
 8. Zaidi N, Okoh A, Yigitbas H, *et al*. Laparoscopic microwave thermosphere ablation of malignant liver tumors: an analysis of 53 cases. *J Surg Oncol*, 2016, 113: 130–134.
 9. Lee KF, Wong J, Hui JW, *et al*. Long-term outcomes of microwave versus radiofrequency ablation for hepatocellular carcinoma by surgical approach: A retrospective comparative study. *Asian J Surg*, 2017, 40: 301–308.
 10. Long J, Zheng JS, Sun B, *et al*. Microwave ablation of hepatocellular carcinoma with portal vein tumor thrombosis after transarterial chemoembolization: a prospective study. *Hepatol Int*, 2016, 10: 175–184.
 11. Couinaud C. Surgical anatomy of the liver. Several new aspects. *Chirurgie*, 1986, 112: 337–342.
 12. Inoue Y, Hayashi M, Komeda K, *et al*. Resection margin with anatomic or nonanatomic hepatectomy for liver metastasis from colorectal cancer. *J Gastrointest Surg*, 2012, 16: 1171–1180.
 13. Liu JX, Zhang YF, Zhu H, *et al*. Prediction of perioperative outcome after hepatic resection for pediatric patients. *BMC Gastroenterol*, 2019, 19: 201.
 14. Pringle JH. V. Notes on the arrest of hepatic hemorrhage due to trauma. *Ann Surg*, 1908, 48: 541–549.
 15. Chen WQ, Zheng RS, Baade PD, *et al*. Cancer statistics in China, 2015. *CA Cancer J Clin*, 2016, 66: 115–132.
 16. Liu PH, Hsu CY, Hsia CY, *et al*. Surgical resection versus radiofrequency ablation for single hepatocellular carcinoma ≤ 2 cm in a propensity score model. *Ann Surg*, 2016, 263: 538–545.
 17. Pompili M, De Matthaeis N, Saviano A, *et al*. Single hepatocellular carcinoma smaller than 2 cm: are ethanol injection and radiofrequency ablation equally effective? *Anticancer Res*, 2015, 35: 325–332.
 18. Xu Y, Shen Q, Wang N, *et al*. Microwave ablation is as effective as radiofrequency ablation for very-early-stage hepatocellular carcinoma. *Chin J Cancer*, 2017, 36: 14.
 19. Lee DH, Lee JM, Lee JY, *et al*. Radiofrequency ablation of hepatocellular carcinoma as first-line treatment: long-term results and prognostic factors in 162 patients with cirrhosis. *Radiology*, 2014, 270: 900–909.
 20. Cavagnaro M, Pinto R, Lopresto V. Phantoms in hyperthermia and thermal ablation applications at microwave frequencies: a review. In 2019 European Microwave Conference in Central Europe (EuMCE) 2019 May 13 (pp. 538–541). IEEE.
 21. Stauffer PR, Rossetto F, Prakash M, *et al*. Phantom and animal tissues for modelling the electrical properties of human liver. *Int J Hyperthermia*, 2003, 19: 89–101.
 22. Xu Y, Shen Q, Wang N, *et al*. Percutaneous microwave ablation of 5–6 cm unresectable hepatocellular carcinoma: local efficacy and long-term outcomes. *Int J Hyperthermia*, 2017, 33: 247–254.
 23. Galanakis N, Kehagias E, Matthaiou N, *et al*. Transcatheter arterial chemoembolization combined with radiofrequency or microwave ablation for hepatocellular carcinoma: a review. *Hepat Oncol*, 2018, 5: HEP07.
 24. Vietti Violi N, Duran R, Guiu B, *et al*. Efficacy of microwave ablation versus radiofrequency ablation for the treatment of hepatocellular carcinoma in patients with chronic liver disease: a randomised controlled phase 2 trial. *Lancet Gastroenterol Hepatol*, 2018, 3: 317–325.
 25. Facciorusso A, Di Maso M, Muscatiello N. Microwave ablation versus radiofrequency ablation for the treatment of hepatocellular carcinoma: A systematic review and meta-analysis. *Int J Hyperthermia*, 2016, 32: 339–344.
 26. Laeseke PF, Lee FT Jr, Sampson LA, *et al*. Microwave ablation versus radiofrequency ablation in the kidney: high-power triaxial antennas create larger ablation zones than similarly sized internally cooled electrodes. *J Vasc Interv Radiol*, 2009, 20: 1224–1229.
 27. Zhao H, Ding WZ, Wang H, *et al*. Prognostic value of precise hepatic pedicle dissection in anatomical resection for patients with hepatocellular carcinoma. *Medicine*, 2020, 99: e19475.
 28. Shindoh J, Makuuchi M, Matsuyama Y, *et al*. Complete removal of the tumor-bearing portal territory decreases local tumor recurrence and improves disease-specific survival of patients with hepatocellular carcinoma. *J Hepatol*, 2016, 64: 594–600.
 29. Li XQ, Liu S, Li H, *et al*. Proper hepatic pedicle clamping during hepatectomy is associated with improved postoperative long-term prognosis in patients with AJCC stage IIIB hepatocellular carcinoma. *Oncotarget*, 2016, 7: 24623–24632.

DOI 10.1007/s10330-021-0514-4

Cite this article as: Wang D, Zhu S, Zhu P, *et al*. Ultrasound-guided No Touch liver pedicle microwave ablation in hepatocellular carcinoma treatment. *Oncol Transl Med*, 2021, 7: 209–215.

SMARCC1* copy number variation is related to metastatic colon cancer: an investigation based on TCGA data

Libo Feng¹, Yu Liu², Dong Xia¹, Xiaolong Chen¹ (✉)

¹ Department of Gastrointestinal Surgery, Southwest Medical University, Luzhou 646000, China

² Department of Electrocardiogram, Affiliated Hospital of Southwest Medical University, Luzhou 646000, China

Abstract

Objective There are no well-defined genetic indicators for distant metastatic illness in patients with colon cancer (CC). The discovery of genetic changes linked to metastatic CC might aid in the development of systemic and local therapeutic approaches. Using The Cancer Genome Atlas (TCGA), we examined the relationship between copy number variation (CNV) of SWI/SNF-related matrix-associated actin-dependent regulator of chromatin subfamily C member 1 (*SMARCC1*) and distant metastatic illness in patients with CC.

Methods Genetic sequencing data of all relevant CC patients and clinical features were collected from TCGA using R. There were 506 CC patients with CNV and clinical outcome data. The CNV of *SMARCC1* was examined for its correlation with distant metastatic disease using the TCGA CC dataset (M1 vs. M0). After adjusting for age, sex, T stage, N stage, adjuvant chemotherapy, microsatellite instability (MSI), and surgical margin status, univariate and multivariate logistic regression analyses were performed.

Results *SMARCC1* CNV was linked to distant metastatic disease ($P = 0.012$ and 0.008 in univariate and multivariate analysis, respectively); positive lymph nodes and margin status were also associated with distal metastases (all $P < 0.01$). MSI, T stage, N stage, adjuvant treatment, sex, race, and MSI were not associated with metastases (all $P > 0.05$).

Conclusion *SMARCC1* CNV is associated with distant metastatic disease in patients with CC. In individuals with CC, such genetic profiles might be utilized therapeutically to support optimal systemic treatment options against local treatments for CC, such as radiation therapy, pending additional confirmation.

Key words: colon cancer (CC); copy number variation (CNV); genetic marker

Received: 9 September 2021

Revised: 21 September 2021

Accepted: 5 October 2021

According to Global Cancer Statistics (Globocan 2018), led by the International Agency for Research on Cancer (IARC) of the World Health Organization (WHO), the worldwide incidence of newly developed colorectal cancer (CRC) in 2018 was approximately 1.85 million, making it the 3rd most common malignant tumor. Approximately 880,000 died of CRC, making it the 2nd most common cause of cancer-related deaths^[1]. In addition, around 20% of all current patients with CRC have distant metastatic illness^[1]. Despite advancements in screening and therapy, patients with CRC still have a poor 5-year overall survival rate^[1]. Some genes linked to the existence and progression of CRC, as well as treatment response indicators, have been identified^[2–4]; however, genetic markers linked to metastatic CRC are

still lacking. Surgical resection, chemotherapy, radiation, and targeted therapy may be applied in the treatment of CRC depending on the stage and location of the original tumor. In individuals with rectal adenocarcinoma, radiation treatment improves local control and overall survival^[5]. Copy number variation (CNV) is caused by genome rearrangement and refers to an increase or decrease in the copy number of large genome fragments with lengths of more than 1 kb, mainly showing deletion and duplication at the submicroscopic level^[6–7]. CNV is an important component of the structural variation (SV) of the genome. The mutation rate of CNV sites is much higher than that of single nucleotide polymorphisms (SNPs), which are an important pathogenic factor in human disease^[6].

Correspondence to: Xiaolong Chen. Email: 1870747218@qq.com

* Supported by a grant from the Joint Project of Southwest Medical University-Three Affiliated Hospitals (No. 2017-ZRQN-028).

© 2021 Huazhong University of Science and Technology

For a variety of malignancies, CNVs have been utilized to assess prognosis and subsequent therapy profiles, such as *MYCN* amplification in neuroblastoma [8]. CNV of genes in primary CRC tumors and their corresponding metastatic disease locations has long been studied, but little is known about how CNVs of genes in the primary tumor of CRC are associated with localized illness and distant metastases [9–14]. One key component of the SWI/SNF complex involved in epigenetic control of genome transcription is the SWI/SNF-related, matrix-associated, actin-dependent regulator of chromatin subfamily C member 1 (*SMARCC1*) [15–18]. It is thought to act as a tumor suppressor in a variety of malignancies, including pancreatic and renal carcinomas [19–20]. However, its involvement in CRC is unclear and controversial. Using a dataset of 524 individuals with colon cancer (CC) from The Cancer Genome Atlas (TCGA), we evaluated the relationship of *SMARCC1* CNV with distant metastatic disease.

Materials and methods

Patient data

In July 2021, a cohort of 524 samples (506 cases were determined after data integration) from original tumor specimens were chosen from the TCGA database using R based on the availability of metastatic staging and copy number data. The results presented here are based on data downloaded from the TCGA Research Network (<http://cancergenome.nih.gov/>) on July 22nd.

Clinicopathological data

Clinical data on age, sex, race/ethnicity, and staging were obtained from the TCGA data portal. The TCGA data portal also included pathologic information such as tumor size, tumor location, resection margins, lymph node status, and metastatic status upon diagnosis.

CNV analysis

The TCGA level 3 CNV data for colorectal cancer were obtained from the TCGA data portal. Each sample was processed and normalized using TCGA level 3 CNV (Affymetrix Genome-Wide SNP Array 6.0). The study was conducted using mean copy number estimations of regions that overlapped the whole genome. The gene was classified using the Genomic Identification of Significant Targets in Cancer (GISTIC) algorithm. CNV was characterized as a copy number ≥ 1 or ≤ 1 .

Statistical analysis

The univariate relationship of *SMARCC1* CNV with variables in the CC set was investigated using the chi-squared test or Fisher's exact test, as applicable. A logistic regression model was used to perform a univariate

study of metastatic disease (M1 vs. M0) using predictors and variables. A logistic regression model was used to conduct a multivariate analysis of metastatic disease (M1 vs. M0) by inputting all factors in the model and utilizing a backward variable selection technique with an alpha level of removal of 0.1. The model was modified to include *SMARCC1* CNV, chemotherapy, N stage, and T stage. R (version 4.1.0) was used for all analyses, and the threshold for significance was set at 0.05. Following the discovery of a link between *SMARCC1* CNV and distant metastatic disease in the colorectal cohort, *SMARCC1* CNV data were analyzed to determine whether the CNV represented a gain or a loss, and the majority of the CNVs were homozygous deletions, indicating copy number loss.

Results

A total of 506 individuals with CC were included in the CC copy number analysis group (Table 1). The median age was 68 years (range, 31–90 years).

Pathological characteristics

Patients with distant metastatic disease were identified in 68 (13.4%) of the CC copy number analysis cohort, whereas 204 (40.3%) had positive nodal disease.

Genetic analysis for all patients

There were 22 samples with CNV of *SMARCC1*, with homozygous deletions resulting in a reduction in copy number. *SMARCC1* CNV was shown to have a statistically significant relationship with distant metastatic disease ($P = 0.017$) in the univariate analysis. *SMARCC1* CNV was shown to have no link to positive nodal disease, positive resection margins, sex, race, or T stage (Table 2).

The occurrence of distant metastatic disease was observed to be related to the existence of *SMARCC1* CNV in the univariate analysis of metastatic disease (Table 2; $P = 0.012$). Distant metastases were also connected with N1-2 nodal disease ($P < 0.001$), R1-2 ($P < 0.001$) resection, Adjuvant treatment ($P < 0.001$), but had no relation with MSI ($P = 0.993$), T3 or T4 advanced local disease ($P = 0.984$), adjuvant chemotherapy ($P = 0.985$), sex ($P = 0.530$), and race ($P = 0.500$).

On multivariate analysis (Table 2), the presence of *SMARCC1* CNV was associated with distant metastatic disease ($P = 0.008$), as well as N1-2 nodal disease ($P < 0.001$). The data for race and MSI were removed from the multivariate model to determine the amount of NA data.

Discussion

An examination of data of 506 individuals using the TCGA revealed that *SMARCC1* CNV was independently associated with distant metastatic disease in CC. We used

Table 1 Sample characteristics of patients with colon cancer included in copy number analysis ($n = 506$)

Characteristic	Number (%)
Age in years (mean \pm standard deviation)	66.45 \pm 12.41
Gender	
Male	259 (51.2)
Female	245 (48.4)
NA	2 (0.4)
Race	
White	244 (48.2)
Non-white*	77 (15.2)
NA	185 (36.6)
Adjuvant chemotherapy	
Yes	4 (0.8)
No	500 (98.8)
NA	2 (0.4)
M stage	
M0	372 (73.5)
M1	68 (13.4)
NA	66 (13.0)
N stage	
N0	300 (59.3)
N1–2	204 (40.3)
NA	2 (0.4)
T stage	
T1–2	98 (19.4)
T3–4	405 (80.0)
NA	3 (0.6)
Microsatellite instability	
MSI	85 (16.8)
MSS	14 (2.8)
NA	407 (80.3)
Margins status**	
R0	371 (73.3)
R1–2	279 (55.1)
NA ^a	106 (20.9)

* Non-white contains Asian, Black, Hispanic and African–American;

** Margin status refers to microscopic (R1) or macroscopic (R2) residual disease, or no microscopic residual disease (R0); MSI, microsatellite instability; MSS, microsatellite stability; ^a NA: Not Available, means not mentioned any of the above two

multivariate analysis, which included age, sex, surgical margin status, T stage, N stage, MSI, and adjuvant chemotherapy, to corroborate our findings. According to our data, *SMARCC1* CNV is strongly linked with distant metastatic disease in individuals with all types of CC. Furthermore, our findings imply that CNV of *SMARCC1* might be a valuable genetic marker for personalizing CC treatment and identifying individuals who would benefit from more aggressive treatment methods.

Table 2 Univariate and multivariate analysis for presence of distant metastatic disease ($n, \%$)

Characteristic	M0	M1	Univariate analysis	Multivariate analysis*
			<i>P</i> value	<i>P</i> value
<i>SMARCC1</i> copy number			0.012	0.008
Variation	12 (3)	7 (10)		
No variation	360 (97)	61 (90)		
Gender			0.53	0.18
Famel	185 (50)	31 (46)		
Male	187 (50)	37 (54)		
Adjuvant chemotherapy			0.985	0.998
Yes	4 (1)	0 (0)		
No	368 (99)	68 (100)		
N stage			< 0.001	< 0.001
N1–2	116 (31)	58 (85)		
N0	256 (69)	10 (15)		
T stage			0.984	0.988
T1–2	86 (23)	0 (0)		
T3–4	286 (77)	68 (100)		
Margin Status			< 0.001	< 0.001
R0	305 (82)	31 (46)		
R1–2	5 (9)	24 (35)		
NA	62 (17)	1 (19)		
Microsatellite instability*			0.993	
MSI	56 (15)	13 (19)		
MSS	11 (3)	0 (0)		
NA	305 (82)	55 (81)		
Race*			0.5	
White	170 (46)	32 (47)		
Non-white	45 (12)	11 (16)		
NA	157 (42)	25 (37)		

* many NAs were presented, so we ticked Microsatellite instability and Race out for smooth analysis by R

When various genetic markers, such as mutations, gene expression, methylation status, and CNV, were included in the TCGA analysis, no indication of a substantial genetic relationship with distant metastatic illness was found^[21]. Our work is unusual in that it uses a larger database with more samples of distant metastatic illness to determine a CNV of a single gene that is independently linked with distant metastatic disease. Low *SMARCC1* expression was linked to the development of extrahepatic metastases in a study of 30 individuals with CC^[22]. In line with these findings, the majority of *SMARCC1* CNVs in our population were homozygous deletions, suggesting that the gene was downregulated. *SMARCC1* CNV is linked to more aggressive CC, as evidenced by the relationship with nodal disease and distant metastasis in our cohort.

The new cohort included a large number of samples

of both colectomy and metastatic illness, allowing for a more statistically powerful correlation analysis. Nodal disease was linked to distant metastasis and increases with advanced T stage. The molecular route of tumorigenesis is another element that influences the development of distant metastatic diseases. Hereditary non-polyposis CC is linked to tumors that initially present in the left colon with a reduced risk of metastasis, as well as MSI. Several studies have found that distinct molecular and clinical characteristics exist in various parts of the colon [2, 9, 23–24]; thus, we adjusted for MSI when looking for a link between *SMARCC1* CNV and distant metastatic illness. *SMARCC1* CNV was not found to be associated with MSI/MSS on univariate analysis ($P = 0.879$), and *SMARCC1* was independently associated with distant metastatic disease ($P = 0.018$) in the multivariate analysis, despite the expected trend between distant metastatic disease in the CC cohort and microsatellite stability (MSS) ($P = 0.993$) in the multivariate analysis. These data show that the link between *SMARCC1* CNV and distant metastatic illness is not based on genetic differences between right- and left-sided primary malignancies.

Multiple studies have demonstrated that the number of lymph nodes sampled after CC surgery is related to the outcome in stage II CC, suggesting that further therapy might prevent the disease from spreading [25–27]. With increased evidence of tumor dissemination in the early stages of CC, additional indications, such as *SMARCC1* CNV, may be beneficial in directing therapy toward a more aggressive regimen aimed at avoiding tumor spread. Future research with a longitudinal design will be required to elucidate *SMARCC1*'s role as a molecular marker that affects therapy, allowing for greater association with the development of advanced illness with distant metastases.

We note that, in addition to the retrospective approach, this study has limitations. The data came from individuals who had their original tumor resected; thus, there were no cases of advanced, unresectable illness in the study. Some clinical information, such as race/ethnicity, was not recorded, and some CNVs may be linked more with various nationalities/backgrounds [28]. Only the capacity to compare genetic changes with the occurrence of metastatic illness was possible in the retrospective analysis. The lack of a prospective component following genetic analysis restricts the application of the findings and prevents the identification of variables linked to development of distant metastasis. Although prior studies have found somatic alterations and CNV in the genomes of several cancer types, no previous study has linked *SMARCC1* CNV at the original location to distant metastatic illness. The link might have an effect on therapeutic options and could even be used as a marker for targeted molecular therapy.

Conclusions

We found a statistically significant association between *SMARCC1* CNV and distant metastatic disease in CC and rectal adenocarcinoma in our sample. *SMARCC1* CNV may be utilized clinically to support optimal systemic treatment methods against more aggressive local treatments in patients with CC, including radiation therapy for rectal adenocarcinoma, pending additional confirmation in longitudinal investigations.

Conflicts of interest

The authors indicated no potential conflicts of interest.

References

1. Bray F, Ferlay J, Soerjomataram I, et al. Global cancer statistics 2018: GLOBOCAN estimates of incidence and mortality worldwide for 36 cancers in 185 countries. *CA Cancer J Clin*, 2018, 68: 394–424.
2. Cancer Genome Atlas Network. Comprehensive molecular characterization of human colon and rectal cancer. *Nature*, 2012, 487: 330–337.
3. Fodde R. The APC gene in colorectal cancer. *Eur J Cancer*, 2002, 38: 867–871.
4. Markowitz S D, Bertagnolli M M. Molecular origins of cancer: Molecular basis of colorectal cancer. *N Engl J Med*, 2009, 361: 2449–2460.
5. van Gijn W, Marijnen CA, Nagtegaal ID, et al. Preoperative radiotherapy combined with total mesorectal excision for resectable rectal cancer: 12-year follow-up of the multicentre, randomised controlled TME trial. *Lancet Oncol*, 2011, 12: 575–582.
6. Stankiewicz P, Lupski JR. Structural variation in the human genome and its role in disease. *Annu Rev Med*, 2010, 61: 437–455.
7. Conrad DF, Pinto D, Redon R, et al. Origins and functional impact of copy number variation in the human genome. *Nature*, 2010, 464: 704–712.
8. Mace A, Kutalik Z, Valsesia A. Copy Number Variation. *Methods Mol Biol*, 2018, 1793: 231–258.
9. Vakiani E, Janakiraman M, Shen R, et al. Comparative genomic analysis of primary versus metastatic colorectal carcinomas. *J Clin Oncol*, 2012, 30: 2956–2962.
10. Lee H, Flaherty P, Ji HP. Systematic genomic identification of colorectal cancer genes delineating advanced from early clinical stage and metastasis. *BMC Med Genomics*, 2013, 6: 54.
11. Xie T, Cho YB, Wang K, et al. Patterns of somatic alterations between matched primary and metastatic colorectal tumors characterized by whole-genome sequencing. *Genomics*, 2014, 104: 234–241.
12. Lee SY, Haq F, Kim D, et al. Comparative genomic analysis of primary and synchronous metastatic colorectal cancers. *PLoS One*, 2014, 9: e90459.
13. Mekenkamp LJ, Haan JC, Israeli D, et al. Chromosomal copy number aberrations in colorectal metastases resemble their primary counterparts and differences are typically non-recurrent. *PLoS One*, 2014, 9: e86833.
14. Gonzalez-Gonzalez M, Fontanillo C, Abad M M, et al. Identification of a characteristic copy number alteration profile by high-resolution single nucleotide polymorphism arrays associated with metastatic sporadic colorectal cancer. *Cancer*, 2014, 120: 1948–1959.
15. Hohmann AF, Vakoc CR. A rationale to target the SWI/SNF complex for cancer therapy. *Trends in Genetics*, 2014, 30: 356–363.

16. Alver BH, Kim KH, Lu P, *et al.* The SWI/SNF chromatin remodelling complex is required for maintenance of lineage specific enhancers. *Nature Communications*, 2017, 8: 14648.
17. Reisman D, Glaros S, Thompson EA. The SWI/SNF complex and cancer. *Oncogene*, 2009, 28: 1653–1668.
18. Savas S, Skardasi G. The SWI/SNF complex subunit genes: Their functions, variations, and links to risk and survival outcomes in human cancers. *Crit Rev Oncol Hematol*, 2018, 123: 114–131.
19. Wang G, Lv Q, Ma C, *et al.* SMARCC1 expression is positively correlated with pathological grade and good prognosis in renal cell carcinoma. *Transl Androl Urol*, 2021, 10: 236–242.
20. Xiao ZM, Lv DJ, Yu YZ, *et al.* SMARCC1 Suppresses Tumor Progression by Inhibiting the PI3K/AKT Signaling Pathway in Prostate Cancer. *Front Cell Dev Biol*, 2021, 9: 678967.
21. Lee H, Flaherty P, Ji HP. Systematic genomic identification of colorectal cancer genes delineating advanced from early clinical stage and metastasis. *BMC Med Genomics*, 2013, 6: 54.
22. Macartney-Coxson DP, Hood KA, Shi HJ, *et al.* Metastatic susceptibility locus, an 8p hot-spot for tumour progression disrupted in colorectal liver metastases: 13 candidate genes examined at the DNA, mRNA and protein level. *BMC Cancer*, 2008, 8: 187.
23. Missiaglia E, Jacobs B, D'Ario G, *et al.* Distal and proximal colon cancers differ in terms of molecular, pathological, and clinical features. *Ann Oncol*, 2014, 25: 1995–2001.
24. Sugai T, Habano W, Jiao YF, *et al.* Analysis of molecular alterations in left- and right-sided colorectal carcinomas reveals distinct pathways of carcinogenesis: proposal for new molecular profile of colorectal carcinomas. *J Mol Diagn*, 2006, 8: 193–201.
25. Lee D, Wang KY, Sagar PM, *et al.* S1 Sacrectomy for re-recurrent rectal cancer: our experience with reconstruction using an expandable vertebral body replacement device. *Dis Colon Rectum*, 2018, 61: 261–265.
26. Xingmao Z, Hongying W, Zhixiang Z, *et al.* Analysis on the correlation between number of lymph nodes examined and prognosis in patients with stage II colorectal cancer. *Med Oncol*, 2013, 30: 371.
27. Storli K, Sondenaa K, Furnes B, *et al.* Improved lymph node harvest from resected colon cancer specimens did not cause upstaging from TNM stage II to III. *World J Surg*, 2011, 35: 2796–2803.
28. Redon R, Ishikawa S, Fitch KR, *et al.* Global variation in copy number in the human genome. *Nature*, 2006, 444: 444–454.

DOI 10.1007/s10330-021-0522-2

Cite this article as: Feng LB, Liu Y, Xia D, *et al.* SMARCC1 copy number variation is related to metastatic colon cancer: An investigation based on TCGA data. *Oncol Transl Med*, 2021, 7: 216–220.

CircBAGE2 (hsa_circ_0061259) regulates CCND1 and PDCD10 expression by functioning as an miR-103a-3p 'sponge' to alter the proliferation and apoptosis of prostate cancer cells*

Chunlei Zhang^{1,2}, Dan Liu¹ (Co-first author), Qinqin Tian¹, Qi Yang^{1,2}, Xiaoyuan Zi¹ (✉), Yinghao Sun¹ (✉)

¹ Department of Urology, Changhai Hospital, Navy Military Medical University, Shanghai 200433, China

² Department of Urology, The 940 Hospital of Joint Logistics Support Force of Chinese PLA, Lanzhou 730050, China

Abstract

Objective The aim of the article is to explore the function of circBAGE2 (hsa_circ_0061259) in prostate cancer (PCa) cells.

Methods Sequencing results of circBAGE2 were verified by quantitative RT-PCR (qRT-PCR) and Sanger sequencing. Agarose gel electrophoresis was used to detect the resistance of GAPDH, BAGE2, and circBAGE2 to RNase R and their expression as cDNA and gDNA in 22RV1 cells. The biological functions of circBAGE2 were investigated by CCK8 assay and flow cytometry in 22RV1 cells transfected with siRNAs. Multiple databases were used to predict the target binding sites between circRNAs, miRNAs, and mRNAs. Western blotting was used to detect the expression of CCND1 and PDCD10.

Results CircBAGE2 was significantly upregulated in PCa samples and PCa cells compared to that in matched normal tissues and normal cells, and CircBAGE2 knockdown inhibits cell proliferation and promotes apoptosis. Downregulation of circBAGE2 compromised the expression of CCND1 and PDCD10. The 3' UTRs of CCND1 and PDCD10 were matched by miR-103a-3p, which shared binding sites with circBAGE2.

Conclusion CircBAGE2 contributes to PCa progression by upregulating CCND1 and PDCD10 expression through its role as a 'sponge' of miR-103a-3p. CircBAGE2 may be a potential therapeutic target for PCa.

Key words: prostate cancer (PCa); circBAGE2; CCND1; PDCD10

Received: 14 September 2020

Revised: 12 November 2020

Accepted: 21 May 2021

Prostate cancer (PCa) is the most frequently diagnosed malignancy and the second leading cause of death in men worldwide [1–2]. In Asian countries, such as China, the incidence of PCa has increased annually. Clinically, serum prostate-specific antigen (PSA) levels are currently detected in diagnostic studies. However, serum PSA has several detection flaws involving false positives, which cause overdiagnosis and subsequent overtreatment [3]. Therefore, it is necessary to develop a more accurate and sensitive biomarker to guide the diagnosis, prognosis, and therapy of PCa.

With recent developments in bioinformatics and the application of RNA sequencing, the biological activity of circular RNAs (circRNAs) is receiving increasing attention. CircRNAs are a class of noncoding RNAs that are emerging as key new members of the gene regulatory milieu, which are produced by back-splicing events within genes [4]. The expression analysis of circRNA transcripts revealed that numerous circRNAs seem to be specifically expressed in various tissues, including PCa [5]. Some reports have identified that circRNAs, such as circSMARCA5 [6], circFOXO3 [7], and circZMIZ1 [8] play

✉ Correspondence to: Yinghao Sun, Email: sunyhsmmu@126.com; Xiaoyuan Zi, Email: zi_xiaoyuan@163.com

* Supported by grants from the Natural Science Foundation of Gansu Province (No. 20JR5RA601) and In-hospital Project of The 940 Hospital of Joint Logistics Support Force of Chinese PLA (No. 2021yxky057).

© 2021 Huazhong University of Science and Technology

important roles in PCa. However, many circRNAs and their mechanisms remain unclear.

In order to further explore the biomarkers of PCa and the underlying mechanisms, we previously performed a circRNA sequencing analysis and identified some significantly upregulated and downregulated circRNAs in PCa cell lines [9]. Among them, circBAGE2 (hsa_circ_0061259) is one of the most upregulated circRNAs in 22RV1 cell line compared to RWPE-1 cell line, and is therefore considered responsible for the progression of PCa. In addition, BAGE genes in its linear transcript are silent in normal cells and expressed in some tumors and cancer cell lines [10–11]. Therefore, we further explored the mechanism and function of circBAGE2 in the 22RV1 cell line. The present study aimed to investigate the role of circBAGE2 in PCa progression.

Materials and methods

Ethics statement

This study was approved and supervised by the Ethics Committee of the Navy Military Medical University (Shanghai, China). Human PCa tissues and adjacent normal tissues were obtained from patients undergoing surgery at the Changhai Hospital of Navy Military Medical University, Shanghai, China. All tumors and paired adjacent normal tissues were confirmed by pathologists. Written informed consent was obtained from the patients for research purposes.

Cell culture

RWPE-1, 22RV1, PC3, and LNCaP cells were purchased from the American Type Culture Collection (ATCC), USA. 22RV1, PC3, and LNCaP cells were cultured in RPMI-1640 medium (Gibco, Carlsbad, CA, USA), F12 (ham) medium (Gibco, Carlsbad, CA, USA), and RPMI-1640 medium (Gibco, Carlsbad, CA, USA), respectively. RWPE-1 cells were cultured in PEpiCM medium (ScienCell, USA). All media were supplemented with 10% FBS and 1% penicillin-streptomycin, and all cell lines were cultured at 37 °C and 5% CO₂. The medium was changed every 2 days, and cells were digested at room temperature with 0.5 mL 0.25% trypsin/EDTA (Gibco, Carlsbad, CA, USA) per well and grown to 70%–80% confluency.

Total RNA and circRNA extraction

Total RNA was extracted from cultured cell lines and tissues using RNAiso Plus (Takara, Dalian, China), according to the manufacturer's instructions. To remove linear RNAs and enrich circRNAs, 3 units/μg of RNase R (Epicenter, Madison, WI, USA) was used to digest the total extracted RNA for 15 min at 37 °C. RNA quantity and quality were evaluated using a NanoDrop 2000 c

spectrophotometer (Thermo, Wilmington, DE, USA), and RNA integrity was assessed by 2% agarose gel electrophoresis.

Agarose gel electrophoresis

Agarose was dissolved in a TAE buffer in a microwave oven at a concentration of 1.5% with Gelred dye, and then placed in an electrophoresis tank by adding samples containing 6 × loading buffer after cooling. The reaction was performed at 90 V for 30 min. A gel camera system (G-box-chemi-R5, Hong Kong Gene Co., Ltd., China) was used to capture the images.

PCR

PCR analyses of the expression levels of the circRNAs were performed using Premix Ex Taq II (Takara, Dalian, China) in 20 μL reaction volume, including 1 μL of cDNA, 10 μL of 2 × Master Mix, 0.3 μL of Forward Primer (10 μM), 0.3 μL of Reverse Primer (10 μM), and 8.4 μL of double distilled water. The cycling conditions were as follows: 95 °C for 10 min, followed by 40 cycles at 95 °C for 20 s, 60 °C for 30 s, 72 °C for 45 s, and 72 °C for 7 min in a PCR System (Bio-Rad, CA, USA). All primers are shown in Table 1.

Quantitative RT-PCR (qRT-PCR)

cDNA was synthesized from 500 ng of total RNA using PrimeScript RT Master Mix (Takara, Dalian, China), according to the manufacturer's instructions. qRT-PCR analyses of the expression levels of the circRNAs were performed using SYBR Premix Ex Taq II (Takara, Dalian, China). qRT-PCR was performed in a 20 μL reaction volume, including 1 μL of cDNA, 10 μL of 2 × Master Mix, 0.3 μL of forward primer (10 μM), 0.3 μL of reverse primer (10 μM), and 8.4 μL of double distilled water. The reaction was performed with the protocol; 95 °C for 10 min, followed by 40 cycles at 95 °C for 10 s and 60 °C for 60 s in a real-time PCR System (ABI, CA, USA). GAPDH was used as a reference, and samples were amplified in triplicate wells, and the relative level was calculated using the 2^{-ΔΔC_q} method. All primers are shown in Table 1.

Gene transfection

Cells were transfected with corresponding specific siRNA or control siRNA (10 mM, 7.5 μL siRNA/125 μL OPTI-MEM) using Lipofectamine RNAiMax (5 μL in 125 μL OPTI-MEM) (Invitrogen, Carlsbad, CA, USA), in accordance with the manufacturer's recommendations. Briefly, the cells were incubated with siRNAs and Lipofectamine RNAiMax mixture for 15 min at room temperature. Cells were then cultured in medium without antibiotics, after washing with OPTI-MEM twice. The following siRNA sequences were used: siRNA-1 for circBAGE2 sense: 5'-CGGUCAAACA

Table 1 Primers of all moleculars used in PCR and qRT-PCR

Primer name	Primer sequence (5'-3')-F	Primer sequence (5'-3')-R
circ-BAGE2	AACTGGCATGGGTAAACCAG	TGTTCTGGACAAAGCAGGAA
BAGE2 (cDNA)	AATACAGTGAGCCCACCTCGT	TTTCAGCTTTGACCTGCCTCGG
BAGE2 (gDNA)	TGTAAGCACTTTGGAGCCACTATCA	TTCAGGAGCTTGGTCAATGTGTCT
CCND1	CGCCCTCGGTGTCCTACTTCAA	GTTCTCGCAGACCTCCAGCAT
PDCD10	CGCAGGGCACTTGAACACCAA	TCGGTTGGCACTTACGAACACA
GAPDH	AAGAAGGTGGTGAAGCAGG	GTCAAAGGTGGAGGAGTGG GG
circ-GUCY1A2	GCTCCTATGCAGACCACTCC	TTTCTGCATCCCTGTAACCA
circ-ETV3	ACGGGGAATTTGTCATCAAG	AATGGGTAGTTGGGCATCAC
circ-KCNN2	GGATAATTGCCGCATGGA	CTGCTCCATTGTCCACCA
circ-MIR663A	CTACCGTTCTGCCTCCGA	CGCGTCTCGTCTCACTCA
circ-KRT6A	GCGTTGGACAAGTCAACATC	GAAGTGAAGCCACCTCCAAC
circ-CD276	AGCTTACCTGCTTCTGTGAG	ATCCTGCCAGAACACCTCAG
circ-ZFP57	TGGCCAGAATCTTTCTGCAT	TCCTGGTAAAGACCCTCTG
circ-PSMA7	CTCATCGTGGGTTTCGACTT	ATGCAGACGTTGTATCCAA
circ-RPPH1	GGGCTCTCCCTGAGCTTC	CAAGGGACATGGGAGTGG

GCGAUGUGTT-3'; antisense: 5'-CACAUUGCUGUU UGGACCGTT-3'; and siRNA-2 for circBAGE2 sense: 5'-CAAACAGCGAUGUGCAUUUTT-3'; antisense: 5'-AAAUGCACAUCGUGUUUGTT-3'. Cells were harvested 48 h after transfection and expression levels were determined using qRT-PCR.

Cell proliferation assays

Cell proliferation was assayed using the Cell Counting Kit-8 (CCK-8) assay (Dojindo, Japan), according to the manufacturer's protocol. The cells were plated in 96-well plates (3×10^5 cells/well). Cell proliferation was detected every 24 h according to the manufacturer's protocol. Briefly, 10 μ L of CCK-8 solution was added to each well and incubated for 2 h at 37 °C. The solution was then spectrophotometrically measured at 450 nm.

Cell cycle and cell apoptosis assays

Cell lines, seeded in 6-well plates (3×10^5 cells/well), were assayed using the Cell Cycle Staining Kit (MultiSciences, Hangzhou, China) and the Annexin V-FITC/PI Apoptosis DetectionKit (MultiSciences, Hangzhou, China), according to the manufacturer's protocol. After 24 h of treatment with or without siRNAs, the cells were harvested and washed twice with cold PBS. For cell cycle analysis, the trypsin-harvested cells were incubated with 1 mL DNA staining solution and 10 μ L permeabilization solution for 30 min at room temperature. For the cell apoptosis assay, cells were incubated with 5 μ L Annexin V-FITC and 3 μ L PI solution in 500 μ L binding buffer for 5 min at room temperature. Fluorescence was measured using a MACSQuant Analyzer 10 (Miltenyi Biotec GmbH, Germany) and analyzed using FlowJo 7.6.1 software (CA, USA).

Western blotting

Cellular protein (25 μ g) was loaded onto a 12% SDS-PAGE gel and then transferred to PVDF membranes. After blocking with 5% BSA in TBST for 2 h at room temperature, membranes were incubated with primary antibodies against CCND1, PDCD10 (1:1000 dilution, CST, Beverly, MA, USA) and GAPDH (1:10000 dilution, CST, Beverly, MA, USA) at 4 °C overnight, followed by incubation with appropriate HRP-conjugated secondary antibody (1:1000 dilution, CST, Beverly, MA, USA) at room temperature for 2 h. The membranes were then exposed using a chemiluminescent detection system (Syngene G, Box, America). Quantitative densitometric analyses of immunoblots were performed using the ImageJ software (Ver. 1.48, Bethesda, MD, USA), and the relative ratios were calculated.

Annotation and functional prediction of circBAGE2

The circRNA-miRNA-mRNA network of circBAGE2 was constructed using CloudSeq's homemade software based on miR and a and TargetScan (CloudSeq Inc., Shanghai, China), combined with Cytoscape (<http://www.cytoscape.org/>).

Statistical analysis

Each experiment was performed in triplicates. All data are represented as the mean \pm SEM. Student's *t*-test and one-way analysis of variance were used to determine statistical significance. Differences were considered statistically significant at $P < 0.05$.

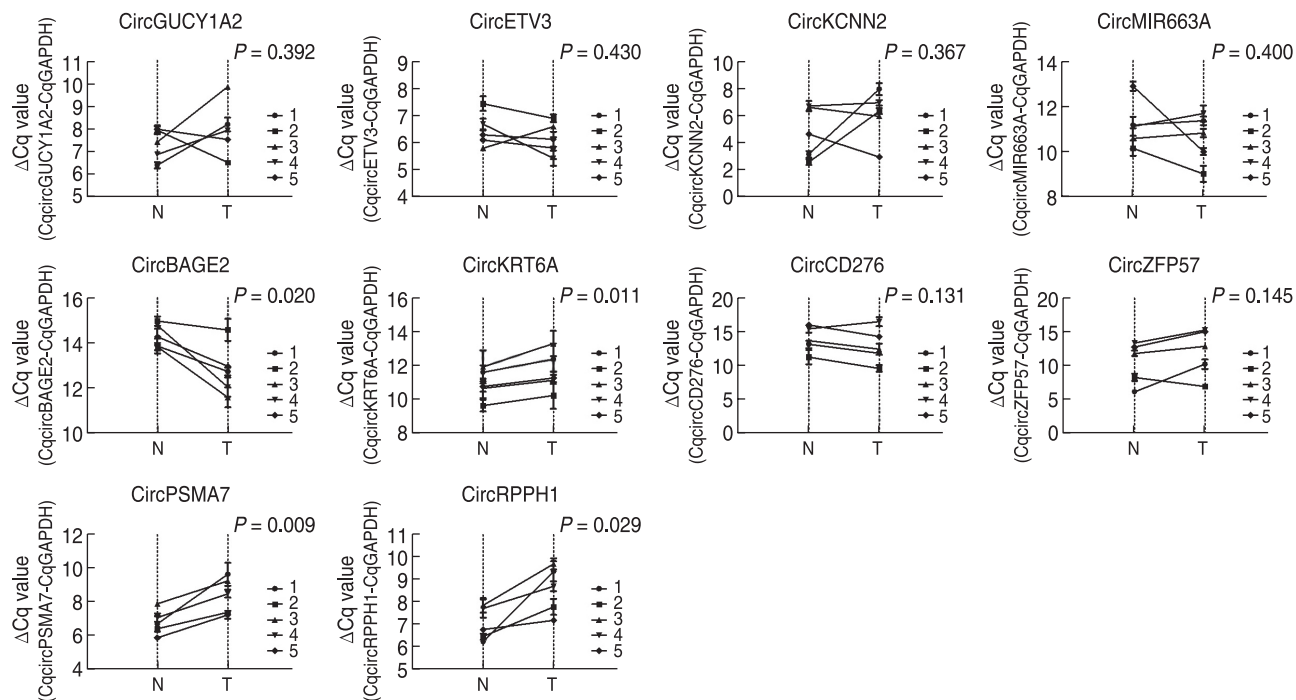


Fig. 1 The expression levels of candidate circRNAs for validation in 5 pairs of human prostate cancer tissue and adjacent normal tissue samples via qRT-PCR: circGUCY1A2, circETV3, circKCNN2, circMIR663A, circBAGE2, circKRT6A, circCD276, circZFP57, circPSMA7 and circRPPH1. N: normal tissues; T: tumor tissues

Results

Expression of circBAGE2 in human PCa tissues

The expression levels of five significantly upregulated and downregulated circRNAs in 22RV1 cell line compared to RWPE-1 cell line [9] were detected in five samples of human PCa tissues and their paired adjacent normal tissues by qRT-PCR using GAPDH as the internal standard, targeting circGUCY1A2, circETV3, circKCNN2, circMIR663A, circBAGE2, circKRT6A, circCD276, circZFP57, circPSMA7, and circRPPH1. As shown in Fig. 1, circBAGE2 was identified as the only upregulated circRNA in cancer tissues compared to the corresponding normal tissues, with statistical significance ($P < 0.05$). Meanwhile, circKRT6A, circPSMA7, and circRPPH1 were downregulated in cancer tissues compared to normal tissues.

Characterization of circBAGE2 in human PCa cell lines

CircBAGE2 was significantly upregulated in 22RV1 cells compared to RWPE-1 cells when normalized to GAPDH by qRT-PCR and nucleic acid electrophoresis (Fig. 2a and 2b). The distinct product of the expected size amplified using outward-facing primers was confirmed by Sanger sequencing (Fig. 2c). Using PCR and nucleic acid electrophoresis, circBAGE2 was confirmed to be

more resistant to RNase R treatment than the line control BAGE2 (Fig. 2d). As expected, PCR assays alone did not produce amplification in genomic DNA with circBAGE2 primers using cDNA and genomic DNA of 22RV1 as templates, which ruled out the possibility of genomic rearrangement (Fig. 2e).

Silencing circBAGE2 inhibited proliferation and increased apoptosis of human PCa cell lines *in vitro*

The expression of circBAGE2 was suppressed by the two siRNAs (Fig. 3a). CircBAGE2 knockdown significantly decreased the viability of 22RV1 cells (Fig. 3b). As shown in Fig. 3c and 3d, 22RV1 cells transfected with siRNAs were arrested in the G1-phase. In addition, downregulation of circBAGE2 led to a substantial increase in cell apoptosis (Fig. 3e and 3f).

Prediction of target genes related to circBAGE2

Based on circRNA-miRNA-mRNA network analysis tools, 12 miRNAs containing binding sites with circBAGE2 were predicted: miR-450a-2-3p, miR-7-5p, miR-766-5p, miR-103a-3p, miR-107, miR-377-3p, miR-1236-5p, miR-301b-3p, miR-603, miR-520f-3p, miR-301a-3p, and miR-134-5p (Fig. 4a). CircBAGE2 had two binding sites for miR-103a-3p (Fig. 4b). Further analysis showed that miR-103a-3p matched the 3'UTR of CCND1 and

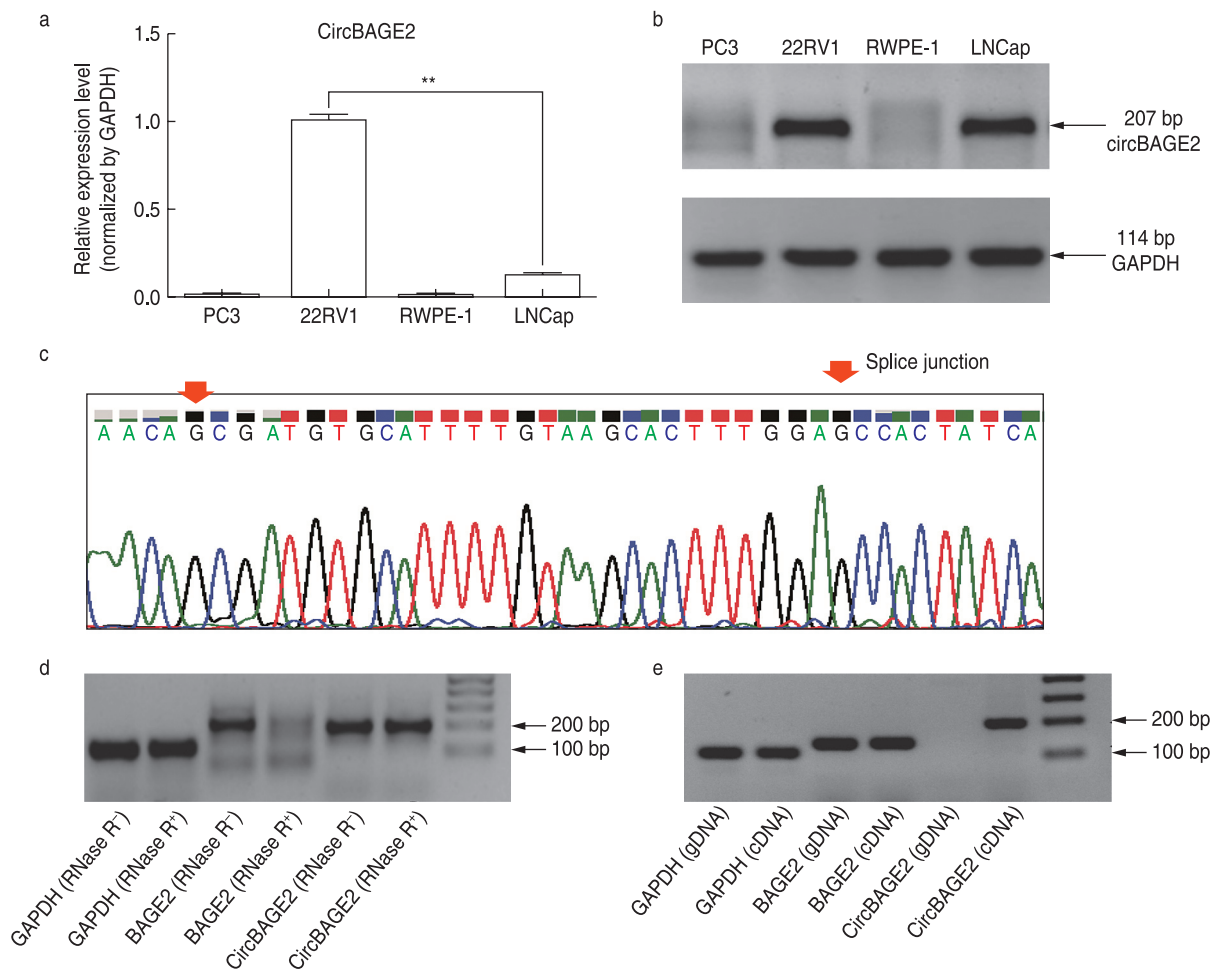


Fig. 2 Characterization of circBAGE2 in human prostate cancer cells. (a and b) The expression levels of circBAGE2 in 4 human prostate cancer cell lines by qRT-PCR and agarose gel electrophoresis. (c) Sanger sequencing of the product amplified by primers of circBAGE2. (d) The resistance to RNase R of GAPDH, BAGE2 and circBAGE2 in 22RV1. (e) The expression levels of GAPDH, BAGE2 and circBAGE2 using cDNA and genomic DNA (gDNA) of 22RV1 as templates. ** $P < 0.01$

PDCD10 (Fig. 4c). CCND1 and PDCD10 expression was significantly decreased by co-transfection with siRNAs in 22RV1 at the mRNA (Fig. 4d) and protein levels (Fig. 4e and 4f), as detected by qRT-PCR and western blotting.

Discussion

CircRNAs have recently been identified as a natural family that may regulate gene expression in mammals [12–13], which are important regulators of many cellular processes, such as embryonic development, cell cycle control, cellular senescence, cell signaling, and response to cellular stress [4]. All these functions are critical for cancer progression. Therefore, circRNAs may have a vital relationship with cancer, including PCa.

In our previous studies, we successfully constructed circRNA libraries of PCa cell lines and identified many

differentially expressed circRNAs [9]. circBAGE2 was one of the most upregulated circRNAs in 22RV1 compared with those in the RWPE1 cell line. In this study, we found that the expression level of circBAGE2 was significantly upregulated in human PCa tissues compared to the corresponding normal tissues.

BAGE family genes code for tumor-specific antigens that are highly expressed in different histological types of tumors. BAGE2 is expressed in a significant number of tumors, including melanoma, bladder cancer, lung cancer, mammary and prostatic carcinoma, and neuroblastoma [10]. Many published studies have indicated that BAGE2 may play an important role in cancer progression and could therefore be a good candidate as a new, highly informative epigenetic biomarker for cancer diagnosis [11, 14–15]. These studies imply that circBAGE2, which is highly expressed in PCa as the corresponding circRNA of BAGE2, may also perform key functions in PCa. In this

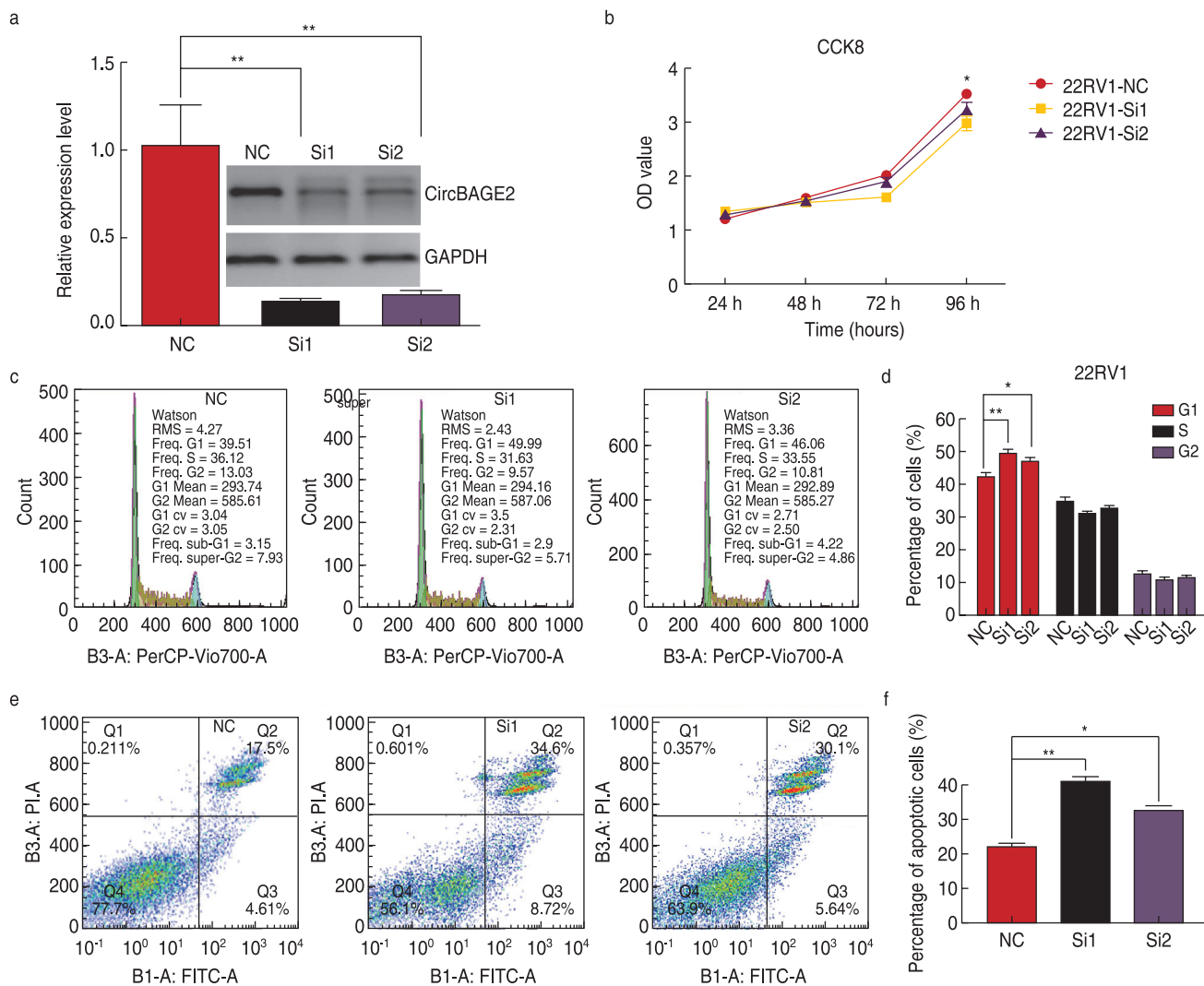


Fig. 3 Effects of circBAGE2 on the biological functions of 22RV1. (a) Effects of two different small interfering RNAs (siRNAs) against circBAGE2 analyzed by qRT-PCR. (b) CCK-8 assay of 22RV1 transfected with two siRNAs of circBAGE2. Cell cycle assay (c and d) and cell apoptosis assay (e and f) of 22RV1 transfected with two siRNAs of circBAGE2 by flow cytometry. ** $P < 0.01$, * $P < 0.05$, NC: negative control, Si1: siRNA1, Si2: siRNA2

study, we found that circBAGE2 knockdown inhibited cell proliferation and promoted cell apoptosis, which verified our hypothesis.

CircRNAs have been proposed to act through several mechanisms, including as miRNA sponges [16], binding with proteins or affecting translation [17], and as splicing modifiers of transcription [18]. Among them, the most important mechanism is the binding of circRNAs to specific miRNAs or groups of miRNAs, to sequester them and suppress their function in a phenomenon termed the competitive endogenous RNA hypothesis [16, 19]. Thus, we constructed a targeted circRNA-miRNA-mRNA network based on sequence-pairing prediction to explore the underlying mechanisms.

CircBAGE2 was predicted to have two binding sites with

miR-103a-3p, which has been shown to be upregulated in several types of cancer, including colorectal [20] and endometrial cancer [21], and is hypothesized to induce the proliferation, migration, and invasion of cancer cells. Early reports have demonstrated that the expression level of miR-103 was significantly decreased in PCa cells [22] and could suppress PCa proliferation and migration by downregulating the oncogene PDCD10 [23]. CCND1 plays a critical role in promoting the G1-S transition of the cell cycle in many cell types [24-25]. Mutations and overexpression of CCND1 are known to lead to alterations in cell cycle progression, and are frequently observed in a variety of tumors and could thus contribute to tumor progression in cancers such as non-small cell lung cancer [26] and PCa [27]. Considering our target analyses of miR-

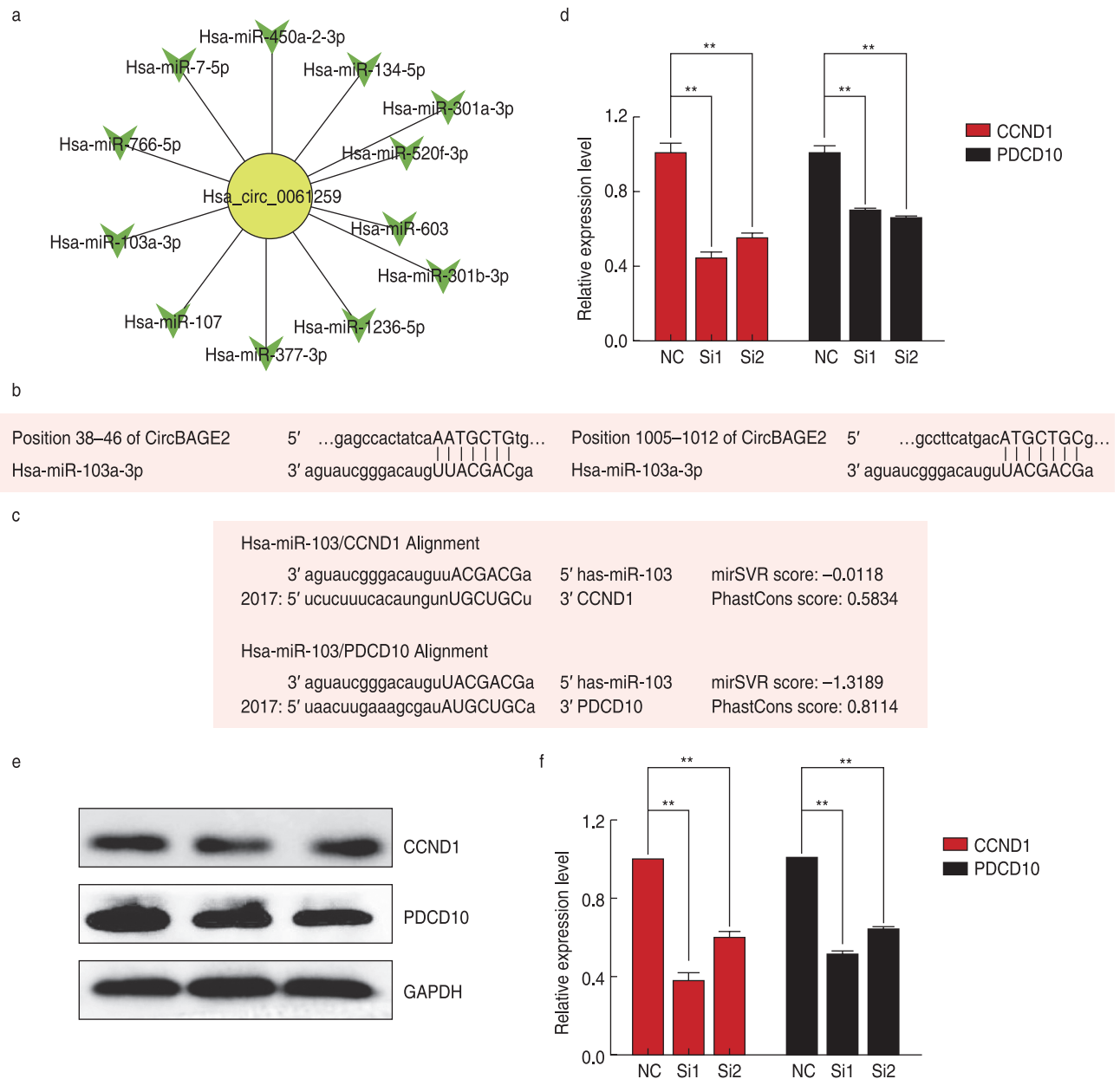


Fig. 4 Prediction of the targets of circBAGE2 based on circRNA-miRNA-mRNA network. (a) Network of circBAGE2 and targeted miRNAs. (b) Binding sites shown by solid lines of circBAGE2 with miR-103a-3p. (c) 3' UTRs of mRNAs (CCND1 and PDCD10) matched by miR-103a-3p. (d) Expression levels of mRNAs (CCND1 and PDCD10) detected by qRT-PCR following knockdown of circBAGE2 with siRNAs. Protein expression levels of CCND1 and PDCD10 analyzed by western blotting (e) and quantified with Image J (f) following knockdown of circBAGE2 using siRNAs. GAPDH was used as a control. ** $P < 0.01$, NC: negative control, Si1: siRNA1, Si2: siRNA2

103a-3p using miR and a and TargetScan, CCND1 and PDCD10 may be candidate genes. In the present study, the downregulated expression of PDCD10 and CCND1 after circBAGE2 knockdown confirmed the underlying mechanism by which circBAGE2 might regulate CCND1 and PDCD10 expression by functioning as an miR-103a-3p ‘sponge’ to alter the proliferation and apoptosis of the 22RV1 cell line.

To the best of our knowledge, this study is the first to systematically analyze the role of circBAGE2 in PCa progression. Therefore, this study may provide a therapeutic strategy or predictor for patients with PCa. Nevertheless, deeper mechanisms or animal experiments *in situ* still need to be studied.

Conflicts of interest

The authors indicated no potential conflicts of interest.

References

- Siegel RL, Miller KD, Jemal A. Cancer statistics, 2018. *CA Cancer J Clin*, 2018, 68: 7–30.
- Nong SJ, Guan YB, Wang ZW, *et al*. Significant association between IL-18 and OCT4 gene polymorphisms in susceptibility and clinical characteristics of prostate cancer. *Oncol Transl Med*, 2019, 5: 123–130.
- Yao JJ, Xu C, Fang ZY, *et al*. Androgen receptor regulated microRNA miR-182-5p promotes prostate cancer progression by targeting the ARRDC3/ITGB4 pathway. *Biochem Biophys Res Commun*, 2016, 474: 213–219.
- Haque S, Harries LW. Circular RNAs (circRNAs) in health and disease. *Genes (Basel)*, 2017, 8: 353.
- Zheng QP, Bao CY, Guo WJ, *et al*. Circular RNA profiling reveals an abundant circHIPK3 that regulates cell growth by sponging multiple miRNAs. *Nat Commun*, 2016, 7: 11215.
- Kong Z, Wan XC, Zhang YL, *et al*. Androgen-responsive circular RNA circSMARCA5 is up-regulated and promotes cell proliferation in prostate cancer. *Biochem Biophys Res Commun*, 2017, 493: 1217–1223.
- Kong Z, Wan XC, Lu YL, *et al*. Circular RNA circFOXO3 promotes prostate cancer progression through sponging miR-29a-3p. *J Cell Mol Med*, 2020, 24: 799–813.
- Jiang H, Lv DJ, Song XL, *et al*. Upregulated circZMIZ1 promotes the proliferation of prostate cancer cells and is a valuable marker in plasma. *Neoplasma*, 2020, 67: 68–77.
- Zhang CL, Xiong J, Yang Q, *et al*. Profiling and bioinformatics analyses of differential circular RNA expression in prostate cancer cells. *Future Sci OA*, 2018, 4: FSOA340.
- Ruault M, van der Bruggen P, Brun ME, *et al*. New BAGE (B melanoma antigen) genes mapping to the juxtacentromeric regions of human chromosomes 13 and 21 have a cancer/testis expression profile. *Eur J Hum Genet*, 2002, 10: 833–840.
- Lana E, Brun ME, Rivals I, *et al*. BAGE hypomethylation is an early event in colon transformation and is frequent in histologically advanced adenomas. *Cancers (Basel)*, 2009, 1: 3–11.
- Hansen TB, Jensen TI, Clausen BH, *et al*. Natural RNA circles function as efficient microRNA sponges. *Nature*, 2013, 495: 384–388.
- Jeck WR, Sorrentino JA, Wang K, *et al*. Circular RNAs are abundant, conserved, and associated with ALU repeats. *RNA*, 2013, 19: 141–157.
- Grunau C, Brun ME, Rivals I, *et al*. BAGE hypomethylation, a new epigenetic biomarker for colon cancer detection. *Cancer Epidemiol Biomarkers Prev*, 2008, 17: 1374–1379.
- Zhang SQ, Zhou XL, Yu H, *et al*. Expression of tumor-specific antigen MAGE, GAGE and BAGE in ovarian cancer tissues and cell lines. *BMC cancer*, 2010, 10: 163.
- van Rossum D, Verheijen BM, Pasterkamp RJ. Circular RNAs: novel regulators of neuronal development. *Front Mol Neurosci*, 2016, 9: 74.
- Li ZY, Huang C, Bao C, *et al*. Exon-intron circular RNAs regulate transcription in the nucleus. *Nat Struct Mol Biol*, 2015, 22: 256–264.
- Ashwal-Fluss R, Meyer M, Pamudurti NR, *et al*. circRNA biogenesis competes with pre-mRNA splicing. *Mol Cell*, 2014, 56: 55–66.
- Tay Y, Rinn J, Pandolfi PP. The multilayered complexity of ceRNA crosstalk and competition. *Nature*, 2014, 505: 344–352.
- Geng L, Sun B, Gao B, *et al*. MicroRNA-103 promotes colorectal cancer by targeting tumor suppressor DICER and PTEN. *Int J Mol Sci*, 2014, 15: 8458–8472.
- Yu DQ, Zhou HJ, Xun QY, *et al*. MicroRNA-103 regulates the growth and invasion of endometrial cancer cells through the downregulation of tissue inhibitor of metalloproteinase 3. *Oncol Lett*, 2012, 3: 1221–1226.
- Porkka KP, Pfeiffer MJ, Waltering KK, *et al*. MicroRNA expression profiling in prostate cancer. *Cancer Res*, 2007, 67: 6130–6135.
- Fu XL, Zhang W, Su YS, *et al*. MicroRNA-103 suppresses tumor cell proliferation by targeting PDCD10 in prostate cancer. *Prostate*, 2016, 76: 543–551.
- Wang Q, He GP, Hou MM, *et al*. Cell cycle regulation by alternative polyadenylation of CCND1. *Sci Rep*, 2018, 8: 6824.
- Lamb J, Ramaswamy S, Ford HL, *et al*. A mechanism of cyclin D1 action encoded in the patterns of gene expression in human cancer. *Cell*, 2003, 114: 323–334.
- Gautschi O, Ratschiller D, Gugger M, *et al*. Cyclin D1 in non-small cell lung cancer: a key driver of malignant transformation. *Lung Cancer*, 2007, 55: 1–14.
- Jiang JH, Eliaz I, Sliva D. Suppression of growth and invasive behavior of human prostate cancer cells by ProstaCaid™: mechanism of activity. *Int J Oncol*, 2011, 38: 1675–1682.

DOI 10.1007/s10330-020-0454-4

Cite this article as: Zhang CL, Liu D, Tian QQ, *et al*. CircBAGE2 (hsa_circ_0061259) regulates CCND1 and PDCD10 expression by functioning as an miR-103a-3p 'sponge' to alter the proliferation and apoptosis of prostate cancer cells. *Oncol Transl Med*, 2021, 7: 221–228.

Evaluation of endocrine therapy combined with intensity modulated radiation therapy in patients with advanced prostate cancer

Xiulong Ma¹, Hongbing Ma¹, Dongli Ruan² (✉)

¹ Department of Radiotherapy, The Second Affiliated Hospital, Xi'an Jiaotong University, Xi'an 710004, China

² Department of Urology, Xijing Hospital, Air Force Military Medical University, Xi'an 710032, China

Abstract

Objective The aim of this study was to study the effect of endocrine therapy combined with intensity-modulated radiation therapy in patients with advanced prostate cancer.

Methods The clinical data of 231 patients with advanced prostate cancer treated with radiotherapy in our hospital from May 2010 to March 2018 were collected. A total of 135 patients were treated with endocrine therapy combined with intensity-modulated radiotherapy, and 96 patients were treated with intensity-modulated radiotherapy only because of drug allergy, serious adverse reactions, and economic reasons. Two months after the end of the treatment, the short-term curative effect was evaluated using imaging reexamination. The total prostate-specific antigen (TPSA) and free prostate-specific antigen (FPSA) were detected before and 2 months after the end of the treatment. All patients were followed up for at least 3 years, and the metastasis-free survival rate and cumulative survival rate of the two groups were calculated.

Results The remission rates (RRs) of the observation and control groups were 64.45% and 46.87%, respectively; the difference was not statistically significant ($P > 0.05$); however, the efficacy distribution of the endocrine therapy combined with intensity-modulated radiotherapy group was significantly better than that of the intensity-modulated radiotherapy group ($P < 0.05$). There was no significant difference in clinical efficacy between the two groups in different TNM stages and Gleason grades. After treatment, the levels of TPSA and FPSA were significantly decreased compared with those before treatment; however, the decrease in the endocrine therapy combined with the intensity-modulated radiation therapy (IMRT) group was significantly higher than that in the IMRT group ($P < 0.05$). Although there were no significant differences in the 1-year and 3-year cumulative survival rates between the two groups, the 1-year and 3-year metastasis-free survival rates of the endocrine therapy combined with the IMRT group were 60% and 38.17%, respectively, which were significantly higher than those of the IMRT group (37.5% and 20.83%, $P < 0.05$).

Conclusion Endocrine therapy combined with IMRT significantly improved the clinical efficacy of advanced prostate cancer, reduced PSA (prostate specific antigen) levels, and improved the metastasis-free survival rates.

Key words: conformal intensity-modulated radiation; endocrine therapy; prostate cancer; metastasis-free survival rate

Received: 18 April 2021
Revised: 22 July 2021
Accepted: 10 August 2021

Prostate cancer is one of the most common malignant tumors of the urinary system. The incidence rate in recent years has been increasing^[1-2]. In China, the incidence rate of prostate cancer is the highest among male urogenital tumors^[3]. The main treatment methods for prostate cancer are surgical treatment, radiotherapy, and endocrinology. However, the overall age of the patients was large and combined with other internal diseases. Such patients

are not suitable for radical prostatectomy, and some patients are unwilling to undergo surgery. Radiotherapy is the appropriate choice for these patients. Intensity-modulated radiation therapy (IMRT) is one of the standard therapies for prostate cancer. A large number of studies have confirmed that IMRT can increase the target dose, reduce the adverse reactions of normal tissues, and lead to an overall higher survival rate (OS) of patients^[4-5].

This study aimed to investigate the effect of endocrine therapy combined with IMRT in patients with advanced prostate cancer.

Materials and method

General information

The clinical data of 231 patients with advanced prostate cancer treated with radiotherapy in our hospital from May 2010 to March 2018 were collected. The inclusion criteria were as follows: ①patients with a pathological diagnosis of prostate cancer who were not suitable for surgical treatment or unwilling to undergo surgery; ②positron emission tomography (PET) and MRI showed TNM stage III and IV. Exclusion criteria: ①chronic prostatitis and benign prostatic hyperplasia; ②brain metastasis occurred; ③ combined with malignant tumors from other sources; ④complicated with infection, heart, cerebrovascular, liver, kidney, and blood system and other serious primary diseases; ⑤complicated with severe urinary tract infection, urinary tract stenosis, bladder stones; ⑥other diseases associated with detrusor overactivity or detrusor physical and dysuria symptoms; and ⑦patients who had undergone surgical castration before treatment. Among the 231 patients, 135 were treated with endocrine therapy combined with intensity-modulated radiotherapy, and 96 were treated with intensity-modulated radiotherapy only because of drug allergy, serious adverse reactions, and economic reasons. There were no significant differences in age, TNM stage, Gleason score, and PSA level between the two groups (Table 1).

Treatment methods

IMRT: After simulated CT localization (Siemens as20 CT simulator), scanning from L4 to 3 cm below the ischial tubercle, with a slice thickness of 3 mm, the gross tumor volume (GTV), including the whole prostate, bilateral seminal vesicles, and pelvic lymph node drainage area, was delineated by CT scan and pelvic magnetic resonance imaging; the clinical target volume (CTV) was the same as the GTV. Based on the CTV, 1 cm was used as the planning target volume (PTV). After delineation of each target, the radiotherapy plan was made according to the actual situation of each patient. We used 6MeV X-ray, pvt2.23gy/time, 5 times/week, a total of 35 times, with a total dose of 78.05gy; 95% PTV volume received a dose

≥ 76 Gy. The V50 of adjacent sensitive organs such as the rectum and bladder was ≤ 50%, and the V50 of the femoral head (bilateral) was ≤ 5%.

Endocrine therapy: Goserelin Acetate Sustained-Release Depot, 3.6 mg, subcutaneous injection, once every 28d days, did not need to adjust the dose for patients with liver and kidney dysfunction and elderly patients; oral bicalutamide at a dose of 50 mg once per day, regular review of blood routine and liver function, when abnormal liver function occurred during treatment, the treatment was stopped. During the treatment, the drug can be stopped when the serum PSA level is less than 0.2 ng/mL and the lowest value is maintained for 3–6 months. Half a year after drug withdrawal, the total prostate-specific antigen (TPSA) and free prostate-specific antigen (FPSA) were reexamined once a month, half a year later, every two months, and every three months after two years. If biochemical recurrence occurred during the follow-up period (Serum PSA exceeds the minimum value of 2ng/mL), the drug can be used according to the above methods.

Observation indexes

Two months after the end of the treatment, the short-term curative effect was determined by the evaluation results of the imaging reexamination [6]. Complete remission (CR): the tumor completely subsided and was maintained for more than 4 weeks, partial remission (PR): tumor regression ≥ 50% and maintained for more than 4 weeks; no change (NC), tumor regression < 50% or increase < 25%, progression of disease (PD): tumor enlargement ≥ 25% or new lesions. The total remission rate (RR) was calculated using the Cr and PR.

TPSA and FPSA levels were detected before and 2 months after treatment. All patients were followed up by telephone or through in-hospital follow-up, including clinical follow-up, PSA monitoring, imaging examination, treatment-related complications, and evaluation of the quality of life. Generally, they were followed up every 3 months within the first 2 years and every 6 months after the first 2 years. If any abnormality is found during follow-up, the follow-up interval should be shortened if necessary. All patients in this study were followed up for at least 3 years to calculate the metastasis-free survival rate and the cumulative survival rate.

Table 1 Comparison of general condition between two groups before treatment

Groups	Number of cases	Age (years)	Gleason score	TPSA (ng/mL)	FPSA (ng/mL)
Observation	135	72.36 ± 8.66	7.385 ± 0.664	315.62 ± 135.37	165.83 ± 78.51
Control	96	73.89 ± 10.28	7.28 ± 1.67	296.45 ± 103.86	152.35 ± 81.96
<i>t</i> value		35.381	15.14	76.342	48.233
<i>P</i> value		0.851	0.135	0.885	0.286

Statistical methods

SPSS 22.0 was used to analyze and process the data. Continuous data were expressed as the mean and standard deviation while categorical data were expressed as frequencies and percentages (%). The comparison of RR, metastasis-free survival rate, and cumulative survival rate between groups was performed using the chi-square test. Comparisons between groups were performed using the *t*-test for continuous variables. The efficacy distributions of CR, PR, NC, and PD were analyzed using the rank-sum test for categorical data. The threshold for statistical significance was set at $P \leq 0.05$.

Results

Comparison of clinical efficacy between the two groups

The RR of the observation group and the control group were 64.45% and 46.87%, respectively ($\chi^2 = 3.65, P > 0.05$). However, the efficacy distribution of endocrine therapy combined with IMRT was significantly better than that of IMRT alone ($z = 4.15, P < 0.05$; Table 2).

Comparison of the clinical efficacy of the two groups in different stages and grades (Table 3 and 4)

There was no significant difference in RR between the IMRT + endocrine therapy and IMRT groups in stage III and IV patients ($\chi^2 = 2.76, P = 0.38$). There was no significant difference in RR between the IMRT + endocrine therapy and IMRT groups in Gleason grades 4 and 5 patients ($\chi^2 = 3.25, P = 0.57$).

Comparison of PSA levels between the two groups before and after treatment (Table 5)

Before treatment, there was no statistically significant difference between the levels of TPSA and FPSA in the two groups ($P > 0.05$). After treatment, PSA levels in both groups decreased significantly; however, TPSA and FPSA levels in the IMRT + endocrine therapy group decreased more significantly than those in the IMRT group ($P < 0.05$).

Comparison of adverse reactions between the two groups (Table 6)

The common adverse reactions of the two groups were acute bladder irritation symptoms such as frequent micturition, urgency, and pain of micturition; intestinal irritation symptoms such as diarrhea, constipation, and abdominal pain; Grade 1–2 skin reactions such as erythema and pigmentation in the treatment area; anemia, leukopenia, thrombocytopenia, and other myelosuppression reactions. Most of the adverse reactions were grade 1–2, and most patients could tolerate them. A few patients with severe symptoms were treated with active symptomatic treatment, and the symptoms were significantly relieved. All patients could cooperate to complete the entire course of treatment. There was no significant difference in bladder irritation, intestinal irritation, grade 1–2 skin reaction, and grade 1–2 myelosuppression between the two groups during the follow-up period.

Comparison of the survival rates between the two groups (Table 7)

There were no significant differences in the 1-year and 3-year cumulative survival rates between the two groups

Table 2 Comparison of clinical efficacy between the two groups [*n* (%)]

Groups	Number of cases	CR	PR	NC	PD	RR
Observation	135	26 (19.26)	61 (45.19)	39 (28.88)	9 (6.66)	87 (64.45)
Control	96	10 (10.42)	35 (36.46)	32 (33.33)	19 (19.79)	45 (46.87)

Table 3 Comparison of the clinical efficacy of two groups in different stages [*n* (%)]

Groups	TNM stage	Number of cases	CR	PR	NC	PD	RR
Observation	III	72	17 (23.61)	41 (56.94)	14 (19.44)	0 (0.00)	58 (80.55)
	IV	63	9 (14.29)	20 (31.75)	25 (39.68)	9 (14.29)	29 (46.03)
Control	III	52	7 (13.46)	21 (40.38)	20 (38.46)	4 (7.69)	28 (53.84)
	IV	44	3 (6.82)	14 (31.82)	12 (27.27)	15 (34.09)	17 (38.64)

Table 4 Comparison of the clinical efficacy of two groups with different grades [*n* (%)]

Groups	Gleason grade	Number of cases	CR	PR	NC	PD	RR
Observation	4	54	17 (31.48)	26 (48.15)	8 (14.81)	3 (5.56)	43 (79.63)
	5	81	9 (11.11)	35 (43.21)	31 (38.27)	6 (7.41)	44 (54.32)
Control	4	46	6 (13.04)	19 (41.30)	20 (43.48)	1 (2.17)	25 (54.35)
	5	50	4 (8.00)	16 (32.00)	12 (24.00)	18 (36.00)	20 (40.00)

($P > 0.05$); however, the 1-year and 3-year metastasis-free survival rates of the IMRT + endocrine therapy group were 60% and 38.17%, respectively, which were significantly higher than those of the IMRT group (37.5% and 20.83%, $P < 0.05$).

Discussion

With the increasingly prominent aging phenomenon, the number of prostate cancer patients is increasing. Prostate cancer is one of the main causes of male deaths in European and American countries [7]. Especially in advanced prostate cancer, some patients often miss the best treatment time, and the prognosis is often poor [8]. The choice of safe and effective treatment for elderly patients with prostate cancer has also aroused widespread concern. Fan *et al.* [9] conducted a 10-year follow-up of laparoscopic radical prostatectomy for elderly patients with prostate cancer over 80 years of age and concluded that radical prostatectomy is not suitable for elderly patients above the age of 80 years. Radical radiotherapy is considered the standard treatment for localized prostate cancer. At present, comprehensive treatment based on it plays an important role in reducing the recurrence rate and improving the quality of life of patients with prostate cancer. Wang Xing *et al.* [10] found that compared with simple castration, radiotherapy combined with drug castration can effectively prolong the PFS and OS of elderly patients with advanced prostate cancer.

At present, external radiotherapy for prostate cancer mainly includes stereotactic radiotherapy (SBRT) and IMRT. It has a good curative effect, wide indications, few complications; it is also safe and effective. It is one of the most important treatment methods for patients with prostate cancer. For locally advanced prostate cancer, ionizing radiation can kill and destroy the cancer tissue to different degrees, thereby reducing the tumor volume. In view of the large radiation dose and relative complexity of SBRT, some researchers have questioned its safety [11]. There are also studies showing that [12] SBRT is cheaper and more convenient and suitable for replacement therapy for localized prostate cancer. Hamdy *et al.* [13] compared the quality of life of patients with SBRT and radical prostatectomy through prospective research and found that the two treatment methods were associated with decreased quality of life of urination and intestinal tract within 1 month. The quality of life of SBRT patients gradually recovered 6 months after treatment and recovered 36 months after treatment. The quality of life scores of radical prostatectomy patients at all time points was lower than the baseline level. With the continuous improvement of radiotherapy technology and medical equipment, IMRT advocates that different doses can be obtained by different target areas through the output of non-uniform radiation doses, which can moderately increase the local radiation dose of the tumor and the total radiation dose of the target area, and reduce the radiation dose to surrounding normal tissues and organs (such as the rectum and the bladder). It is superior to conventional

Table 5 Comparison of PSA levels between the two groups before and after treatment

Groups	TPSA (ng/mL)		FPSA (ng/mL)	
	Before treatment	After treatment	Before treatment	After treatment
Observation	70.46 ± 13.46	15.25 ± 4.87	13.56 ± 3.94	2.67 ± 0.59
Control	60.35 ± 12.86	31.98 ± 5.36	12.89 ± 2.63	3.86 ± 0.73
<i>t</i> value	0.26	16.35	0.38	12.36
<i>P</i> value	> 0.05	< 0.05	> 0.05	> 0.05

Table 6 Comparison of adverse reactions between the two groups [*n* (%)]

Groups	Number of cases	Bladder irritation	Intestinal irritation	Grade 1-2 skin reaction	Grade 1-2 myelosuppression
Observation	135	59 (43.7)	32 (23.7)	49 (36.3)	50 (37.0)
Control	96	35 (36.46)	16 (16.67)	26 (27.08)	29 (30.21)
χ^2 value		8.213	1.69	2.17	1.16
<i>P</i> value		> 0.05	> 0.05	> 0.05	> 0.05

Table 7 Comparison of survival rate between the two groups [*n* (%)]

Groups	Number of cases	Metastasis free survival rates		Cumulative survival rates	
		1 year	3 years	1 year	3 years
Observation	135	81 (60)	50 (38.17)	125 (92.59)	85 (62.96)
Control	96	36 (37.5)	20 (20.83)	86 (89.58)	51 (53.13)
χ^2 value		4.35	6.27	0.17	0.68
<i>P</i> value		< 0.05	< 0.05	> 0.05	> 0.05

and three-dimensional radiotherapy in increasing the radiation dose and controlling rectal radiation [14]. The EAU prostate cancer guidelines also pointed out that [15] simple transperineal continuous low-dose brachytherapy is a clear, reliable, and reproducible modality for the treatment of low-risk prostate cancer. There are also a few cases in our center with good clinical effects. Due to the small sample size, we need to increase the sample size and draw a conclusion after long-term follow-up. In this study, IMRT was used in both groups and had a good clinical effect. The PSA level was significantly lower than that before treatment, and there was no significant difference in the cumulative survival rate between the two groups.

Androgen dependence is the basis for endocrine therapy for prostate cancer. Reducing androgen levels and inhibiting the synthesis of androgens by the adrenal glands can help to inhibit the conversion of testosterone to dihydrotestosterone, block the binding of androgens and androgen receptors to a certain extent, and inhibit or control the growth of prostate cancer cells. Mandel [16] conducted a randomized, double-blind, parallel controlled trial on 1218 patients with hormone-sensitive and non-metastatic prostate cancer. The results of long-term survival analyses revealed that compared with placebo, oral bicalutamide (150 mg) once a day can reduce the mortality of locally progressive prostate cancer, improve the overall survival rate, and prolong the average survival time of 1.8 years. However, bicalutamide did not improve the survival of patients with localized prostate cancer. In this study, goserelin acetate sustained-release depot combined with bicalutamide was used for endocrine therapy, which can help to reduce the serum androgen level of patients with prostate cancer, promote the death of androgen-sensitive cells *in vivo*, inhibit tumor growth, alleviate tumor metastasis to a certain extent, inhibit the proliferation of cancer cells after radiotherapy, and enhance the effect of radiotherapy. According to the results of this study, although there was no significant difference in clinical efficacy between the IMRT + endocrine therapy group and the IMRT group, the levels of TPSA and FPSA decreased more significantly than those in the IMRT group, and the 1-year and 3-year metastasis-free survival rates were significantly higher than those in the IMRT group, with the differences being statistically significant.

PSA, as a specific biomarker of prostate cancer, can be increased in prostate cancer, benign prostatic hyperplasia, prostatitis, and other non-malignant diseases. Compared with digital rectal examination and transrectal prostate ultrasound, PSA is a better predictor of prostate cancer; however, the correlation between PSA levels and prostate cancer risk in Chinese men is significantly weaker than that in Western countries [17]. The main purpose of

prostate cancer screening with PSA as the main detection method is to reduce the mortality of prostate cancer in the screening population without affecting the quality of life of the population [18]. The basic purpose of prostate cancer follow-up is to detect changes in serum PSA levels after treatment. The prostate gland still exists after radiotherapy; therefore, the PSA level decreases slowly. PSA may reach its lowest value 3 years after the end of radiotherapy. At present, there is still controversy regarding the optimal cut-off value for determining the prognosis of the lowest PSA level after radical radiotherapy. Generally, the lower the cut-off value, the higher the cure rate. It is generally believed that the prognosis of patients with the lowest PSA level reaching 0.5 ng/mL after 3–5 years is better [19]. Whether endocrine therapy was used at the same time, biochemical recurrence was considered when the PSA level exceeded the minimum PSA level of ≥ 2 ng/mL after radiotherapy [20]. The follow-up PSA level in this study was limited to the change in PSA level two months after treatment. The levels of TPSA and FPSA in the IMRT + endocrine therapy group decreased more significantly than those in the IMRT group ($P < 0.05$). The follow-up of PSA was not comprehensive, and no further studies were carried out; however, no biochemical recurrence was found during the follow-up period.

Common acute complications of external radiotherapy include frequent micturition, urgency of micturition, nocturia, hematuria, diarrhea, tenesmus, hematochezia, and perianal skin ulceration; these symptoms generally disappear a few weeks after radiotherapy, which is a reversible pathological change [21–22]. The most obvious delayed complication of external radiotherapy is rectal bleeding; however, less than 1% of rectal bleeding seriously affects life and requires surgical treatment. Other possible complications include hemorrhagic cystitis, which generally improves after nonsurgical treatment [21–22]. Compared with surgical treatment, radiotherapy rarely causes urinary incontinence and urethral stricture and has less effect on erectile function than surgical treatment. Retrospective studies have shown that radiotherapy for prostate cancer can increase the risk of rectal cancer and bladder cancer; however, these small-probability adverse events do not affect the choice of radiotherapy for prostate cancer patients [21–22]. There was no significant difference in the incidence of complications between the two groups. After giving positive symptomatic treatment, they were significantly improved and could complete the entire course of the treatment.

In conclusion, endocrine therapy combined with intensity-modulated radiotherapy has a good clinical effect on patients with advanced prostate cancer; the decrease in PSA levels and the 1-year and 3-year metastasis-free survival rates are significantly improved. However, the long-term prognostic effect still needs to be

determined after follow-up.

Conflicts of interest

The authors indicated no potential conflicts of interest.

References

- Chen W, Zheng R, Baade PD, *et al.* Cancer statistics in China, 2015. *CA Cancer J Clin*, 2016, 66: 115–132.
- Pang C, Guan Y, Li H, *et al.* Urologic cancer in China. *Jpn J Clin Oncol*, 2016, 46: 497–501.
- Su Q, Li L, Zhang M. Diagnostic values of SI, TPSA and FPSA for prostate cancer. *Labeled Immunoassays Clin Med*, 2018, 25: 445–449.
- Luo HC, Cheng HH, Fu ZC, *et al.* The clinical effects for the prostate cancer patients treated reduced clinical target volume of intensity-modulated radiotherapy. *J Clin Oncol*, 2016, 21: 1019–1023.
- Liu YP, Xu J, Zhang LS, *et al.* An analysis of interfractional and intrafractional prostate motion in hypofractionated precise radiotherapy for prostate cancer. *Chin J Radiat Oncol (Chinese)*, 2016, 25: 1199–1203.
- Dell' Oglio P, Zaffuto E, Boehm K, *et al.* Long-term survival of patients aged 80 years or older treated with radical prostatectomy for prostate cancer. *Fyr J Surg Oncol*, 2017, 43: 1581–1588.
- Kaufman HL, Wang W, Manola J, *et al.* Phase II randomized study of vaccine treatment of advanced prostate cancer (E7897): a trial of the Eastern Cooperative Oncology Group. *J Clin Oncol*, 2016, 22: 2122–2132.
- Ward JF, Slezak JM, Blute ML, *et al.* Radical prostatectomy for clinically advanced (cT3) prostate cancer since the advent of prostate-specific antigen testing: 15-year outcome. *BJU Int*, 2015, 95: 751–756.
- Zhang F, Zhang SD, Xiao CL, *et al.* Perioperative parameters and prognosis analysis of patients aged 80 years or older treated with radical prostatectomy for prostate cancer. *Acta Sci Nat Univ Pekinensis*, 2018, 50: 822–827.
- Wang X, Jiang Z, Rong WW. Efficacy and safety of drug castration with radiotherapy in treatment of prostate cancer. *China J Modern Med (Chinese)*, 2020, 30: 111–116.
- Zhao SG, Chang SL, Spratt DE, *et al.* Development and validation of a 24-gene predictor of response to postoperative radiotherapy in prostate cancer: A matched, retrospective analysis. *Lancet Oncol*, 2016, 17: 1612–1620.
- Gao QN. Stereotactic body radiation therapy versus conventional intensity-modulated radiation therapy for the treatment of prostate cancer. *Nat J Androl*, 2019, 25: 424–429.
- Hamdy FC, Donovan JL, Jane JA, *et al.* 10-year outcomes after monitoring, surgery, or radiotherapy for localized prostate cancer. *N Engl J Med*, 2016, 375: 14–15.
- Zheng J, Tao LS, Chen YS, *et al.* Clinical analysis of intensity modulated radiotherapy combined with endocrine therapy for 42 patients with advanced prostate cancer. *Int J Urol Nephrol*, 2017, 37: 70–73.
- Mottel N, Bellmunt J, Briers E, *et al.* EAU guidelines on prostate cancer. 2017, [2017-04-22].
- Mandel P, Kriegmair MC, Kanphake JK, *et al.* Tumor characteristics and oncologic outcome after radical prostatectomy in men 75 years old or older. *J Urol*, 2016, 196: 89–94.
- Chen R, DD Sjoberg, Huang Y, *et al.* Prostate specific antigen and prostate cancer in Chinese men undergoing initial prostate biopsies compared with Western cohorts. *J Urol*, 2017, 197: 90–96.
- Fleshner K, Carlsson SV, Roobol MJ. The effect of the USPSTF PSA screening recommendation on prostate cancer incidence patterns in the USA. *Other*, 2017, 14.
- Ray ME, Thames HD, Levy LB, *et al.* PSA nadir predicts biochemical and distant failures after external beam radiotherapy for prostate cancer: a multi-institutional analysis. *Int J Radiat Oncol Biol Phys*, 2006, 64: 1140–1150.
- lii MR, Hanks G, Thames H, *et al.* Defining biochemical failure following radiotherapy with or without hormonal therapy in men with clinically localized prostate cancer: recommendations of the RTOG-ASTRO Phoenix Consensus Conference. *Int J Radiat Oncol Biol Phys*, 2006, 65: 965–974.
- Matzinger O, Duclos F, Bergh A, *et al.* Acute toxicity of curative radiotherapy for intermediate- and high-risk localised prostate cancer in the EORTC trial 22991. *Eur J Cancer*, 2009, 45: 2825–2834.
- Rma B, Crc C, Mf D, *et al.* Pelvic complications after prostate cancer radiation therapy and their management: an international collaborative narrative review. *Eur Urol*, 2019, 75: 464–476.

DOI 10.1007/s10330-021-0491-1

Cite this article as: Ma XL, Ma HB, Ren DL. Evaluation of endocrine therapy combined with intensity modulated radiation therapy in patients with advanced prostate cancer. *Oncol Transl Med*, 2021, 7: 229–234.

A case of sorafenib-induced severe thrombocytopenia during treatment of unresectable hepatocellular carcinoma

Xiaoying Quan, Xiaoyan Chen, Lei Lei, Chunzhi Wu, Xiaoli Jia, Bin Ye (✉)

Department of Medical Oncology, the Sixth People's Hospital of Chengdu, Chengdu 610051, China

Abstract

An 81-year-old male with unresectable hepatocellular carcinoma underwent transarterial chemoembolization (TACE) combined with sorafenib. Platelet count was normal before and after TACE treatment, after which oral administration of sorafenib (400 mg po bid) was initiated. During this period, the patient experienced significant diarrhea, so the dosage was reduced to 200 mg po bid. Later, the patient showed obvious gingival bleeding with progressive exacerbation, and his blood routine examination showed a platelet count of 2×10^9 cells/L. The patient was clinically diagnosed with extreme severe thrombocytopenia. The patient was advised to stop taking sorafenib and was immediately treated with hemostasis, platelet transfusion, and suspended red blood cells. After the above treatment, the patient's symptoms improved, and he was discharged. Up to the date of follow-up, there was no further bleeding.

Key words: thrombocytopenia; sorafenib; hepatocellular carcinoma

Received: 22 April 2021
Revised: 21 May 2021
Accepted: 23 June 2021

An 81-year-old male patient presenting with “diagnosis of liver cancer more than one month, gingival bleeding for six days, and aggravation for one day” was admitted to our department on November 10, 2020. On September 8, 2020, the patient had undergone abdominal color ultrasonography and a large mass in the right lobe of the liver (maximum diameter approximately 9 cm) was suspected to be liver cancer. The patient sought further treatment and tumor marker results showed AFP was 8.45 ng/mL and CA199 was > 1000 U/mL. Abdominal enhanced computed tomography (CT) revealed a mixed low-density mass in the anterior right lobe and left medial lobe of the liver (approximately 10.3 cm long straight through), multiple similar enhanced nodules in the liver (maximum diameter, 2.4 cm), and tumor thrombus in the right anterior branch of the portal vein. On September 22, 2020, clinical diagnosis of liver cancer through “superselective hepatic arteriography, hepatic artery chemotherapy perfusion, and tumor supplying artery embolization” of the right femoral artery under local anesthesia was made. Intraoperative angiography showed a large, ill-defined, and irregular contrast agent staining of the mass shadow in the right lobe, with abundant pathological blood vessels and no

early manifestation of portal vein branches. The patient was administered fluorouracil 1000 mg, epirubicin 50 mg chemotherapy infusion, tumor supplying artery iodized oil, and PVA embolization in the right and left hepatic arteries. The patient was discharged from the hospital after receiving protective liver function treatment. Later, on October 12, 2020, he began to take 400 mg po bid sorafenib (Bayer Medical & Healthcare Corporation, trade named Duojime, German). On October 24, 2020, he developed diarrhea, which was not taken seriously and was treated. On October 28, 2020, he presented with worsening diarrhea and was administered antidiarrhea therapy. Considering drug-related side effects, the dose of sorafenib was reduced to 200 mg p.o. bid. However, on November 4, 2020, a small amount of gingival bleeding occurred in the patient, which could stop by itself. The patient did not receive further diagnosis and treatment, and continued sorafenib administration until November 10, 2020. The gingival bleeding worsened, and the skin of the limbs, head, and face was scattered in the petechiae, so he was admitted to our department at 19:04 on November 10, 2020.

Physical examination on admission: T 36.5°C, P 88 times/min, R 20 times/min, BP 140/81 mmHg, slightly

poor nutrition, scattered petechias in the skin of the limbs, head and face without petechias. Double lung breathing sounds were thick, and no dry or wet rales were heard. Abdominal tenderness, no rebound pain, muscle tension, liver, spleen, and subcostal were not touched; the rest of the examination did not show positive signs. He had hypertension for more than ten years with the highest systolic blood pressure >180 mmHg, which was treated with oral nifedipine sustained-release tablets 10 mg po qd. No sign of diabetes, coronary heart disease, or other chronic diseases. No history of hepatitis, tuberculosis, or other infectious diseases. No history of blood transfusion or donations. No history of food or drug allergies. There was no significant family history.

The results of the auxiliary examination after admission showed that hepatitis B markers were negative. Blood routine indicated the white blood cell count was 7.86×10^9 cells/L, hemoglobin was 105 g/L, platelet count was 2×10^9 cells/L, C-reactive protein was 104.38 mg/L, and procalcitonin was 0.320 ng/mL. Liver function showed albumin was 33.4 g/L, alanine aminotransferase was 39 U/L, aspartate aminotransferase was 43 U/L, lactate dehydrogenase was 226 U/L, and α -hydroxybutyrate dehydrogenase was 176 U/L. Coagulation resulted prothrombin time was 14.8 s, partial prothrombin time was 55.4 s, fibrinogen was 6.19 g/L, and D-dimer was 1.30 mg/L. Tumor markers indicated AFP was 3.4 ng/mL and CA199 was 218.3 U/mL. Myocardial enzymology demonstrated hypersensitive troponin T was 28.59 ng/L and B-type natriuretic peptide precursor was 765.60 ng/L. Kidney function, electrolytes, and routine urine tests revealed no definite abnormalities. Contrast-enhanced head, chest, and abdominal CT (November 11, 2020) revealed postoperative changes in hepatocellular carcinoma (HCC) showing multiple nodules, masses, and lipiodol deposition in the liver, with the largest being approximately 10.2 cm \times 6.6 cm. In the arterial phase of the enhanced scan, there was still significant enhancement, and the portal vein and venous phase decreased, suggesting that the tumor was still active, while contrast-enhanced scanning of the remaining sites showed no abnormal enhancement.

After admission, the patient was instructed to stop taking sorafenib immediately, and was administered tranexamic acid and phenolic sulfoethylamine to stop bleeding, platelet infusion, interleukin-11 elevated platelets, amino acid and fat milk for nutritional support, and blood pressure management. No gingival bleeding was observed after treatment. At 07:20 on October 11, 2020, the patient developed fever with a body temperature of 38.2°C, accompanied by chills without chills. Blood culture was performed, and the body temperature returned to normal after hypothermia treatment, and anti-infective treatment was administered cefazoxime

sodium 2 g q12h. On October 11, 2020 solstice during November 13, 2020, the patient received five infusions of irradiated platelets. Routine blood examination (November 14, 2020) indicated a hemoglobin level of 56 g/L and a platelet count of 2×10^9 cells/L. The hematology department of our hospital considered secondary thrombocytopenic purpura in consultation and advised using terbium and gamma globulin to increase platelet count. A platelet matching antibody test negative. On November 14, 2020, the patient presented once with myelinolysis and weak positive occulted blood in stool. Considering severe anemia with gastrointestinal bleeding, he was prescribed fasting, pantoprazole for acid inhibition and hemostasis, infusion of suspended red blood cells to correct anemia, and recombinant human thrombopoietin and immunoglobulin to boost platelets. On November 18, 2020, routine blood analysis indicated a hemoglobin level of 37 g/L, and a platelet count of 67×10^9 cells/L. Due to continued positive fecal occultation blood, acid suppression and hemostasis and transfusion of suspended red blood cells to correct anemia were maintained. On November 23, 2020, the patient had a good appetite, strong mental disposition, and no black stool. Routine blood examination showed a hemoglobin level of 72 g/L and a platelet count of 107×10^9 cells/L. After the above treatment, the patient's symptoms improved significantly and he was discharged to the hospital for rest on November 27, 2020.

Discussion

Primary HCC is a malignant tumor with high clinical morbidity and mortality. Due to its insipient onset, rapid progression, and difficulty in detection in the early stages, most patients are diagnosed in the middle and advanced stages, losing the opportunity for radical surgery, resulting in poor prognosis, with a median survival of only a few months^[1]. Currently, transarterial chemoembolization (TACE) is an effective treatment for middle-to-advanced liver cancer that cannot be surgically resected, and its short-term efficacy has been clinically confirmed^[2-3]. However, the long-term efficacy of TACE treatment is not ideal, because incomplete embolization of lesions causes ischemia and hypoxia in the tumor microenvironment, stimulates the secretion of large amounts of vascular endothelial growth factors by the remaining tumor cells, promotes tumor angiogenesis, and leads to tumor recurrence and metastasis. The development of sorafenib provides a new direction for the treatment of patients, as an oral multi-target molecular targeted drug that can inhibit the growth of tumor cells through the Raf/MEK/ERK pathway and block tumor angiogenesis^[4]. Recently, some studies have confirmed that sorafenib can improve the prognosis of patients with advanced HCC and, combined with TACE, can significantly prolong the time

of disease progression and overall survival, which could benefit patients with advanced HCC^[5-9].

Although TACE combined with sorafenib therapy has become a focus of intense research, its treatment-related toxicity is also under investigation. According to a number of studies^[8-10], common adverse reactions to TACE treatment include fever, liver pain, nausea, and vomiting, while common adverse reactions of TACE combined with sorafenib treatment were mainly mild to moderate side effects including hand and foot skin syndrome, diarrhea, and fatigue. However, one study have shown^[11] that myelosuppression was mainly mild to moderate in the TACE group alone, with seven cases of grade I/II leukopenia (12.5%), five of grade I/II thrombocytopenia (8.93%), and two of grade III thrombocytopenia (3.57%). In the TACE combined with sorafenib group, there were four cases of grade I/II leukopenia (7.14%), one of grade III leukopenia (1.79%), seven of grade I/II thrombocytopenia (12.5%), and one of grade III thrombocytopenia (1.79%). Another study reported^[12] two patients (2.8%) with grade III thrombocytopenia from treatment with TACE alone, and ten patients (13.0%) with grade III thrombocytopenia who were treated with TACE combined with sorafenib. The above reports suggested that combination therapy did not significantly increase the probability of treatment-related side effects, and severe grade IV thrombocytopenia was not reported.

The patient in our study was elderly with unresectable liver cancer who was treated with TACE combined with sorafenib. No fever, abdominal pain, abnormal liver function, bone marrow depression, or other complications were found after TACE treatment. The patient began to take sorafenib orally 22 days after the operation, and diarrhea and bleeding gums occurred more than ten days after beginning oral sorafenib administration, resulting in a platelet count of 2×10^9 cells/L. Therefore, we analyzed patients with thrombocytopenia that were closely associated with sorafenib. On the one hand, the peak of chemotherapy-related side effects mainly occurred on the seventh to fourteenth day of chemotherapy, while no myelosuppression was observed in these patients after TACE. The dose of TACE chemotherapy drugs was much lower than in normal intravenous chemotherapy. On the other hand, a separate study showed serious adverse reactions of sorafenib mainly included hand-foot syndrome, fatigue, diarrhea, and hypertension^[13]. However, myelosuppression usually presents as grade I/II white blood cells and neutropenia, while there was no severe thrombocytopenia^[14]. The reason for thrombocytopenia may be related to the anti-tumor mechanism of sorafenib, which inhibits vascular endothelial growth factor receptor and platelet-derived growth factor receptor, and can act against tumor angiogenesis. Therefore, sorafenib is associated with

adverse reactions after recognition and binding to the corresponding receptors in normal tissues and organs of the body.

Conclusion

The patient in this study developed severe thrombocytopenia after oral administration of sorafenib. Clinicians must therefore closely monitor routine blood tests and blood coagulation indices of patients being treated with sorafenib and be alert to bleeding caused by thrombocytopenia to ensure the safety of medication.

Conflicts of interest

The authors indicated no potential conflicts of interest.

References

1. Bray F, Ferlay J, Soerjomataram I, *et al.* Global cancer statistics 2018: GLOBOCAN estimates of incidence and mortality worldwide for 36 cancers in 185 countries. *CA Cancer J Clin*, 2018, 68: 394–424.
2. Raoul JL, Forner A, Bolondi L, *et al.* Updated use of TACE for hepatocellular carcinoma treatment: How and when to use it based on clinical evidence. *Cancer Treat Rev*, 2019, 728–736.
3. Ogasawara S, Ooka Y, Koroki K, *et al.* Switching to systemic therapy after locoregional treatment failure: Definition and best timing. *Clin Mol Hepatol*, 2020, 26: 155–162.
4. Ahmed A, Abdelgalil, Hamad M, *et al.* Sorafenib. *Profiles Drug Subst Excip Relat Methodol*, 2019, 44: 239–266.
5. Cai R, Song R, Pang P, *et al.* Transcatheter arterial chemoembolization plus sorafenib versus transcatheter arterial chemoembolization alone to treat advanced hepatocellular carcinoma: a meta-analysis. *BMC Cancer*, 2017, 17: 714.
6. Li L, Zhao WZ, Wang MM, *et al.* Transarterial chemoembolization plus sorafenib for the management of unresectable hepatocellular carcinoma: a systematic review and meta-analysis. *BMC Gastroenterol*, 2018, 18: 138.
7. Kok VC, Chen Y, Chen YY, *et al.* Sorafenib with transarterial chemoembolization achieves improved survival vs. sorafenib alone in advanced hepatocellular carcinoma: a nationwide population-based cohort study. *Cancers*, 2019, 11: 985.
8. Cheng Z, He L, Guo Y, *et al.* The combination therapy of transarterial chemoembolisation and sorafenib is the preferred palliative treatment for advanced hepatocellular carcinoma patients: a meta-analysis. *World J Surg Oncol*, 2020, 18: 243.
9. Li H, Li S, Geng J, *et al.* Efficacy evaluation of the combination therapy of sorafenib and transarterial chemoembolization for unresectable HCC: a systematic review and meta-analysis of comparative studies. *Ann Transl Med*, 2020, 8: 540.
10. Ren B, Wang W, Shen J, *et al.* Transarterial chemoembolization (TACE) combined with sorafenib versus TACE alone for unresectable hepatocellular carcinoma: a propensity score matching study. *J Cancer*, 2019, 10: 1189–1196.
11. Wu FX, Chen J, Bai T, *et al.* The safety and efficacy of transarterial chemoembolization combined with sorafenib and sorafenib monotherapy in patients with BCLC stage B/C hepatocellular carcinoma. *BMC Cancer*, 2017, 17: 645.
12. Masatoshi K, Kazuomi U, Masafumil, *et al.* Randomised, multicentre

prospective trial of transarterial chemoembolisation (TACE) plus sorafenib as compared with TACE alone in patients with hepatocellular carcinoma: TACTICS trial, *Gut*, 2019, 69: 1492–1501.

13. Li Y, Gao ZH, Qu XJ. The adverse effects of sorafenib in patients with advanced cancers. *Basic Clin Pharmacol*, 2015, 116: 216–221.
14. Ziogas DC, Papadatos-Pastos D, Thillai K, *et al.* Efficacy and safety of sorafenib in patients with advanced hepatocellular carcinoma: age is not a problem. *Eur J Gastroenterol Hepatol*, 2017, 29: 48–55.

DOI 10.1007/s10330-021-0492-2

Cite this article as: Quan XY, Chen XY, Lei L, *et al.* A case of sorafenib-induced severe thrombocytopenia during treatment of unresectable hepatocellular carcinoma. *Oncol Transl Med*, 2021, 7: 235–238.

Special IgD- λ type multiple myeloma based on bone marrow cell morphology: A case report

Xiaofang Zhang, Yanqing Zhang, Yungang Zhang, Chuanke Wan, Ling Xu, Ruimin Li (✉)

Clinical Laboratory, Handan Central Hospital, Handan 056000, China

Abstract

We aimed to explore the changes of laboratory indexes of IgD- λ type multiple myeloma with special cell morphology, and to improve the cognition of IgD- λ type MM. To explore the changes of laboratory indexes of IgD- λ type 1 multiple myeloma with special cell morphology, and to improve the cognition of IgD- λ type MM. The morphology of bone marrow cells, immunofixation electrophoresis, serum free light chain (sFLC) and other detection indexes of a patient with IgD- λ type MM treated in Handan Central Hospital in December 2020 were analyzed. The patient bone marrow smears showed 62% of abnormal cells—which were distributed in clusters and resembled lymphoma and metastatic cancer cells. The Flowcytometry indicates that the cell is a plasma cell tumor. Immunoglobulin IgG, IgA and IgM were all lower than the normal range. There is a monoclonal light chain λ component in immunofixation electrophoresis. The serum free light chain λ was 2700.00 mg/L, light chain κ/λ is 0.0023, the high of serum calcium, LDH, β 2 microglobulin. IgD- λ type MM is a rare type of MM. The age of onset is young, the invasiveness is strong, the prognosis is poor, the clinical manifestation is complex, and it is easy to be misdiagnosed or missed. The analysis of the clinical symptoms and laboratory characteristics of the disease plays a positive role in the diagnosis, treatment and prognosis of the disease.

Key words: IgD- λ type multiple myeloma; bone marrow cell morphology; immunofixation electrophoresis; serum free light chain

Received: 4 September 2021

Revised: 21 September 2021

Accepted: 13 October 2021

A 66-year-old man sought treatment from the Department of Cardiology at a local hospital. His main symptoms were cough and shortness of breath, accompanied by dizziness, weakness, and edema of the lower limbs for since over half a month prior, which led the doctor to suspect “pulmonary heart disease.” The laboratory examination results were: white blood cell count (WBC) $3.04 \times 10^9/L$, red blood cell count (RBC) $3.05 \times 10^9/L$, hemoglobin (Hb) 97 g/L, and platelet count (Plt) $87 \times 10^9/L$. However, hematological diseases could not be excluded, and the patient was admitted to the Handan Central Hospital for further treatment. Since the disease onset, the patient had a poor mental diet, normal stools, hematuria, no significant changes in body weight, moderate anemia, edema of both lower extremities, no bleeding point or ecchymosis in the systemic skin and mucosa, no palpable superficial lymph node enlargement, red pharynx congestion, coarse respiratory sounds in

both lungs, no rrrhoea, no fever, and a blood pressure of 122/69 mmHg. The laboratory examination results were as follows: calcium 2.64 mmol/L, globulin 18.1 g/L, lactate dehydrogenase 1136 U/L, ferritin 1129.00 ng/L, uric acid 884.3 $\mu\text{mol/L}$, WBC $3.9 \times 10^9/L$, RBC $2.58 \times 10^{12}/L$, Hb 81 g/L, Plt $65 \times 10^9/L$. His quantitative immunoglobulin (Ig) levels were: IgG 0.45 g/L, IgA 0.63 g/L, IgM 0.14 g/L, and IgE 5 IU/mL. The blood light chain ration κ was 402 mg/dL, ration λ 280 mg/dL, and κ/λ 1.4357. His blood free light chain κ was 6.1 mg/L, blood free light chain λ 2700.00 mg/L, and blood free light chain κ/λ 0.0023. His serum β 2 microglobulin was quantified at 3.78 mg/L.

The monoclonal proliferation of abnormal plasma cells is a specific pathological feature of multiple myeloma, but most malignant tumor plasma cells are well-differentiated, morphologically similar to normal plasma cells, and are easy to identify. The confusing aspect of this case was the bone marrow smear: hyperplasia was significantly active,

✉ Correspondence to: Ruimin Li. Email: zyxzxr666@126.com

© 2021 Huazhong University of Science and Technology

and abnormal protoplast cells accounted for 62%. The cells were of different sizes, irregular shapes, contained rich cytoplasm, stained gray-blue, and contained some vacuoles, along with coarser chromatin with markedly large nucleoli that were scattered or clustered and fused (Fig. 1a–c). The following were noted: (1) possible lymphoma with bone marrow infiltration; (2) metastatic cancer was not excluded. In the patient's bone marrow smears, there were more abnormal cells distributed as clusters, which were morphologically similar to metastatic cancer cells. Some cells adhered to the clusters, and the cytoplasm appeared fused, but closer observation revealed a more cytoplasm-like superposition. However, single cells were relatively regular with clear nucleoli, which is more similar to lymphoid hematopoietic system cells, and morphologically indistinguishable from lymphoma cells and metastatic cancer cells.

IgD type multiple myeloma (MM) can manifest at a younger age and predominantly affects male individuals. Patient survival time is short, and the disease can be difficult to detect in its early stages. Most patients are in stage III period when symptoms appear. λ light chain type is more common, and such patients are more prone to anemia, kidney damage, hypercalcemia, and extramedullary infiltration, with a poor prognosis^[1-3]. Therefore, early diagnosis is of great significance for the clinical treatment of IgD type MM, quality of life improvement, and prognosis assessment. In this case, serum protein electrophoresis revealed M protein bands, immunofixation electrophoresis for blood Ig (G, A, and M), κ , λ : monoclonal light chain component λ was observed in region λ , and immunofixation electrophoresis for blood IgD: monoclonal IgD λ component was observed

in region β (Fig. 1d–f). His urine trace albumin was 4.65 g/24 h. Urine light chain λ ration was 378.00 mg/L, and the urine free light chain κ/λ was 0.0049 mg/L. FISH(CKS1B/CDKN2C) (1Q21.1p32.3) 40% (1Q21) and 20% (1p32) were detected as positive for chromosome-related CKS1B gene deletion. Currently, the most sensitive method that can identify monoclonal free light chains is the detection of serum free light chain (sFLC) levels, and the sFLC κ/λ ratio can reflect the clonality of plasma cells^[4-5]. However, this requires a high proliferation rate of tumor cells, while 1q21 amplification indicates a poor prognosis in IgD MM^[6].

Flow cytometry (FCM) revealed plasma cell tumors, with abnormal cell populations accounting for 14.68% of the nuclear cells. Due to the destruction of plasma cells by FCM, the proportion of abnormal cells was significantly lower than that of the bone marrow smears. The cells expressed CD56 and cLambda and partially expressed CD138, but did not express CD38, CD19, CD45, and cKappa. We considered that the early plasma cells were more primitive, which may be related to the special morphological manifestation of bone marrow cells. The morphological characteristics of myeloma cells are also different in different pathological stages and can be used to guide the clinical treatment, judge the curative effect, and evaluate the prognosis of myeloma cells^[7-8] (Fig. 2).

In conclusion, in the diagnosis of IgD MM, the morphological study of bone marrow cells, immunofixation electrophoresis, and the detection of sFLC are of great clinical significance. In this case, in addition to the special cell morphology, the patient had a high plasma cell number, a high LDH and β_2 -microglobulin expression, and a high sFLC λ level, all

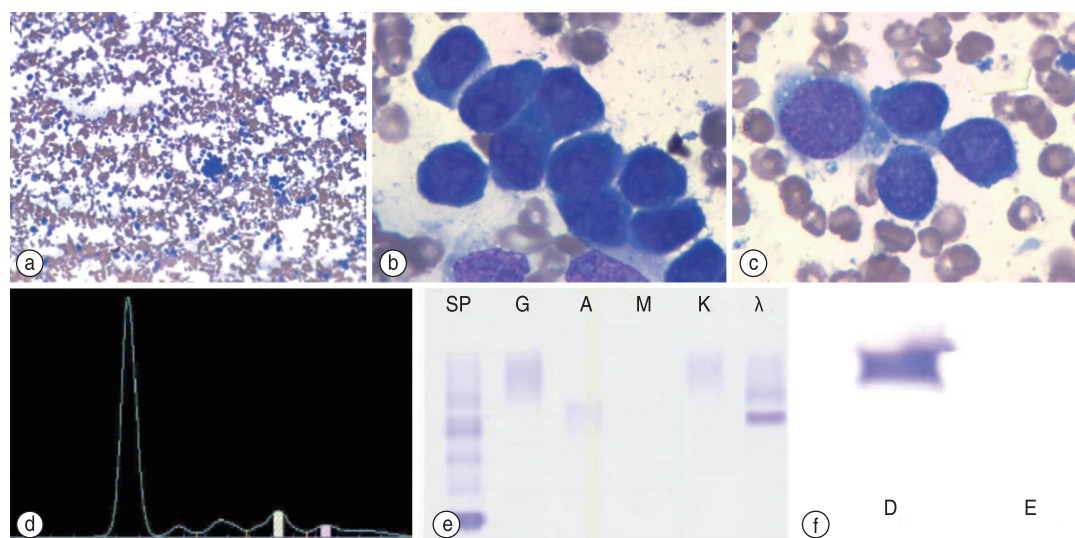


Fig. 1 Bone marrow image showing pancytopenia and a large number of abnormal cells (a) (Wright Giemsa 10 × 100). Bone marrow image showing abnormal plasma cells accounting for 62% (b–c) (Wright Giemsa 10 × 100). A detailed M-band appeared on serum protein electrophoresis (d). Serum immunofixation electrophoresis revealed a monoclonal light chain, which is a D-type immunoglobulin (e–f)

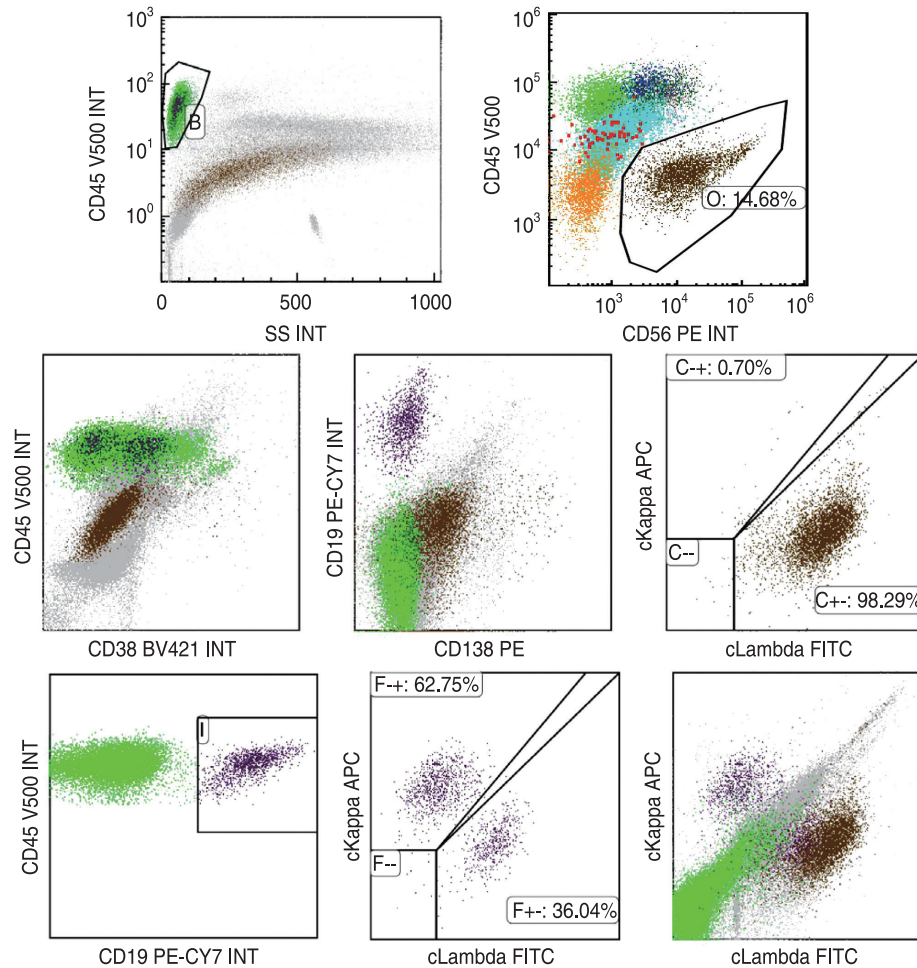


Fig. 2 Flow cytometry (FCM) revealing plasma cell tumors, with abnormal cell populations accounting for 14.68% of nuclear cells. Due to the destruction of plasma cells by FCM, the proportion of abnormal cells was significantly lower than that of the bone marrow smears. The cells expressed CD56 and cLambda and partially expressed CD138, but did not express CD38, CD19, CD45, and cKappa

suggesting a higher tumor burden and a more aggressive tumor invasion.

Conflicts of interest

The authors indicated no potential conflicts of interest.

References

1. Chen L, Fan F, Deng J, *et al.* Clinical characteristics and prognosis of immunoglobulin D myeloma in the novel agent era. *Ann Hematol*, 2019, 98: 963–970.
2. Chen J, Fang M, Chen X, *et al.* N-glycosylation of serum proteins for the assessment of patients with IgD multiple myeloma. *BMC Cancer*, 2017, 17: 881.
3. Liu W, Liu J, Song Y, *et al.* Union for China Leukemia Investigators of the Chinese Society of Clinical Oncology, Union for China Lymphoma Investigators of the Chinese Society of Clinical Oncology. Mortality of lymphoma and myeloma in China, 2004–2017: an observational study. *J Hematol Oncol*, 2019, 12: 22.
4. Wang PF, Xu Y, Yan S, *et al.* The roles of serum free light chain ratio

- in the diagnosis and prognosis of newly diagnosed multiple myeloma. *Zhonghua Xue Ye Xue Za Zhi (Chinese)*, 2016, 37: 377–382.
5. Bhole MV, Sadler R, Ramasamy K. Serum-free light-chain assay: clinical utility and limitations. *Ann Clin Biochem*, 2014, 51(Pt 5): 528–542.
6. Modi J, Kamal J, Eter A, *et al.* Immunoglobulin D multiple myeloma with rapidly progressing renal failure. *J Clin Med Res*, 2015, 7: 653–655.
7. Xiang Y, Zeng H, Liu X, *et al.* Thymidine kinase 1 as a diagnostic tumor marker is of moderate value in cancer patients: A meta-analysis. *Biomed Rep*, 2013, 1: 629–637.
8. Chen XZ, Zhang WH, Yang K, *et al.* Quantitative comparisons of summary receiver operating characteristics (sROC) curves among conventional serological tumor biomarkers for predicting gastric cancer in Chinese population. *Tumour Biol*, 2014, 35: 9015–9022.

DOI 10.1007/s10330-021-0506-6
 Cite this article as: Zhang XF, Zhang YQ, Zhang YG, *et al.* Special IgD-A type multiple myeloma based on bone marrow cell morphology: A case report. *Oncol Transl Med*, 2021, 7: 239–241.

Contribution Invitation of Oncology and Translational Medicine

Oncology and Translational Medicine is an international professional academic periodical on oncology and translational medicine. The Journal, with the authors from around world, especially from China, is dominated in introducing the clinical experience of diagnosis and treatment as well as leading scientific research achievement in the tumor and translational medicine domain, in addition to report basic theory researches which help instruct the clinical practice of oncology and closely connect with the discipline. All the manuscripts are published in English, bimonthly issued both internal and external, 48–64 pages, 16 opens domains, art paper in offset printing, with layout by international customs, unified issuing number: ISSN 2095-9621 / CN 42-1865/R.

Oncology and Translational Medicine uses an online submission system. After reading the Information for Contributors, you must go to <http://otm.tjh.com.cn> to submit.

Manuscripts' arrangements are expected to meet the *Uniform Requirement for Manuscripts Submitted to Biomedical Journals (the 5th edition)* basically, which was laid down by Internal Medical Journals Edition Committee. Specific requirements for manuscripts are as follows:

Submission process

Manuscripts must be submitted by one of the authors of the manuscript, and should not be submitted by anyone on their behalf. The submitting author takes responsibility for the article during submission and peer review. Manuscripts should be scientific, advanced, pragmatic, concise, clear, well-arranged, well-informed and data-accurate. Provided the manuscript is to be printed, full text will be published in English. To facilitate rapid publication and to minimize administrative costs, *Oncology and Translational Medicine* accepts online submission.

During submission you will be asked to provide a cover letter. Please use this to explain why your manuscript should be published in the journal and to elaborate on any issues relating to our editorial policies detailed in the instructions for authors.

Files can be submitted as a batch, or one by one. The submission process can be interrupted at any time – when users return to the site, they can carry on where they left off. Each manuscript should include title page, abstract, key words, text, acknowledgement, authors' disclosures of potential conflicts of interest, reference, tables, charts and captions, starting each of these sections on a new page, numbered consecutively, beginning with the title page.

Title page: It contains the title of the article, which should be concise but informative. The names of all authors are to be placed under the title in sequence, and personal signatures in the same sequence are a must. Pay attention to accuracy of the title, the names of all authors with their affiliations and the contacting methods in English (address, postcode, telephone and fax number, Email address, etc.).

Abstract and key words: A structural abstract of no more than 250 words is to be put on the second page. It should embody four parts, objectives, methods, results and conclusion. It's desirable to employ the third person to write, not "this article" or "the author" in stead of. Supply three to eight key words or short phrases, and terms from the medical subject heading (MeSH) list Index Medicus should be adopted, each word being separated by semicolon.

Figures and Tables: Each figure and table is demanded to be numbered consecutively with the order given in the text, typed in separate sheets, and headed by a concise title. Attach all tables after the text. Place explanatory materials in footnotes below the table, and illustrate in footnotes all non-standard abbreviations used in table. The Journal takes the "Three Lines" form of table, requiring the data of the table in accordance with the significant digits of the same index (in the text). Only professional quality glossy photographs and black and white drawings are acceptable. Table numbers, subjects, names of the authors and an arrow indicating "top" should be affixed to the back of each table with soft pencil. If any images of people are involved, it must be granted by the persons in written. Magnification and staining should be indicated when pertinent (esp. pathological pictures concerned).

References: References should be listed in the order as mentioned in the text using Vancouver style. References are supposed to be sequentially listed according to GB7714-87 The Rules of References after the Manuscript, being marked by numbers in square brackets in the order as mentioned in the text. The authors must have read the references themselves. List the authors of the reference up to three and, "et al" if more than three. Names of journals should be abbreviated on the basis of the Index Medicus. Every reference should be symbolized by beginning and ending pages. Authors ought to check all references for accuracy and, at the same time, to correct text citation, listing all the citation orderly in Arabian number at the bottom of the text before submitting the articles. The following are two examples of reference style:

1 Bold RJ, Ota DM, Ajani JA, *et al.* Peritoneal and serum tumor markers predict recurrence and survival of patients with respectable gastric cancer. *Gastric Cancer*, 1999, 2: 1–7.

2 Weinstein L, Swartz MN. Pathologic properties of invading microorganisms. In: Sodeman WA Jr, Sodeman WA, eds. *Pathologic physiology: mechanisms of disease*. 8th ed. Philadelphia: Saunders, 1974. 457–472.

Assistance with the process of manuscript preparation and submission is available from the customer support team (dmedizin@sina.com).

Publication and peer review processes

Submitted manuscripts will be sent to peer reviewers, unless they are either out of scope or below threshold for the journal, or the presentation or written English is of an unacceptably low standard. They will generally be reviewed by two experts with the aim of reaching a first decision as soon as possible. Statistical reviewers are also used where required (for a full list of our statistical advisers, please click here). Reviewers are asked to declare any competing interests and have to agree to open peer review, which works on two levels: the authors receive the signed report and, if the manuscript is published, the same report is available to the readers. Reviewers are asked whether the manuscript is scientifically sound and whether it is of sufficient significance for publication. In cases where there is strong disagreement either among peer reviewers or between the authors and peer reviewers, advice is sought from a member of the journal's Editorial Board. The journal allows a maximum of two revisions of any manuscript. All appeals should be directed to the Medical Editor. The ultimate responsibility for editorial decisions lies with the Editor-in-Chief.

Other specification

Numbers are required in Arabian. Units of measurement are to be presented in metric units, such as m, cm, mm, mmHg, μm , nm, L, dL, mL, μL , kg, g, mg, μg , kcal, $^{\circ}\text{C}$, etc. Abbreviations and terms in simplified forms should be displayed in whole words or phrases at the first time, directly followed by its abbreviation, for example, nasopharyngeal cancer (NPC). When the terms are to be mentioned the second time, the shortened forms in question are acceptable. The abbreviations ought to be standard ones. Any abbreviations in title and abstract are not allowed.

If some Funds subjects of the studies are involved in the manuscripts, be it winning national, ministerial, provincial funds or concerning the special and strategic program, all should be given clear indication in the title page (the Funds number is to be needed), and the copy of the Funds certificate a plus.

It's advisable of you to send us a English-polish certificate from foreign experts (English or American for the best), with

inclusion of their personal signatures. Without such certificate, we will invite foreign specialist accordingly to examine and revise your manuscript at the cost on your part. Please indicate your approval when contribute.

Manuscripts must be accompanied by a introduction letter from the author's institution. The letter should contain (1) institution's review and remarks over the manuscript, (2) a statement of no duplicate publication or submission elsewhere of any part of the text, (3) a statement that no secretes or classified information are involved, (4) a statement of no signature or other relationships problems that might lead to a conflict of interest.

To reduce errors in typesetting and to speed up publication, authors are encouraged to submit manuscripts on disk. Disks should not be sent until the manuscript has been accepted and all revisions have been made. The revised manuscript should be saved in paper pattern as well as in pure text pattern, and the saving pattern must clearly indicated on the disk. The editors will not accept a disk without accompanying printouts of all the files on the disk nor without the original manuscript.

Under conditions prescribed by Copyright Law and under considerations of some context of the Journal, manuscripts which are acknowledged receipts but no further notice in the following 3 months may be in the course of examine. If contribution elsewhere is a want, please contact with the editor first because double contribution to different journals with the same manuscripts are not permitted. Keep all the manuscripts for no original manuscript will be returned.

Authors are responsible for the manuscripts they submitted. The Journal, on the basis of Copyright Law, is entitled to revise and abridge the manuscripts. Any amendments concerning the original meaning will be referred to the author for consideration.

Once the manuscript was adopted into the inclusion of the press, the Journal has the rights to publish the manuscript by means of electronic medium or in disc edition. Any part of the manuscript should on no condition be reprinted without our approval.

Every manuscript will be charged 50 yuan (RMB) for being taken care of. When post the manuscript, please remit the money via post office simultaneously (Do not enclose the money with the manuscript). After inclusion of the manuscript, a relevant fees for space of page is to be added. The publisher will provide three copies of the journal free of charge, if the manuscript is accepted.

Address of Editorial Office: Editorial Office of *Oncology and Translational Medicine*, Tongji Hospital, 1095 Jiefang Dadao, Wuhan 430030, China; Tel.: +86-27-69378388; Email: dmedizin@sina.com; Website: <http://otm.tjh.com.cn>.



中国科技核心期刊

(中国科技论文统计源期刊)

收录证书

CERTIFICATE OF SOURCE JOURNAL

FOR CHINESE SCIENTIFIC AND TECHNICAL PAPERS AND CITATIONS

ONCOLOGY AND TRANSLATIONAL MEDICINE

经过多项学术指标综合评定及同行专家
评议推荐，贵刊被收录为“中国科技核心期
刊”（中国科技论文统计源期刊）。

特颁发此证书。

中国科学院
中国科学技术信息研究所

Institute of Scientific and Technical Information of China

北京复兴路 15 号 100038

www.istic.ac.cn

2020年12月





Call For Papers

Oncology and Translational Medicine

(CN 42-1865/R, ISSN 2095-9621)

Dear Authors,

Oncology and Translational Medicine (OTM), a peer-reviewed open-access journal, is very interested in your study. If you have unpublished papers in hand and have the idea of making our journal a vehicle for your research interests, please feel free to submit your manuscripts to us via the Paper Submission System.

Aims & Scope

- Lung Cancer
- Liver Cancer
- Pancreatic Cancer
- Gastrointestinal Tumors
- Breast Cancer
- Thyroid Cancer
- Bone Tumors
- Genitourinary Tumors
- Brain Tumor
- Blood Diseases
- Gynecologic Oncology
- ENT Tumors
- Skin Cancer
- Cancer Translational Medicine
- Cancer Imageology
- Cancer Chemotherapy
- Radiotherapy
- Tumors Psychology
- Other Tumor-related Contents

Contact Us

Editorial office of Oncology and
Translational Medicine
Tongji Hospital
Tongji Medical College
Huazhong University of Science
and Technology
Jie Fang Da Dao 1095
430030 Wuhan, China
Tel.: 86-27-69378388
Email: dmedizin@tjh.tjmu.edu.cn;
dmedizin@sina.com

Oncology and Translational Medicine (OTM) is sponsored by Tongji Hospital, Tongji Medical College, Huazhong University of Science and Technology, China (English, bimonthly).

OTM mainly publishes original and review articles on oncology and translational medicine. We are working with the commitment to bring the highest quality research to the widest possible audience and share the research work in a timely fashion.

Manuscripts considered for publication include regular scientific papers, original research, brief reports and case reports. Review articles, commentaries and letters are welcome.

About Us

- Peer-reviewed
- Rapid publication
- Online first
- Open access
- Both print and online versions

For more information about us, please visit:

<http://otm.tjh.com.cn>



Editors-in-Chief

Prof. Anmin Chen (Tongji Hospital, Wuhan, China)
Prof. Shiyong Yu (Tongji Hospital, Wuhan, China)